
Intracellular processing of motion information in a network of blowfly visual interneurons

Yishai Michael Elyada

München 2009



Intracellular processing of motion information in a network of blowfly visual interneurons

Dissertation

Zur Erlangung des Doktorgrades

der Naturwissenschaften (Dr.rer.nat.)

der Fakultät für Biologie

der Ludwig-Maximilians-Universität München

Angefertigt am Max-Planck-Institut für Neurobiologie,

Abteilung 'Neuronale Informationsverarbeitung'

Vorgelegt von

Yishai Michael Elyada

München 2009

Hiermit erkläre ich, daß ich die vorliegende Dissertation selbständig und ohne unerlaubte Hilfe angefertigt habe. Sämtliche Experimente wurden von mir selbst durchgeführt, außer wenn explizit auf Dritte verwiesen wird. Ich habe weder anderweitig versucht, eine Dissertation oder Teile einer Dissertation einzureichen bzw. einer Prüfungskommission vorzulegen, noch eine Doktorprüfung durchzuführen.

München, den

1. Gutachter: Dr. Alexander Borst
 2. Gutachter: Dr. Benedikt Grothe
- Tag der mündlichen Prüfung: Dienstag, den 14. 07.2009

Contents

Abstract	9
Chapter 1. Introduction	11
1.1. Visual orientation in flight	11
1.1.1. Optic flow and the optomotor response	12
1.2. Local motion detection	16
1.2.1. The Reichardt detector	17
1.2.2. Evidence in insects	18
1.2.3. Response properties	20
1.3. The fly visual system	22
1.3.1. The compound eye.....	23
1.3.2. The lamina.....	27
1.3.3. The medulla.....	29
1.3.4. The lobula.....	31
1.3.5. The lobula plate.....	31
1.4. Lobula plate tangential cells	34
1.4.1. Lobula plate tangential cells and optic flow integration	34
1.4.2. HS cells	38
1.4.3. CH cells	39
1.4.4. FD cells (CI cells)	40
1.4.5. Bilateral spiking cells – H cells and V cells.....	41
1.4.6. VS cells.....	43
1.4.7. Calcium responses.....	45
1.5. Lateral interactions between VS cells.....	47
1.5.1. Axo-axonal gap junctions	48
1.5.2. Functional significance	49
1.6. Neuronal morphology and intracellular computation.....	51

1.6.1.	Segregation and aggregation of inputs	51
1.6.2.	Non-linear integration in LPTC dendrites	54
1.7.	Goals and project outline	55
Chapter 2.	Methods	57
2.1.	Experiments	57
2.1.1.	Preparation and positioning of the flies	57
2.1.2.	Electrophysiology	59
2.1.3.	Visual stimulation	61
2.1.4.	Electrical responses.....	62
2.2.	Data analysis	63
2.2.1.	Cell identification	63
2.2.2.	Calcium imaging	64
2.3.	Modeling.....	66
2.3.1.	VS cell network model	66
2.3.2.	Model parameters	69
2.3.3.	Modeling visual input.....	70
2.3.4.	Modeling calcium responses.....	71
Chapter 3.	Results	72
3.1.	Two receptive fields in single VS cells	73
3.1.1.	Linearity and homogeneity of calcium responses	73
3.1.2.	Mapping the receptive fields	74
3.2.	Information flow underlying receptive field broadening	77
3.2.1.	Controlling information flow with voltage clamp.....	78
3.2.1.	Clamping out dendritic input to the axon terminal	80
3.3.	Interpolation of dendritic signals in the terminals	83
3.3.1.	Faster reporting of calcium dynamics.....	83
3.3.2.	Frequency response and SNR of the calcium dye.....	85
3.3.3.	Smoothing of dendritic fluctuations in the axon terminal.....	87
3.4.	Functional consequences.....	88
3.4.1.	Compartmental model.....	89

3.4.2.	Quantifying response smoothness	90
3.4.3.	The shunting effect of chemical synapses	92
3.5.	Small field selectivity of VS cell dendrites	95
Chapter 4.	Discussion	100
4.1.	Methodology	100
4.1.1.	Calcium imaging	101
4.1.2.	Single electrode voltage clamp	104
4.1.3.	Local voltage clamp as a tool	105
4.1.4.	The effects of dendritic voltage clamp in VS cells.....	106
4.2.	Relation to previous results	107
4.2.1.	Receptive field broadening in VS cells	107
4.2.2.	Information flow in the lobula plate	108
4.3.	Broad receptive fields and population coding	112
4.3.1.	Noise correlations	113
4.3.2.	Stimulus dimension	114
4.3.3.	Relevance to the VS cell network.....	116
4.4.	Gap junctions	117
4.5.	Separating VS cell input sources	119
4.5.1.	Linear and non-linear integration	120
4.6.	Small field selectivity of VS cell dendrites	121

List of Figures

Figure 1-1: Optic flow fields for different flight maneuvers.....	16
Figure 1-2: The Reichardt detector.....	18
Figure 1-3: Schematic overview of the fly visual system.....	24
Figure 1-4: The fly retina – morphology and light responses.....	25
Figure 1-5: The two motion detection pathways in the lamina	28
Figure 1-6: Lobula plate tangential cells.....	37
Figure 1-7: VS cells and their receptive fields.....	45
Figure 1-8: Single neurons as dual layer neural networks.....	53
Figure 1-9: Narrow dendritic and broad axonal receptive fields in single VS cells	57
Figure 2-1: Access to the lobula plate and the LPTCs.....	59
Figure 2-2: Identification of a VS4 cell by the relative position of its main dendrite.....	64
Figure 2-3: Calculating the region of interest (ROI).....	65
Figure 2-4: Normalizing calcium imaging receptive fields.....	66
Figure 2-5: VS network models used for simulations.....	68
Figure 3-1: Current-calcium influx relationship in VS cell dendrites and axons.....	75
Figure 3-2: Broadening of VS cells' receptive fields within single cells.....	76
Figure 3-3: Broadening of VS cells' receptive fields – population analysis.....	77
Figure 3-4: No broadening of receptive fields in VS1 cells – population analysis.....	78
Figure 3-5: Voltage clamp and current injection in a VS cell network model.....	80
Figure 3-6: Voltage clamping of dendritic input.....	81
Figure 3-7: Voltage clamping of dendritic input – population analysis.....	83
Figure 3-8: Calcium influx modeling results.....	86
Figure 3-9: Calcium influx signal-to-noise ratio analysis.....	87
Figure 3-10: Calcium influx model frequency response.....	87
Figure 3-11: Interpolation of dendritic responses in the axon terminal.....	89
Figure 3-12: Axon terminal coupling results in more robust VS cell population coding ..	92
Figure 3-13: Small-field selectivity in VS cell dendrites	96
Figure 3-14: Vertical size dependence of dendrites and axons.....	97
Figure 3-15: Effect of a lateral grating on dendritic and axonal responses.....	99
Figure 4-1: Schematic of VS cell connectivity with other LPTCs.....	111

Abstract

In the past few decades, the lobula plate of the fly has emerged as one of the leading models for the neural processing of optic flow stimuli that give rise to visual orientation behaviors (for recent reviews see Borst and Haag, 2002; Egelhaaf et al., 2002; Egelhaaf et al., 2002; Borst and Haag, 2007). The relative simplicity and accessibility of this neural system allows researchers to characterize the neural mechanisms that are thought to link the visual stimuli and the resulting behavioral responses. In the lobula plate, a set of 60 motion sensitive lobula plate tangential cells (LPTCs) integrate visual motion information from an array of local motion detectors, which form a retinotopic map of the fly's visual space in the lobula plate. The selective pooling of local, direction selective inputs, together with a network of unilateral and bilateral interactions between LPTCs, shape and tune the response properties of LPTCs to behaviorally relevant optic flow stimuli.

Over the years, lobula plate researchers assembled a formidable array of measurement and perturbation techniques that are usually available only in in-vitro systems. Additionally, the lobula plate and its presynaptic circuitry have been the subject of extensive and detailed modeling which allows a deeper synthetic understanding of the empirical results, as well as a more efficient and detailed way to generate hypotheses.

In this work I used a selection of these tools to explore the role of intracellular processing of visual motion information in lobula plate neurons and the significance of spatial segregation and aggregation of these cells' inputs in the context of their sensory function.

Abstract

Previous work on a network of ten LPTCs of the vertical system (VS cells) resulted in a prediction that due to lateral, gap-junction coupling of neighboring VS cells in their axon-terminals, the receptive fields of these cells should be broader in the axonal region than in the dendritic regions. I tested and confirmed this prediction using in-vivo calcium imaging and intracellular recordings. Using single-electrode voltage clamp I was able to perturb the flow of information in these cells and isolate the source of input responsible for this broadening, confirming that the coupling indeed takes place in the axon terminal.

The separation of feed-forward, synaptic input in the dendrites from lateral, gap-junction coupling in the axon-terminals allowed me to experimentally ask what is the function of the receptive field broadening. Relying on model predictions, I showed that this broadening results in a more stable and smooth representation of optic flow in the output region of the cells than in their input region, when the fly is presented with naturalistic, patchy and non-uniform stimuli. I then showed, using a simplified compartmental model that the separation of axonal gap-junctions from the dendritic synaptic input makes the gap-junction coupling more effective, and is thus necessary to ensure the functionality of the lateral interactions.

Chapter 1. Introduction

1.1. Visual orientation in flight

When a flying insect performs three dimensional maneuvers in space, it has access to three sources of information to monitor and control its maneuvers: wind, inertial and gyroscopic forces, and visual input. Wind can be used mainly to measure the speed of the animal and its angle of flight pitch (Simmons, 1980; Reichert et al., 1985), and inertial and coriolis forces to measure attitude of flight and deviations from it, as well as rotation (Pringle, 1948; Nalbach, 1993; Nalbach and Hengstenberg, 1994; Dickinson, 1999). However, light reflected by the surroundings and entering the animal's visual system can provide information not only about these two variables of flight control, but more importantly, about how the animal's flight relates to the physical structure of its immediate environment. The importance of visual information for flying insects becomes all the more evident when one considers the amount of neural hardware these organisms dedicate to vision. In flies, for example, the optic lobes amount to approximately half of the brain's volume (Strausfeld, 1976).

It is not surprising, therefore, that visual information is considered of primary importance when considering the mechanisms of flight control in insects (for reviews see Buchner, 1984; Collett et al., 1993; Egelhaaf and Kern, 2002; Srinivasan and Zhang, 2004). For example, bees regulate their flight speed using the angular velocity of their visual surrounding

(Srinivasan et al., 1996) and use integrated optic flow to estimate flight distance (Srinivasan et al., 1996; Srinivasan et al., 2000). Flies use visual input to control and stabilize their flight courses (Poggio and Reichardt, 1976; Reichardt and Poggio, 1976; Reichardt and Poggio, 1981; Hausen and Egelhaaf, 1989; Egelhaaf and Borst, 1993b; Egelhaaf and Borst, 1993a; Egelhaaf and Borst, 1993b; Heisenberg et al., 2001), and visual input is also crucial even for orientation behaviors whose primary sensory modality is not visual – for example, *Drosophila* can locate a source of odor only when its surroundings are visually textured, and fail when they are visually uniform (Frye et al., 2003). The experiments that elucidate these robust and reproducible behaviors treat the animal subject as a ‘black box’ that implements a function from the stimulus ensemble to the elicited behaviors. This behavioristic approach leads the neuroscientist to the inevitable question – what is the neural hardware that supports and implements the stimulus-response mapping of visual stimuli to motion responses? To answer this question, one must first consider the system’s relevant stimuli.

1.1.1. Optic flow and the optomotor response

When an organism moves in space, its self-motion generates optic flow, the motion of its visual environment relative to its retina. This autogenic optic flow contains visual motion patterns that can provide information for the organism about its own motion (Gibson, 1958; Lee, 1980; Koenderink, 1986; Warren and Hannon, 1988) and, through parallax motion, about the spatial layout of its physical surroundings (Nakayama and Loomis, 1974; Koenderink and Vandoorn, 1975; Prazdny, 1980). Practically all visual organisms use these optic flow in order to control their motor behavior (for reviews see, e.g., Lappe and Hoffmann, 1999; Srinivasan et al.,

1999), including humans (Pailhous et al., 1990; Barnes, 1993; Patla, 1997), monkeys (Fuchs and Mustari, 1993), rabbits (Baarsma and Collewij, 1974), birds (Fite, 1968; Gioanni et al., 1981; Gioanni, 1988; Eckmeier and Bischof, 2008), turtles (Fite et al., 1979), fish (Keng and Anastasio, 1997; Huang and Neuhauss, 2008) and insects such as beetles (Hassenstein and Reichardt, 1956; Hassenstein and Reichardt, 1956), locusts (Goodman, 1965; Robert and Rowell, 1992; Thorson, 1966), bees (Esch et al., 2001; Srinivasan et al., 1996; Srinivasan et al., 2000) and flies (Hecht and Wald, 1934; Kalmus, 1949; Fermi and Reichardt, 1963; Götz, 1964; McCann and MacGinitie, 1965; Götz, 1968; Eckert, 1973; Buchner, 1976; Srinivasan, 1977; Wagner, 1982; Blondeau and Heisenberg, 1982, reviewed in Reichardt and Poggio, 1976; Poggio and Reichardt, 1976; Reichardt and Poggio, 1981; Egelhaaf and Borst, 1993b; Pflugfelder and Heisenberg, 1995; Heisenberg et al., 2001). In many of these cases, autogenic optic flow is used primarily in order to adjust the visual apparatus for minimal visual slip across the retina, for example by rotating the eyes, head or body in the opposite direction to correct for involuntary deviations from the animals intended trajectory. Additionally, there is much evidence for use of autogenic optic flow for the estimation of distance from objects, for example in the peculiar peering behavior of locusts and praying mantids (Wallace, 1959; Horridge, 1986; Sobel, 1990; Kral, 1998; Kral, 2003) as well as the figure-versus-background tracking responses of flies (Virsik and Reichardt, 1976; Reichardt and Poggio, 1979)

One of the most robust and reproducible behavioral responses to optic flow patterns is the so-called optomotor response in arthropods, including insects (reviewed in Reichardt and Poggio, 1976; Wehner, 1981; Buchner, 1984; Pflugfelder and Heisenberg, 1995). This set of reflexes was extensively characterized in various species of flies (Götz, 1964; Götz, 1968;

Introduction

Blondeau and Heisenberg, 1982; Wehrhahn and Hausen, 1980; Eckert, 1973; Buchner, 1976; Buchner, 1984; Egelhaaf and Borst, 1993b): When presented with a horizontally rotating striped drum flies respond with a horizontal rotation of their body, so as to reduce the visual slip of the pattern on their retina, in a stereotypic visual stabilization reflex (Götz, 1964; Götz, 1968; Reichardt, 1969; Blondeau and Heisenberg, 1982; Collett et al., 1993). However, when presented with a different optic flow pattern, such as front-to-back motion on both sides of the fly, the fly responds with a variation of its forward thrust (Götz, 1968). Another motor behavior elicited by different optic flow patterns is the landing response (Goodman, 1960; Hyzer, 1962), triggered by image expansion in front of the fly (Braitenberg and Taddei-Ferretti, 1966; Wagner, 1982; Borst and Bahde, 1986) or by reducing the ambient light level (Taddei-Ferretti and Perez de Talens, 1973). Yet another behavior is elicited by parallax flow-fields resulting from translational flight near an object that is closer to the fly than the background; in this case the fly tends to orient itself towards the object (Virsik and Reichardt, 1976; Virsik and Reichardt, 1974; Reichardt and Poggio, 1979; Egelhaaf, 1987; Egelhaaf et al., 1988).

From these examples it is clear that different optic flow-fields arising from different flight maneuvers of the fly relative to itself and to its environment elicit different motor responses. It is important to realize in this context that discrimination between different optic flow-fields is only possible by means of global analysis of motion patterns; local motion detectors, subtending only a small part of an organism's visual field, can respond similarly to very different optic flow-fields and would therefore constitute poor discriminators (Figure 1-1). Moreover, local measurements can only detect the component of motion that is parallel to the light intensity gradient, a limitation that results in the so-called "aperture problem" (Marr and



Figure 1-1: Optic flow fields for different flight maneuvers.

The optic flow fields elicited by two different flight maneuvers are represented by red arrow vector diagrams projected on a globe which represents the visual space of the fly. Whereas the two flow-fields are clearly different when taking them into account over the entire visual space, it is difficult to tell them apart by looking at a small part of them, for example the shaded squares to the right-hand side of the fly. Figure adopted from Zbikowski, (2005)

Ullman, 1981; Adelson and Movshon, 1982; Hildreth and Koch, 1987). Theoretical approaches to solving this problem rely usually on integration over space or object contours, given a non-singular distribution of contour orientations (Marr and Ullman, 1981; Adelson and Movshon, 1982). One might therefore expect the nervous system of a visually guided animal to contain elements responsive to global or large-field optic flow-field patterns, elements that would serve as representations of these patterns in order to support flow-field discrimination on a neural level.

Indeed, the nervous systems of many organisms contain large-field neurons that are responsive to optic flow patterns generated by self-motion, including neurons in cortical areas MST (Tanaka and Saito, 1989; Duffy and Wurtz, 1991; Lappe et al., 1996; Gu et al., 2006; Britten, 2008) and VIP (Bremmer et al., 2000; Bremmer, 2005) in monkeys, the accessory optic system in all vertebrate classes (Fite, 1985; Simpson, 1984; Simpson et al., 1988; Wylie and Frost, 1999), the nucleus rotundus in pigeons (Wang and Frost, 1992), the lobula in locusts (Gabbiani et al., 2002; Gabbiani et al., 2004) and the lobula plate in flies (Krapp and

Hengstenberg, 1996; Krapp et al., 1998; Borst and Haag, 2002; Egelhaaf et al., 2002; Egelhaaf and Kern, 2002; Borst and Haag, 2007). I will next review what is known on how these neurons acquire their selectivity for optic-flow field patterns.

1.2. Local motion detection

In order for an organism to integrate motion in a global scope, it must first be able to detect motion locally. The essential requirements from any motion detector are inputs from neighboring locations in space, asymmetrical processing of these inputs, and a non-linear interaction between the two (Poggio and Reichardt, 1973; Buchner, 1984; Borst and Egelhaaf, 1989). Several models can account for local motion detection in visual systems, and these models fall into two broad categories: gradient extraction and correlation detectors (Barlow and Levick, 1965; Hildreth and Koch, 1987; Marr and Ullman, 1981; Reichardt, 1987; Torre and Poggio, 1978; Ullman, 1983 reviewed in Borst and Egelhaaf, 1993). The prevailing model for local motion detection in the fly and in other insects is a kind of correlation detector called the Reichardt detector (Hassenstein and Reichardt, 1956; Reichardt, 1961; Reichardt, 1987; Borst and Egelhaaf, 1989; Borst and Egelhaaf, 1993; Srinivasan et al., 1999), a model which embodies the essential aspects of the correlation model (Poggio and Reichardt, 1973). The correlation model of motion detection provides a good description of many motion-dependent behaviors in various species, from insects through mammals and even humans (van Doorn and Koenderink, 1982b; van Doorn and Koenderink, 1982a; van Santen and Sperling, 1984; Wilson, 1985; Nakayama, 1985; Borst and Egelhaaf, 1989; van den Berg and van de Grind, 1989; Emerson et al., 1992; Ibbotson et al., 1994; Wolf-Oberhollenzer and Kirschfeld, 1994).

1.2.1. The Reichardt detector

In the Reichardt detector (Figure 1-2), input comes from two light-sensitive channels, for example directly from photoreceptors, that are tuned to adjacent locations in space. The first channel's output is time-delayed by means of a first order RC circuit low-pass filter, and the output of this low-pass filter is multiplied by the non-delayed output of the second light sensitive channel. This results in a half-detector that is weakly selective to motion, responding strongly to motion from channel 1 to channel 2, but also weakly to motion from channel 2 to channel 1. Connecting another mirror-symmetric unit to this half-detector and subtracting the

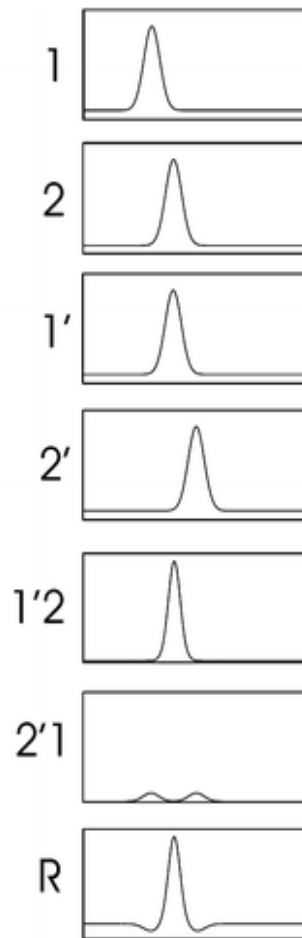
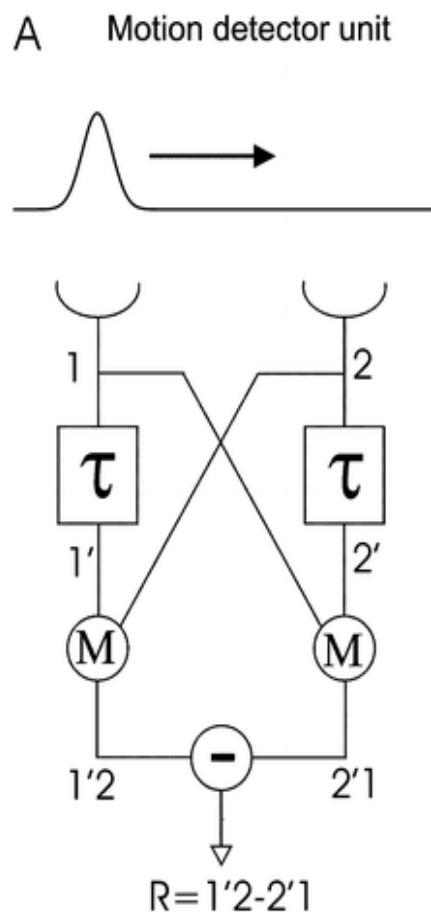


Figure 1-2: The Reichardt detector.

Left: a schematic representation of a Reichardt detector, right: responses to the motion of a spot of light from 1 to 2. The x-axis represents time from left to right. The spot of light triggers a response first in the photoreceptor 1, then with a delay in photoreceptor 2. The response from 1 is delayed by the low-pass filter τ resulting in the response $1'$ which is multiplied with the signal coming from photoreceptor 2, resulting in a strong positive response ($1'2$). The mirror symmetric unit also results in a positive response, albeit much reduced in amplitude ($2'1$). Subtracting these two signals results in a strongly directional selective response (R).

outputs of these two half-detectors results in a complete opponent-motion selective detector that responds positively to motion from channel 1 to channel 2 and negatively from channel 2 to channel 1. Thus, the full-blown Reichardt detector consists of three essential steps – temporal delay, spatial shift and multiplication, and subtraction.

1.2.2. Evidence in insects

The existence of correlation-type motion detectors in the visual system of insects was first suggested in behavioral studies of the optomotor response in the beetle *Chlorophanus*, and later in flies (Hassenstein and Reichardt, 1956; Kunze, 1961; Fermi and Reichardt, 1963; Götz, 1964; Eckert, 1973; Buchner, 1976; Buchner et al., 1978; Buchner, 1984). Subsequently, response properties characteristic of Reichardt detectors were discovered in large-field lobula plate tangential cells (LPTCs) of the fly that pool arrays of local motion detectors (see Lobula plate tangential cells below). Evidence for non-linear processing of neighboring locations in space is found both in the inversion of the optomotor response (Götz, 1964; Götz and Wenking, 1973) and of the responses of LPTCs (Zaagman et al., 1977; McCann and Arnett, 1972) when the grating's spatial frequency is smaller than twice the spacing between adjacent photoreceptors, suggesting a non-linearity that inverts the output of the spatially aliased input channels. That the underlying non-linearity is multiplicative was demonstrated by Fourier analysis of lobula plate cell responses, showing that energy is confined to the first and second temporal harmonic of the stimulus grating's contrast frequency (Egelhaaf and Borst, 1989; Egelhaaf et al., 1989b). Additional support for the existence of a multiplication step comes from the positive and

negative responses, respectively, to apparent motion stimuli consisting of luminance changes in adjacent locations with either the same sign or with opposite signs (Egelhaaf and Borst, 1992).

The subtraction step of the Reichardt detector is required to turn the weakly selective responses of the half-detectors into a strong, opponent direction-selective response (Reichardt, 1961; Borst and Egelhaaf, 1989; Borst and Egelhaaf, 1990). The existence of a subtraction step was initially indicated by experiments in which responses to apparent motion stimuli could not be explained only by a multiplicative interaction (Borst and Egelhaaf, 1990). That this step takes place on the dendrites of lobula plate tangential cells as a local interaction between excitatory, preferred-direction inputs and inhibitory, null-direction inputs was shown in experiments in which the membrane potential of tangential cells was changed, affecting the electrochemical driving force of the excitatory and inhibitory synapses. This was done either by using the cells' own response to preferred direction stimuli (Borst and Egelhaaf, 1990) or by intracellularly perturbing the membrane potentials by current injection (Borst et al., 1995). In the latter case, injection of strong negative currents resulted in the inversion of responses to null-direction motion, implying the existence of two different synaptic reversal potentials that are differentially activated by preferred- and null-direction motion, presumably excitatory and inhibitory. *In-vitro* electrophysiological studies revealed pharmacological profiles of GABAergic and nicotinic cholinergic synapses (Brotz and Borst, 1996), and immunohistological stainings in *Drosophila* confirm the existence of these synapses in the dendrites of tangential cells (Raghu et al., 2007; Raghu et al., 2009). Blockade of GABAergic synapses inverted the responses to null-direction motion from negative to positive, resulting in positive, weakly directional-selective responses to both preferred- and null-direction motion (Single et al., 1997). This demonstrated

that the interaction between null-direction inhibition and preferred-direction excitation is crucial for the emergence of strongly directional-selective responses from the weakly directional-selective inputs.

1.2.3. Response properties

An important characteristic of the Reichardt detector that derives from its mathematical structure, specifically from the spatial distance between its input channels and the time constant of the low-pass filter, is the dependence of its response on various input features such as image velocity, contrast, spatial wavelength spectrum and luminance (Reichardt, 1961; Reichardt, 1987; Borst and Egelhaaf, 1993). The Reichardt detector's dependence on contrast and luminance is a consequence of the direct multiplication of one light-sensitive channel with the non-amplified, filtered version of the other. More interestingly, the dependence of the response on the angular velocity of the stimulus is not linear, or even monotonic. Instead, for a given drifting grating, the steady-state response of a Reichardt detector will peak at a certain optimal angular velocity in which the maxima of the input signals coincide at the multiplication stage, after the temporal delay (Reichardt and Varjú, 1959). Consequently, the optimal angular velocity depends on the spatial wavelength of the grating such that the ratio between the velocity (in deg sec^{-1}) and the wavelength (in deg cycle^{-1}), i.e. the temporal frequency of the drifting grating (in cycle sec^{-1}), is constant (Reichardt, 1961; Buchner, 1984; Götz, 1964; Reichardt, 1987). Such dependence of the motion detectors on the visual features of the stimulus can be seen in the pooled, steady-state responses of large arrays of motion detectors recorded postsynaptically in LPTCs, e.g. H1 (Zaagman et al., 1978; Eckert, 1980; Reisenman et

al., 2003; Single et al., 1997; Haag et al., 2004; Borst et al., 2005; Safran et al., 2007; Srinivasan and Dvorak, 1980; Dvorak et al., 1980, last two in *Lucilia sericata*), HS cells (Egelhaaf and Borst, 1989; Egelhaaf et al., 1989a) and VS cells (Haag et al., 1992; Haag et al., 2004).

The dependence of Reichardt detectors on the visual features of their input also contains a pronounced dynamic component. When presented with a drifting sinusoidal grating, the responses of single Reichardt detectors are modulated by the local structure and features of the grating (Reichardt, 1961; Reichardt, 1987; Egelhaaf and Reichardt, 1987; Egelhaaf and Borst, 1989; Egelhaaf et al., 1989a). When presented with small-field drifting gratings that stimulate only a few motion detectors, the resulting fluctuations can be measured in the axons of LPTCs (Egelhaaf et al., 1989a; Egelhaaf et al., 1989b; Egelhaaf and Borst, 1989). In these experiments, a doubling of the temporal frequency can also be seen, another line of evidence supporting the multiplication step inherent to the Reichardt model. Similar local modulations were also measured by calcium imaging in the fine dendritic tips of LPTCs, thought to be directly postsynaptic to single local motion detectors, but not in the axons of these cells, which pool many of the small dendritic tips (Single and Borst, 1998; Haag et al., 2004). These experiments, conducted with full-field drifting gratings, highlight an important aspect of spatial integration when computing flow-field responses by large-field units. Namely, dendritic integration of many single motion detectors averages out fluctuations caused by the dependence of the motion detectors on the local structure of the visual input, resulting in a smooth representation of global motion of the presented grating (Reichardt and Guo, 1986; Egelhaaf and Reichardt, 1987; Reichardt and Egelhaaf, 1988). The idea of spatial integration of

local motion detectors to overcome local modulations was also raised in the context of complex cells in mammalian visual cortex (Movshon et al., 1978; Holub and Morton-Gibson, 1981).

Thus, the computation of flow-field responses in the fly begins with local motion detection by correlation-based Reichardt detectors and continues with the pooling of these local signals into global flow-field responses. I will next address the question of how this is thought to take place in the visual system of the fly.

1.3. The fly visual system

Light enters the fly's visual system through its compound eyes, which have a panoramic field of vision encompassing almost every direction around the fly's head. The incoming signal is then processed by four optic neuropils before it is sent downstream to motor circuits involved in the control of locomotion and posture. In the first two of these neuropils, the lamina and medulla, local motion is computed by columnar, retinotopic circuits. These circuits project the motion information in a retinotopic manner onto the next neuropil, the lobula complex, which consists of the lobula and the lobula plate. In the lobula plate these local motion signals are integrated by a population of roughly 60 neurons, the lobula plate tangential cells (LPTCs). Through the selective integration of feedforward input from the local motion detectors and the lateral interactions between different LPTCs, these neurons become selective to different optic flow-fields. This information is then projected to descending motor and pre-motor neurons.

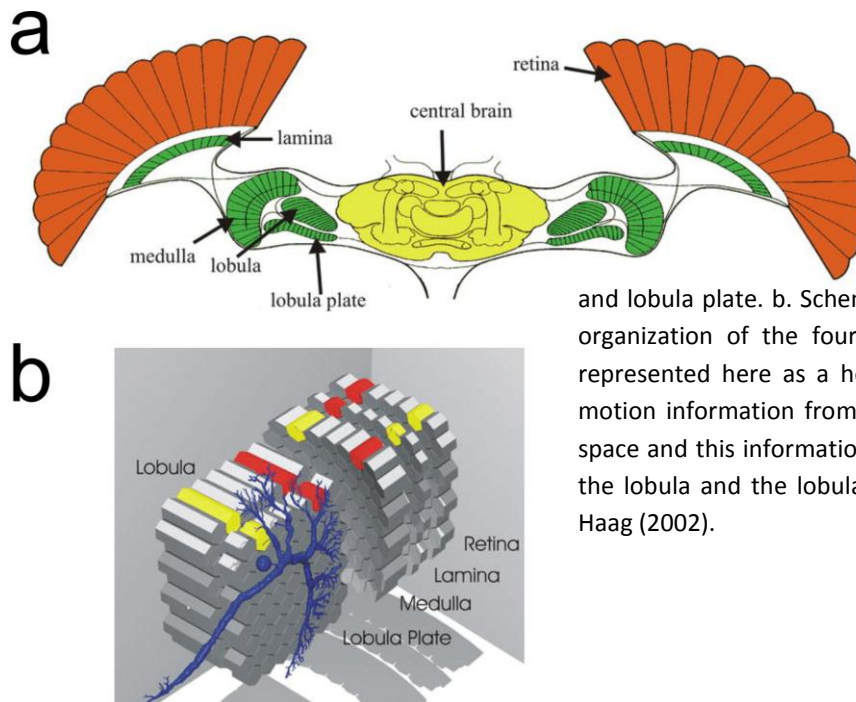


Figure 1-3: Schematic overview of the fly visual system

a. Dorsal view of the fly visual system including the retina and the four main neuropils, the lamina, medulla, lobula

and lobula plate. b. Schematic overview of the columnar organization of the four optic neuropils. Each column, represented here as a hexagonal body, computes local motion information from a small part of the fly's visual space and this information is retinotopically projected to the lobula and the lobula plate. Figures from Borst and Haag (2002).

In the following review of the fly's visual system I will refer to results from *Calliphora* as well as from other fly species such as *Drosophila*, *Musca* and *Sarcophaga*, in which the visual system seems to be largely conserved in both anatomical structure and electrophysiological responses (Buschbeck and Strausfeld, 1996; Shaw, 1989; Fischbach and Dittrich, 1989; Meinertzhagen and Sorra, 2001; Jarvilehto and Zettler, 1973; Joesch et al., 2008).

1.3.1. The compound eye

The compound eye is one of the most studied organs of insect physiology, and an essentially modern description can be found already in the landmark work of Exner (1891). As the retina is the input location for light in this system and is therefore responsible for the initial coding of this input, I will discuss it in relative detail.

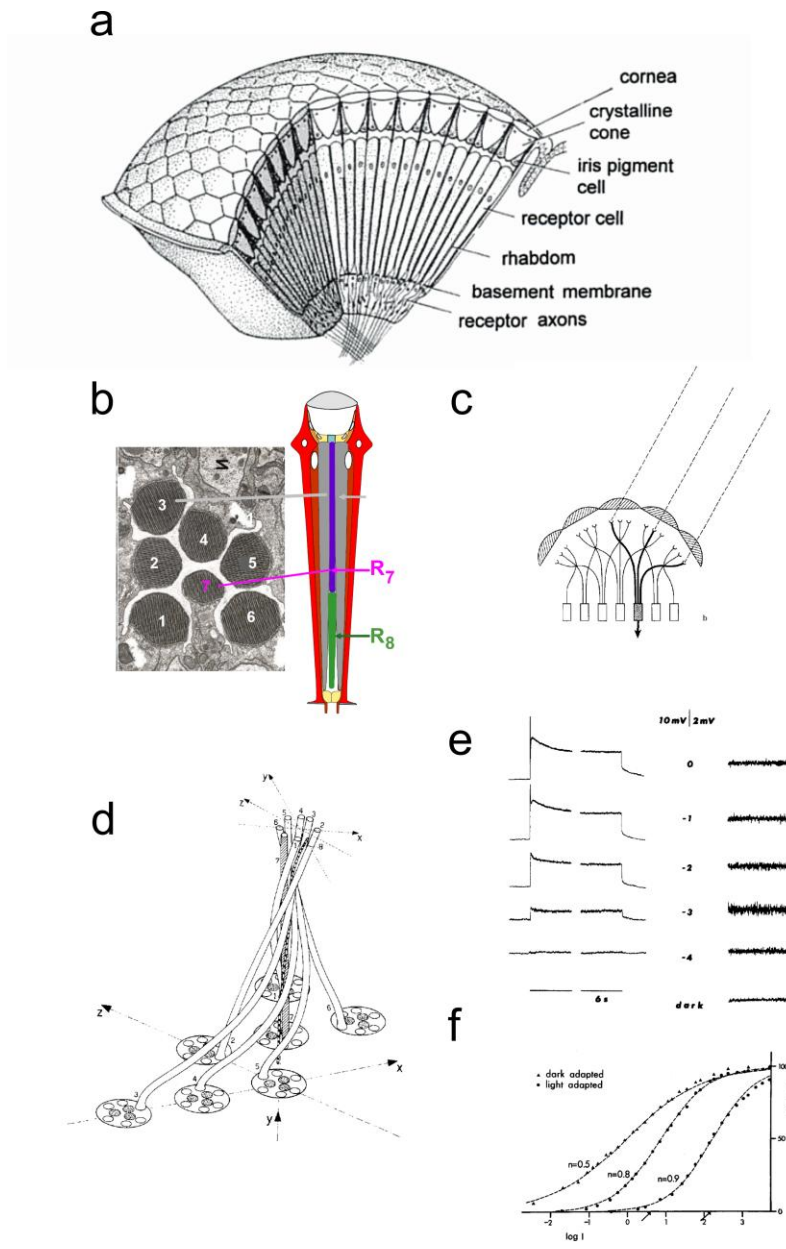


Figure 1-4: The fly retina – morphology and light responses

a. Schematic morphology of an apposition eye from Land and Nilsson (2002a), modified from Duke-Elder (1958). **b.** Left: electron micrograph of *Drosophila* photoreceptors R1-6 and R7, right: schematic of a single ommatidium with photoreceptors R1-6 (gray), R7 (purple) and R8 (green). From Silver Essay, Claude Desplan. **c.** Schematic illustration of the neural superposition principle. Different photoreceptors from adjacent ommatidia receive light from the same direction, this is subsequently pooled in the next synapse by laminar neurons (Braitenberg, 1967, after Kirschfeld, 1967). **d.** Schematic of the 180° twist to conserve retinotopy (Braitenberg, 1967), see text for details. **e.** Left: Responses of *Drosophila* R1-6 photoreceptor to different magnitude light steps, right: corresponding noise levels of the steady-state response (Wu and Pak, 1978). **f.** Log-intensity-response curves from *Calliphora*: dark-accomodated (left curve) or accommodated to light levels indicated by the arrows. From Matic and Laughlin (1981).

In the blowfly, light is captured by a lattice of ca. 5000 hexagonal lenses of receptive structures called ommatidia, that gather incoming light and focus it on the eight photoreceptors, R1-8, of the ommatidium (Figure 1-4a). The resulting spatial resolution in calliphorid flies is about 1-2°, limited mainly by diffraction resulting from the small lenses (20-30 µm radius depending on position within the eye) as well as by the geometry of the lens-photoreceptor arrangement (Smakman et al., 1984; Land and Eckert, 1985, reviewed in Land,

1997). The resulting spatial separation is ca. 120 times worse than that of human fovea (1° compared to $0.5'$ Land, 1997). Perhaps with the exception of redundancy and robustness to damage, it is still unclear why this particular visual adaptation persisted despite obviously superior optical designs such as the single-lens design that exists in the larval and dorsal ocelli (for a discussion of the benefits of the single-lens design see Land, 1997; Land and Nilsson, 2002b). Nevertheless, it seems that this structure underwent structural adaptations to make it a better input device for flow-field analysis. Specifically, the increase of the intra-ommatidial angles along the frontal-lateral axis (Braitenberg, 1967) is thought to deal with the larger retinal velocity, and hence larger temporal smear, of lateral flow-field components during forward flight (Land and Eckert, 1985; Land et al., 1989; Petrowitz et al., 2000). Similarly, the changes in the angle of alignment of the rows of ommatidia is also thought to be an adaptation towards flow-field analysis (Petrowitz et al., 2000; Egelhaaf et al., 2000).

Fly eyes, and dipteran eyes in general, are of the so-called neural superposition type. As in regular apposition eyes, each single ommatidium is an optically separated light channel. However, unlike apposition eyes, in a neural superposition eye the eight photoreceptors within a single ommatidium are aligned to seven different optical axes – R7 and 8 occupy the center channel, and R1-6 the surround (Kirschfeld, 1967). Thus, the six photoreceptors R1-6 from six neighboring ommatidia (Figure 1-4b) are aligned to the same optical axis and view the same point in the fly's visual space (Figure 1-4c).

The axons of these photoreceptors are pooled together in the next neuropil, the lamina (Trujillo and Melamed, 1966; Braitenberg, 1967). Pooling is mediated both by chemical

Introduction

synapses on the lamina and by gap-junction coupling between the axons of photoreceptors (Ribi, 1978). In order to maintain spatial contiguity after the inversion of the image by each one of the facet lenses, this axonal pooling requires a 180° twist of the photoreceptor axons before they synapse on their partners in the lamina (Figure 1-4d; reviewed in Fischbach and Hiesinger, 2008).

At low light intensities, the R1-6 photoreceptors respond with unitary “bumps” to single photons. At higher intensities these bumps fuse into a noisy graded depolarization in response to light steps (Figure 1-4e; Laughlin and Hardie, 1978; Wu and Pak, 1978). The depolarization magnitudes can be fitted by a sigmoid function $V/V_{\max} = I^n / (I^n + \sigma)$, where I is the light intensity and n and σ are parameters that depend on the light adaptation state of the photoreceptors (Figure 1-4f; Matić and Laughlin, 1981). In the $\log I/V$ graphs these sigmoidal curves have a relatively large log linear region spanning about 2 log units around the adaptation light, in which the response function can be treated as logarithmic (Hardie, 1984). The resulting image that is transmitted to the lamina is therefore a retinotopic, pixelated one, where each pixel is provides a log-luminance encoding to its partners in the next neuropil, the lamina.

The pathways that mediate color and motion vision are separate; monochromatic information from R1-6, and not polychromatic information from R7/8, is important for motion detection. This is evident from the absent optomotor response in R1-6 deficient *Drosophila* mutants compared to a normal response in R7 and R7/8 deficient mutants (Heisenberg and Buchner, 1977; Yarnaguchi et al., 2008), as well as from the necessity of the laminar L1 and L2 cells, post-synaptic to R1-6 but not to R7/8, for the optomotor response (Rister et al., 2007).

1.3.2. The lamina

Much is known about the cellular and synaptic arrangement of the lamina and its projections from electron microscopy and genetic labeling. Laminar neurons are grouped into retinotopic columns, “cartridges”, each containing five principle neurons, the laminar monopolar cells L1-5 (Meinertzhagen and Oneil, 1991; Meinertzhagen and Hanson, 1993; Meinertzhagen and Sorra, 2001). Of these, the L1 and L2 neurons are the only neurons necessary for motion vision (Rister et al., 2007). In each cartridge, the L1, L2 and L3 neurons

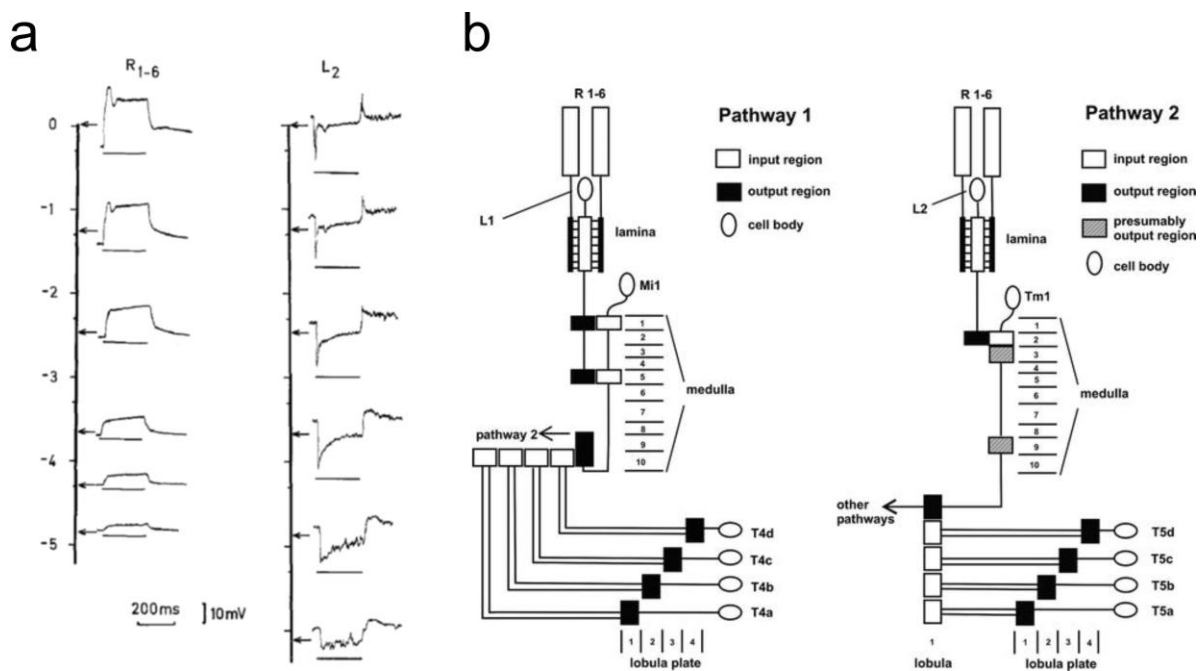


Figure 1-5: The two motion detection pathways in the lamina

a. Comparison of membrane potential responses in *Calliphora* R1-6 photoreceptors and L2 laminar monopolar cells to light intensity steps, highlighting the high-pass filtering characteristic of this synapse (from Jarvilehto and Zettler, 1973). b. Schematic of the two motion detection pathways that separate in the lamina and their downstream components in the medulla, with projections to the lobula plate (modified from Bausenwein et al., 1992) – the Mi1 neuron might correspond to iTm neurons from later work (Strausfeld and Lee, 1991; Douglass and Strausfeld, 1995; Douglass and Strausfeld, 1996).

Introduction

and the amacrine cell amc receive input from single R1-6 photoreceptors (Meinertzhagen and Hanson, 1993), a different photoreceptor from each of six adjacent ommatidia (Figure 1-4f) (Braitenberg, 1967). The histaminergic R1-6-to-L1/2 synapses are inverting (Järvilehto and Zettler, 1971) and have a high-pass characteristic, especially at high luminance (Figure 1-5a; Järvilehto and Zettler, 1973; Coombe et al., 1989) which might be important in the initial filtering stage of motion detection, thought to take place in this neuropil. This interpretation of the role of the lamina in motion detection is also supported by the failure to find any directionally selective responses to motion in the lamina.

In the lamina, the motion processing pathway diverges into two pathways, the L1 pathway and the L2 pathway (Strausfeld, 1984; Bausenwein and Fischbach, 1992). These two pathways are thought to have different contributions to motion processing, for example the L2 pathway participates exclusively in rotation, not translation, responses in walking flies (Katsov and Clandinin, 2008), and the two pathways give rise to different optomotor responses under different pattern contrast conditions (Rister et al., 2007). The L1 neurons project to Mi1 neurons in layers M1 and M5 of the medulla, and the L2 neurons to Tm1 neurons in layer M2 of the medulla (Figure 1-5b).

In the lamina, a few examples of lateral interactions between neighboring light-sensitive channels are known. A short-range form of lateral inhibition was described in the lamina and is thought to explain the sharpening of the receptive fields of laminar monopolar cells relative to their photoreceptor inputs (Zettler and Järvilehto, 1972). This might be the result of ephaptic interactions between photoreceptors which result in the inhibition of adjacent photoreceptors

in the same ommatidium, although contribution of these interactions to the net output of the photoreceptors has not been quantified (in locusts: Shaw, 1975). In the context of motion detection, information must be conveyed laterally between adjacent laminar cartridges in order to temporally compare neighboring parts of the visual field over time. The L4 small monopolar neurons are considered prime candidates for this function, providing reciprocal collaterals to adjacent retinotopic columns (Strausfeld and Campos-Ortega, 1973; Braitenberg and Debbage, 1974). A similar role was also suggested for the amacrine cell and T1 neuron as an asymmetrical delay line between L2 cells in different cartridges (Douglass and Strausfeld, 1995, reviewed in (Douglass and Strausfeld, 2003).

1.3.3. The medulla

The medulla receives projections from laminar monopolar cells as well as directly from the R7/8 photoreceptors of the color pathway. The L1 monopolar cells terminate in layers m1 and m5 and contact the intrinsic medullary cell Mi1 (Bausenwein et al., 1992, iTm in Strausfeld and Lee, 1991; Douglass and Strausfeld, 1995; Douglass and Strausfeld, 1996)), which contacts the motion-sensitive, weakly directionally-selective T4 cells in layer m10. These cells are thought to synapse on lobula plate tangential cells (Strausfeld and Lee, 1991). The L2 monopolar cells project to the m2 layer where they contact the transmedullary Tm1 cells, which project to the T5 cells in the lobula. T5 cells are strongly directionally selective and project to the lobula plate.

Two lines of evidence indicate that the two local motion processing pathways first result in motion-sensitive responses in the medulla. In *Drosophilla*, labeling with radioactive 2-deoxy-

Introduction

glucose shows that different layers of the medulla are labeled when the fly is presented with motion and when it is presented with a full-field flicker in the same temporal frequency (Buchner et al., 1984; Bausenwein and Fischbach, 1992). These activity patterns fit well with the anatomical tracing of the motion-detection L1 and L2 pathways, and the schematic summary of these combined results is shown in Figure 1-5b. More evidence comes from recordings of membrane potentials in medullary neurons, in which motion-sensitive cells have been reported (DeVoe, 1980; Douglass and Strausfeld, 1995; Douglass and Strausfeld, 1996). Both the Tm1 neurons from the L2 pathway and the iTm neurons from the L1 pathway show sustained responses to motion, although a comparison with flicker stimuli of the same frequency is lacking. However, there is very scant evidence for the emergence of directionally-selective responses at this level. The above mentioned T4 cells have qualitatively different responses to different directions of motion, however quantifying this effect has resulted in only very weak direction selectivity (Douglass and Strausfeld, 1996). Recordings in Tm1 cells show a directionally selective frequency doubling, suggesting a non-linear, perhaps multiplicative interaction, but the source of this doubling is still unclear (Douglass and Strausfeld, 1995). Although strongly directionally-selective responses have been recorded in the medulla, these are of centrifugal cells such as CY2 (Douglass and Strausfeld, 1996) and Y18 (Douglass and Strausfeld, 1998), projecting from the lobula plate to the lobula and the medulla.

The paucity of physiological data from medullary cells makes it difficult to construct a functional model of the retinotopic columns and the lateral interactions between them in this neuropil (but see Higgins et al., 2005). However, there are some initial results pointing in the direction of possible lateral interactions in the medulla. Specifically, the M7 layer is labeled by

2-DG when presenting a moving single stripe, but not a grating, in *Drosophila*, suggesting lateral interactions that result in differential responses to full-field and small-field gratings (Bausenwein and Fischbach, 1992). A clearer indication comes from a motion-sensitive (but not direction-selective) medullary neuron that seems to have a center-surround receptive field characteristic of a lateral inhibition architecture (DeVoe, 1980). Lateral connections were also found in Golgi staining of the medulla, the most interesting of which is the GABAergic deep medulla amacrine cell (Douglass and Strausfeld, 1996, m:tan5 in Strausfeld, 1970). This cell spans several adjacent columns in the projection layer of Tm1 and iTm, and is speculated to participate in the lateral interactions that underlie motion detection.

1.3.4. The lobula

The anterior part of the lobula complex, the lobula, consists of six layers (Fischbach and Dittrich, 1989), of which three are labeled by 2-deoxy glucose when the fly is presented with motion stimuli (Buchner et al., 1984). The transmedullary Tm1 neurons project from the medulla to the posterior layer of this neuropil, where they contact the directionally selective bushy T5 neurons (Douglass and Strausfeld, 1995; Douglass and Strausfeld, 1996). Different T5 cells project exclusively to the four different layers of the lobula plate which contain tangential cells selective for the four main axes of motion (Strausfeld, 1976).

1.3.5. The lobula plate

The lobula plate is a flat structure on the posterior side of the lobula complex, and is home to a group of large cells known as lobula plate tangential cells (LPTCs), a subset of which

Introduction

are the focus of my work (Pierantoni, 1976; Hausen, 1976; Hausen, 1982a; Hengstenberg et al., 1982, reviewed in Hausen and Egelhaaf, 1989; Borst and Haag, 2002; Egelhaaf et al., 2002; Borst and Haag, 2007). LPTCs are thought to be a cardinal part of the optomotor response circuitry of the fly, based on a number of important observations, most importantly the shape of their receptive fields and directional selectivity (see next section). Information about local motion, computed by the neurons in the lamina and the medulla, is retinotopically projected as a map of the fly's ipsilateral visual space onto the lobula plate, as was shown by calcium imaging studies in lobula plate tangential cells (Borst and Egelhaaf, 1992; Egelhaaf and Borst, 1995; Durr and Egelhaaf, 1999; Borst and Single, 2000).

The lobula plate is divided into four layers, each containing the dendrites of different LPTCs, as well as other output elements of the lobula plate. LPTCs ramifying in different layers of the lobula plate are sensitive to different directions of motion (Braitenberg, 1972 - *Drosophila*, Dvorak et al., 1975; Pierantoni, 1976; Hausen, 1977; Eckert, 1982; Hengstenberg et al., 1982 - *Calliphora*), giving rise to the idea that four separate retinotopic motion input maps project onto the lobula plate. This idea was corroborated by 2-deoxy glucose labeling experiments, in which motion stimuli in four different directions resulted in labeling of four different layers in the lobula plate (Buchner et al., 1984).

Directionally selective input to the lobula plate is most likely to be supplied at least in part by the bushy T-cells, the medullary T4 and the lobular T5 neurons. These neurons come in four "flavors", each of which stratifies in a different directionally selective layer of the lobula plate, making them good candidates for the four cardinal directions for which LPTCs are

selective (Strausfeld, 1984; Fischbach and Dittrich, 1989; Strausfeld and Lee, 1991). However, direct evidence for contact between the bushy T-cells and LPTCs is lacking – only a single example of a contact between a T4 cell and a LPTC was ever shown (Strausfeld and Lee, 1991), and no such demonstration was made for T5 cells.

The flat and superficial structure of the lobula plate and the large diameters and two-dimensional morphology of the LPTCs makes them relatively easily amenable to a variety of experimental techniques. These include various wide-field optical techniques such as in-vivo calcium imaging (Borst and Egelhaaf, 1992; Single and Borst, 1998; Durr and Egelhaaf, 1999), laser ablation (Warzecha et al., 1992; Warzecha et al., 1993; Farrow et al., 2003; Farrow et al., 2005; Kalb et al., 2006) and UV flash photolysis of caged calcium (Kurtz, 2004; Kurtz, 2007) as well as intra- and extracellular electrophysiological recordings using glass micropipettes (Dvorak et al., 1975; Haag et al., 1997; Haag and Borst, 2004) and tungsten electrodes (Bishop and Keehn, 1966; Eckert, 1980; Bialek et al., 1991; Steveninck et al., 1997), along with less frequently used ablation techniques such as ablation of precursor cells in the larva (Geiger and Nässel, 1981) and targeted microsurgical lesions (Hausen and Wehrhahn, 1983; Hausen and Wehrhahn, 1990). Pharmacological agents such as synaptic agonists and antagonists and channel blockers can also be relatively easily applied to the lobula plate (Warzecha et al., 1993; Brotz and Borst, 1996; Haag et al., 1997).

1.4. Lobula plate tangential cells

In each hemisphere of the fly brain, around 60 uniquely identifiable lobula plate tangential cells pool the incoming signals from the retinotopic array of local motion detectors with their dendrites. The LPTCs process this information both intracellularly within single neurons, and by an extensive network of ipsilateral and heterolateral interactions, before projecting the processed information towards downstream motor circuits. LPTCs respond to visual motion either by graded deflections of their membrane potentials (CH cells), by modulation of their spiking frequency (H1-6, V1-3), or both (HS cells, VS cells, FD cells). LPTCs are categorized by their primary direction selectivity either as selective to horizontal motion (HS, CH, H and FD cells) or vertical motion (VS and V cells), although their motion selectivity in different parts of their receptive fields are more complex. LPTCs acquire their receptive fields by the combined effects of feedforward motion detector input and lateral interactions between LPTCs.

1.4.1. Lobula plate tangential cells and optic flow integration

The lobula plate tangential cells are widely believed to be part of the fly's optomotor response circuitry, implementing the visual motion integration step required for optic flow analysis. LPTCs are ideally situated directly downstream of the local motion detection circuitry in the preceding neuropils, allowing them to integrate the output of these motion detectors and thereby control the post-synaptic motor circuits.

Although still short of a direct corroboration, a number of experiments have accumulated a large body of indirect evidence to this effect. Ablation of HS and VS cell precursors in *Musca* larvae results in reduced optomotor responses to front-to-back motion on the ablated side of the animal (Geiger and Nässel, 1981), and similarly, *Drosophila optomotor-blind*^{H31} mutants in which the entire lobula plate structure is missing lack a walking and tethered flight optomotor response almost completely, compared to the wild-type (Heisenberg et al., 1978; Blondeau and Heisenberg, 1982). Microsurgical lesions that sever the projection pathways of several LPTCs in the protocerebrum result in marked alterations of the optomotor response in *Calliphora* (Hausen and Wehrhahn, 1983; Hausen and Wehrhahn, 1990), and finally, electrical stimulation of different areas in the lobula plate in the absence of visual stimulus results in reproducible yaw, lift and landing responses, similar to those elicited by moving gratings (Blondeau, 1981). However, each of these results, taken on its own, lacks specificity; in the ablation experiments, it is not known what cells other than the LPTCs were ablated in the adult. Similarly, in the microsurgical lesions, other neuronal projections may have been severed as well, or entire neurons killed due to the lesion. In the *optomotor-blind*^{H31} mutant the whole lobula plate structure is missing, which might result in the absence of many other, non-tangential lobula plate neurons, and other structures might be missing from other visual lobes as well. The electrical stimulation experiments also suffer from non-specificity, as the current injections are extracellular and therefore could de- or hyper-polarize cells other than LPTCs.

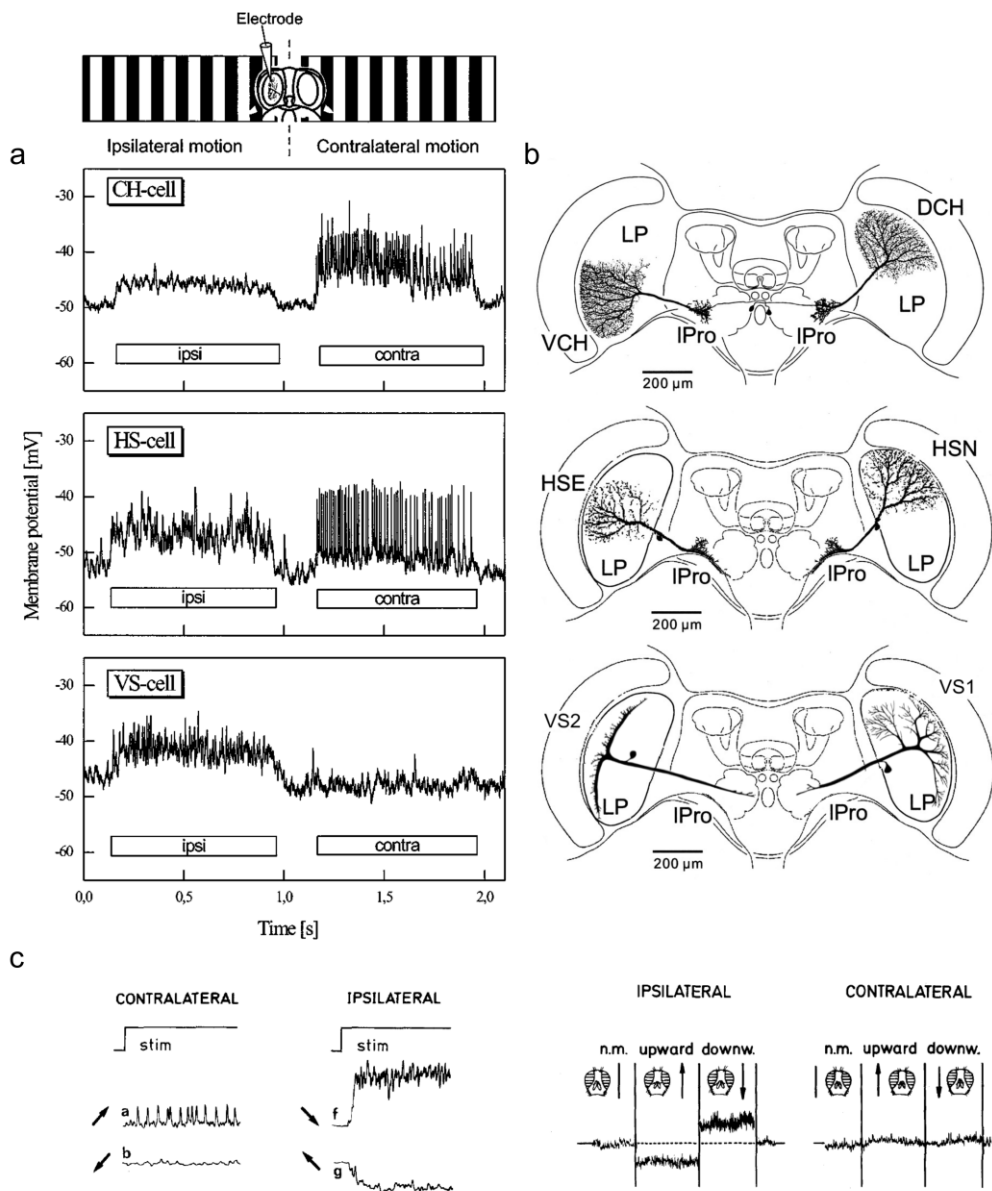


Figure 1-6: Lobula plate tangential cells

(a) Example responses of LPTCs to preferred direction motion on the ipsilateral (first stimulus) and contralateral sides (second stimulus). Top: CH cell, middle: HS cell, bottom: VS cell. Adapted from Haag et al. (1999) (b) Camera lucida tracings of vCH and dCH, HSE and HSN, and VS1 and VS2 cells, with outlines of the fly's brain anatomy. LP – lobula plate, IPro – lateral protocerebrum. Adapted from Krapp et al. (1998; 2001). (c) Responses of an HS cell to gratings drifting in the preferred (upper traces) and null direction (lower traces), on the ipsilateral (right traces) or contralateral (left traces) side. Taken from Hausen (1982b). (d) responses of a frontal VS cell to gratings drifting in the preferred (downward) and null direction (upward), on the ipsilateral (left traces) or contralateral side (right traces). Adapted from Eckert and Bishop (1978).

The most convincing evidence for the participation of LPTCs in the optomotor response is the close agreement between response properties of LPTCs and properties of the optomotor response. Although this is by no means direct evidence, the quantitative and qualitative concurrence is too good to be written off as coincidental or just correlative. The most convincing case was made for the horizontal, output neuron HSE by Hausen. This neuron's responses were shown to be dependent on parameters of the moving grating such as temporal frequency, mean luminance, and spatial position in a way astonishingly similar to the dependence of yaw torque response on these parameters (Hausen, 1977; Hausen, 1981; Hausen, 1982b; Hausen and Wehrhahn, 1989). Moreover, HSE responses are almost independent of stimulus size (Hausen, 1982b), as are the yaw torque responses (Reichardt et al., 1983). The range of the contrast dependency of VS cells is also in close agreement with various optomotor responses (Hengstenberg, 1982), although here it is more difficult to associate the responses of single VS cells with a single optomotor behavior (but see, e.g., Srinivasan, 1977). Such similarities are also found in the responses of the H1 neuron, however this neuron is not an output element of the lobula plate and cannot be considered to be in direct control of downstream elements of the optomotor response circuitry (McCann and Foster, 1971; Zaagman et al., 1977; Eckert, 1980). Another similarity found here is the aforementioned reversal of responses to grating motion both in the H1 neuron and in the optomotor reflex when the spatial wavelength of the grating is between the ommatidial sampling distance and twice that distance (Götz, 1964; Götz and Wenking, 1973; Zaagman et al., 1977; McCann and Arnett, 1972).

Introduction

As mentioned before, in order for a system to evaluate and more importantly differentiate optic flow patterns, two conditions must be met by LPTCs: first, receptive fields of LPTCs must be large in order to implement the integration necessary for large-field motion integration, averaging-out of fluctuations caused by the dependence of the motion detectors on local input features, and avoiding the aperture problem. Second, these receptive fields are required to fit behaviorally relevant optic flow patterns in order to be able to generate the behavioral responses (Franz and Krapp, 2000; Krapp, 2000). This means that in a single optic flow detector, different direction selective responses from different parts of the fly's visual space need to be selectively "bound" together so as to correspond to a particular optic flow field and to be selective to it. I will next review the known neurons that perform this type of selective integration in the lobula plate, with emphasis on the VS cells which are in the focus of my work.

1.4.2. HS cells

The Horizontal system consists of 3 neurons for each hemisphere – the dorsal HSN, medial HSE and ventral HSS (Eckert, 1978; Eckert, 1981; Hausen, 1982a; Hausen, 1982b). HS cell dendrites ramify in the anterior (deeper), horizontal-selectivity layer of the lobula plate, and the cells respond to large-field, horizontal motion with graded membrane potential deflections, positive for front-to-back motion and for back-to-front motion; preferred direction responses are superimposed by pseudo-spikes (Figure 1-6). HSN and HSE cells also respond to motion in the contralateral side with spikelets, triggered by spikes in H1 and H2 neurons (Hausen, 1977; Hausen, 1984; Hausen, 1981; Haag, 1994; Haag et al., 1999; Horstmann et al., 2000; Haag and

Borst, 2001). Although this response was initially considered to have little effect on the average membrane potential of HS cells (Hausen, 1977; Hausen, 1981), contralateral input to HS cells (and CH cells, see below) seems to have a pronounced effect on the calcium levels in these cells, suggesting that these interactions are significant (Egelhaaf et al., 1993). HS cells receive acetylcholine and GABA input from local motion detectors, and are thought to be both output elements of the lobula plate (Hausen et al., 1980) and to supply information through lateral interactions to other LPTCs such as ipsilateral CH cells (Haag and Borst, 2002; Farrow et al., 2003) and the contralateral H2 (HSE only, Farrow et al., 2006).

1.4.3. CH cells

The lobula plate contains two Centrifugal Horizontal (CH) cells, the dorsal dCH and the ventral vCH (Eckert and Dvorak, 1983). Their dendrites also populate the anterior, horizontal-selectivity layer of the lobula plate, and are both pre- and post-synaptic in the lobula plate and post-synaptic in their protocerebral ramification (Gauck et al., 1997). Based on monoclonal antibody staining, it is known that CH cells are GABAergic, and therefore probably supply inhibitory output both in the protocerebrum and in the lobula plate (Meyer et al., 1986). Their ipsilateral input arrives at the lobula plate dendrite (Egelhaaf et al., 1993), but rather than being directly activated by local motion detectors, they receive their input from HS cells via dendro-dendritic gap junctions (Haag and Borst, 2002; Farrow et al., 2003). CH cells respond to ipsilateral horizontal motion with graded deflections of their membrane potential, and have the same preferred direction as HS cells, front-to-back. The cells also respond to contralateral horizontal motion with spikelets triggered by spikes in the contralateral H1 and H2 cells

Introduction

(Hausen, 1977; Hausen, 1984; Hausen, 1981; Eckert and Dvorak, 1983; Haag, 1994; Haag et al., 1999; Horstmann et al., 2000). The contralateral input arrives both at the dendrite and at the protocerebral axon terminal (Egelhaaf et al., 1993), from the contralateral H1 and H2 cells, respectively (Haag and Borst, 2001). V1 also supplies excitatory contralateral input to vCH, but not dCH cells, most probably at the protocerebral terminal (Haag and Borst, 2003). The unidentified Hu cell supplies contralateral inhibitory input to CH cells, most likely also in the protocerebrum.

1.4.4. FD cells (CI cells)

A set of at least 4 different cells called Figure Detection (FD) cells respond selectively to ipsilateral small-field motion and are inhibited by large field motion from both the ipsilateral and contralateral side (Egelhaaf, 1985b; Gauck and Borst, 1999). Not much is known about these cells, but it is thought that they receive ipsilateral input from local motion detectors, and that they are inhibited by GABAergic input from CH cells, probably on their dendrite in the lobula plate (Warzecha et al., 1993; Gauck et al., 1997). Whether or not the FD and CI cells reported in these two studies represent the same cells, these cells are the only small-field selective elements described in the lobula plate, and are therefore thought to participate in the object fixation behavior, in which tethered flies turn towards the position of a small-field stimulus (Egelhaaf, 1985a; Hausen and Wehrhahn, 1989).

FD cells acquire their small-field sensitivity by a combination of large-field selective excitatory responses to horizontal motion and large-field inhibitory responses to the same motion, mediated by CH cells (Warzecha et al., 1993). However, it is still unclear whether the

inhibitory and excitatory signals are dendritically pooled before inhibiting the FD cell, or whether they remain spatially distributed on the dendrite of the FD cell itself. Initial models favored the former interpretation, with different size dependencies of the inhibition and excitation responsible for the emergence of small-field selectivity (Reichardt et al., 1983; Egelhaaf, 1985c). An important drawback of these pooled models is that a pooled signal has less degrees of computational freedom; it will necessarily confound size dependence with dependence on contrast, speed and spatial wavelength. A more recent model considers a distributed, local interaction on the dendrites of the FD cell between the inhibitory input from the CH cell dendrites and the local motion input. According to this model, the activity pattern on the HS cell dendrite is passed on to the CH dendrite via dendro-dendritic gap junctions, resulting in a spatially low-pass filtered (“blurred”) image on the CH dendrite (Egelhaaf et al., 1993; Durr and Egelhaaf, 1999; Haag and Borst, 2002). The blurred, inhibitory signal from the CH cell dendrite is then subtracted from the non-blurred local motion detector input on the FD cell’s dendrite, resulting in motion edge enhancement and small-field selectivity (Cuntz et al., 2003; Hennig et al., 2008).

1.4.5. Bilateral spiking cells – H cells and V cells

A network of bilateral, spiking LPTCs that connect the lobula plates of both hemispheres has been described in relative detail, together with their interactions with other ipsilateral LPTCs. The spiking cells respond to motion with full-blown spikes, presumably necessary to conduct their signal to the contralateral hemisphere. They are either horizontally- or vertically-sensitive (H- and V-cells respectively), and were the first recorded LPTCs (Bishop and Keehn,

Introduction

1966). There are at least six H-cells, H1-6, and two V-cells, V1-2, and the best characterized of these are H1, H2 and V1 (Hausen, 1977; Hausen, unpublished). Another horizontal cell, Hu, is known only from the inhibitory post-synaptic potentials it triggers on CH cells, but its morphology is not known and it might be one of the H3-6 cells.

H1 and H2 receive dendro-dendritic inhibitory GABAergic input from ipsilateral CH cells (Hausen, 1981; Horstmann et al., 2000; Haag and Borst, 2001). The H1 and H2 cells are coupled in their dendrites to the dendrites of VS1, since depolarizing and hyperpolarizing currents injected into the latter cause a rise and fall in the spiking rates of the former (Haag and Borst, 2003). Injecting current into VS2 and VS3, however, does not affect the spiking rate of H1 and H2 (Haag and Borst, 2003), a surprising result considering the electric coupling of VS2 and VS3 with VS1 (see 1.5 below). The V1 cell is postsynaptic to VS1-3 (Krapp et al., 2001; Kurtz et al., 2001; Haag and Borst, 2003), and this contact is mediated by electrical coupling to VS1 (Haag and Borst, 2008), possibly also to VS2 and VS3, although coupling with the latter two cells cannot be distinguished from coupling of VS2 and VS3 to VS1 and that of VS1 to V1 (see below). V1 is presynaptic to the contralateral vCH cells (Krapp et al., 2001; Haag and Borst, 2003) and to the contralateral VS1 (Haag and Borst 2008). The horizontal H1 and H2 and Hu cells, together with the vertically sensitive V1 cell and the unilateral CH, HS and some VS cells, participate in an elaborate bilateral network of interactions which combines information from both eyes to achieve selectivity for yaw rotational flow-fields over thrust translational flow-fields (Horstmann et al., 2000; Hausen, 1981; Haag and Borst, 2001; Krapp et al., 2001; Haag and Borst, 2003; Farrow et al., 2006).

1.4.6. VS cells

The ten neurons of the *Calliphora* Vertical System (VS cells) are T-shaped cells comprised of a horizontally oriented axon and a single, main dendrite spanning the length of the lobula plate in a dorso-ventral strip, from which smaller dendrites branch off (Braitenberg, 1972; Dvorak et al., 1975; Pierantoni, 1976; Hausen, 1976; Bishop and Bishop, 1981; Hengstenberg et al., 1982; Hausen, unpublished; Figure 1-7a). The dendrites of the VS cells span the lobula plate in a tessellated, partially overlapping manner, and receive acetylcholine and GABA input from local motion detectors (Brotz and Borst, 1996; Raghu et al., 2007; Raghu et al., 2009). VS cells respond primarily to ipsilateral large-field, vertical motion by graded deflections of their membrane potential – depolarization for motion in the downward, preferred direction and hyperpolarization for upward, null direction motion. Most pronouncedly in the VS1 neuron, these graded potentials are superimposed by pseudo-spikes – discrete but not full-blown action potentials (Dvorak et al., 1975; Eckert and Bishop, 1978; Soohoo and Bishop, 1980; Hengstenberg, 1982; Haag et al., 1999; Figure 1-6d)¹. All VS cells extend their dendrites into the posterior, vertical-selectivity layer of the lobula plate. The more lateral and medial VS cells (VS1 and VS6-10), also have dendritic ramifications in the anterior, horizontal-selectivity layer (Figure 1-7a; Hengstenberg et al., 1982; Hausen, unpublished). Based on this, it was suggested that these cells are not simply selective for vertical motion, but have complex receptive fields that respond to motion in different directions within different parts of their receptive fields (Hengstenberg et al., 1982). This was in agreement with preliminary results which showed that

¹ To avoid confusion I will refer to action potentials which are not fully blown as ‘pseudo-spikes’, and to excitatory post-electrical synaptic potentials, i.e. spikes in a presynaptic neuron that are transmitted via an electrical synapse, as ‘spikelets’ (see, e.g., Schmitz et al., 2001)

Introduction

VS cells are selective for rotational flow-fields (Hengstenberg and Hengstenberg, 1980; Hengstenberg, 1981), but it was only a decade and a half later that the receptive fields of VS cells were fully characterized over the entire visual space of the fly by intracellular measurement of the local preferred direction and the local motion sensitivity (Krapp and Hengstenberg, 1996; Krapp et al., 1998; Figure 1-7b). These results demonstrated that VS cells

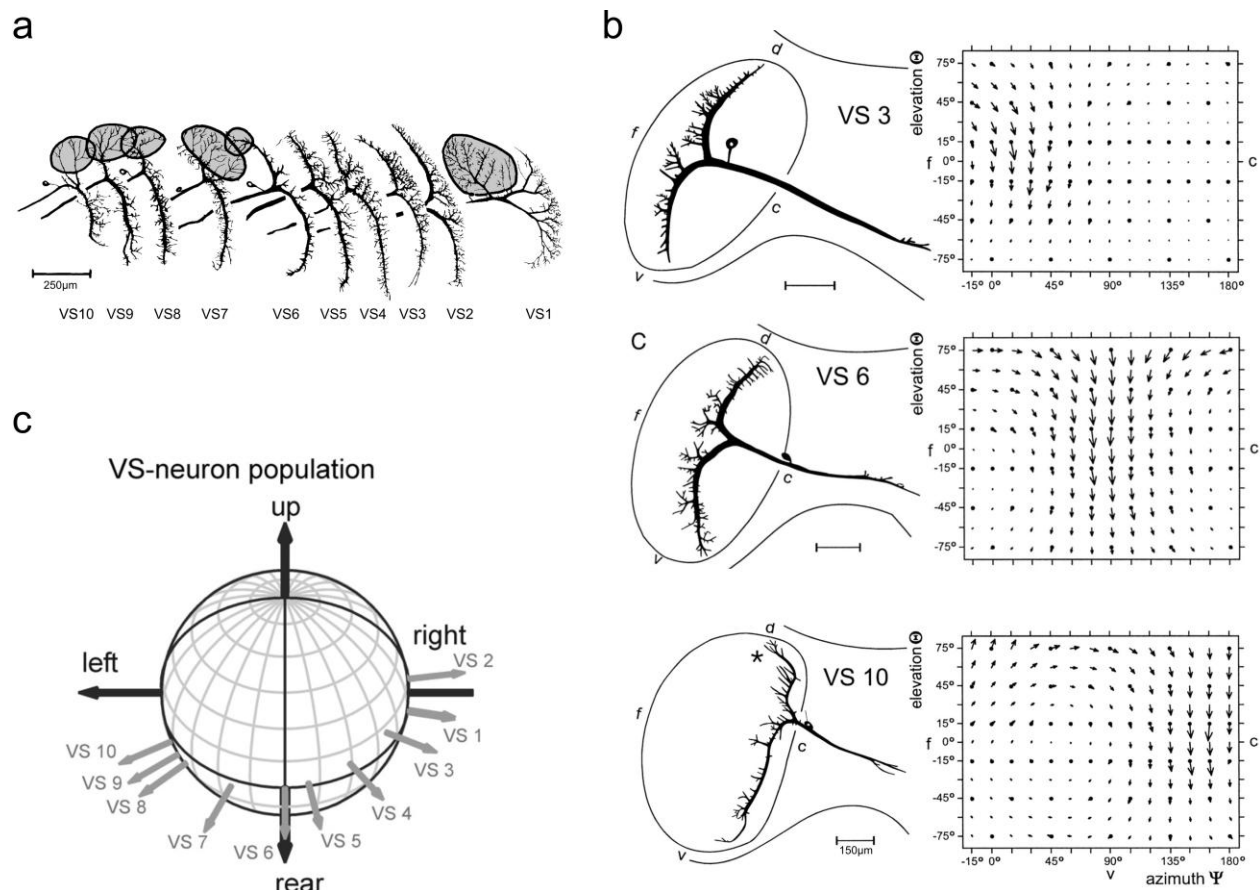


Figure 1-7: VS cells and their receptive fields

(a) Dendrites of the ten VS cells. Shaded areas indicate dendritic arborizations in the anterior, horizontal-selectivity layer of the lobula plate. Modified from Hengstenberg et al. (1982). (b) Examples of three VS cells. Left – camera lucida reconstructions, right – local sensitivity and directional preference, represented as the length and direction of the arrows, respectively. Adapted from Krapp et al. (1998). (c) Estimated preferred axes of rotation for all VS cells of one hemisphere. Adapted from Karmeier et al. (2005a).

respond to visual flow fields arising from horizontal-axis ego-rotations: rotation of the fly around different horizontal axes centered at its own body; essentially pitch, roll and all combinations thereof. Each VS cell has a different axis of preferred rotation, and the set of ten VS cells span an entire hemisphere with their preferred axes of rotation (Figure 1-7c).

VS cells receive retinotopic input from local motion detectors in their dendrites (Borst and Egelhaaf, 1992), and are electrically coupled to neighboring VS cells (Haag and Borst, 2004; see 1.5 below). An inhibitory loop was found in the latter study between lateral VS cells (probably VS1) and medial VS cells (VS7-10), and vice versa; this was later ascribed, at least in one direction, to dendro-dendritic coupling between the medial VS cells and a spiking cell called Vi, an inhibitory neuron that synapses on the dendrite of the ipsilateral VS1 (Haag and Borst, 2007). The medial VS cells receive horizontal input via dendro-dendritic coupling to the dCH cell, a connection that accounts for the horizontal sensitivity in the dorsal, frontal part of their receptive fields (Haag and Borst, 2007).

1.4.7. Calcium responses

Since much of my work is based on *in-vivo* calcium imaging in VS cells, it is important to consider what are the sources and properties of calcium influx in these cells. Calcium influx into LPTCs in response to motion stimuli was first reported in VS and HS cells, and was used to localize sources of input to cells (Borst and Egelhaaf, 1992; Egelhaaf et al., 1993) and to serve as a proxy for the responses of presynaptic motion detectors which are too small to record from directly (Single and Borst, 1998; Haag et al., 2004).

Introduction

Within the relevant voltage range for visual stimuli, calcium influx into LPTCs depends linearly, albeit with different slopes, on membrane potential changes induced by intracellular current injection (Haag and Borst, 2000). In HS and VS cells, the time course of calcium concentration rise is slower in the fine dendritic tips relative to the main axonal arbor, where the injection was made. However, in these experiments the cells were depolarized much beyond their normal activity range (up to -20mV). When stimulated with visual motion, the time courses were more compatible, up to a normalization (Dürr, 1998).

In an in-vitro study, the sources of calcium influx into VS cells was determined to be extrinsic, a mixture of influx through cholinergic receptor channels and voltage-gated calcium channels (Oertner et al., 2001). This was demonstrated by application of the cholinergic agonist carbachol in normal and low-calcium extracellular media; response to carbachol in the latter medium was abolished, showing that external calcium is necessary for the elevation of the intracellular calcium concentration. This experiment also rules out second-messenger driven release from internal stores, as such signaling depends only on the activation of muscarinic cholinergic receptors. Calcium-induced calcium release was also ruled out by experiments in which application of caffeine in a ryanodine-containing medium failed to trigger the elevation of intracellular calcium. Depletion of intracellular calcium stores with thapsigargin also did not affect the carbachol-induced calcium responses. Stimulation with carbachol in a low-sodium medium resulted in almost complete extinction of the membrane potential responses, but the calcium responses remained at almost the control level. The conclusion from this work was that around 80% of the calcium influx in LPTC dendrites comes from ligand-gated channels, and only the remainder from voltage-gated calcium channels.

However, as the authors themselves note, the situation in an in-vitro preparation using carbachol to activate the cholinergic receptors can differ substantially from an in-vivo preparation activated by cholinergic synapses in the visual pathway. A good demonstration of this is the failure of the authors to evoke calcium responses in VS2 and VS3 cells by intracellular depolarization. In the intact fly, hyperpolarization of tangential cells by current injection results in the vanishing of calcium fluctuations that are caused by the responses of local motion detectors to the local texture of the visual stimulus (Single and Borst, 1998). This hints towards a dominant role of voltage-gated calcium channels in tangential cell calcium influx, and a subsequent experimental and modeling study showed that at least 60% of the calcium comes through these channels (Borst and Single, 2000). However, most importantly to my work, that study also made it clear that local activation from synaptic stimulation remains confined to the synapse's dendritic branch, and thus the calcium signal readout, whether from cholinergic or voltage-gated channels, reflects this local synaptic input.

1.5. Lateral interactions between VS cells

Considering the retinotopic projection of motion information onto the lobula plate, a surprising result from the experiments by Krapp et al. is that for each VS cell, the receptive field measured intracellularly in the axon is approximately 3- to 4-fold wider at the horizon than what is expected from the extent of their dendritic arborization in the lobula plate (Krapp and Hengstenberg, 1996; Krapp et al., 1998; Farrow et al., 2005). One explanation considered for these broader receptive fields was lateral interactions between the VS cells. Such interactions

were first speculated by Hengstenberg et al. (1982) based on anatomical evidence of 'axon-collaterals' in VS cells that seemed to project towards the location of similar neighboring axon terminals, but at the time it was not clear whether these protrusions were indeed synaptic connections and how they influenced the receptive fields of VS cells.

1.5.1. Axo-axonal gap junctions

The existence of lateral interactions between VS cells was directly tested by Haag and Borst (2004), using double recordings and current injections in pairs of VS cells. Inward and outward currents injected in VS cells result in positive and negative membrane potential responses in other VS cells, respectively. These responses are smaller the further the distance between injected and recorded VS cells, and reverse their sign for VS cells closer to the edges of the lobula plate (e.g. VS1 and VS7/8). Analyzing the time course of the responses in the recorded cells led the authors to propose a chain-like connectivity model, where each VS cell is connected to its immediate neighbors, with an inhibitory loop between VS1 and VS7/8 (See Figure 2-5). Due to the bi-directional transfer of current, the most likely explanation for the connectivity is electrical synapses. This was verified in an experiment where neurobiotin, which permeates through gap-junctions, was loaded into one cell and its spread within the lobula plate was inspected after it was allowed to diffuse. As expected, the neurobiotin diffused to neighboring cells, indicating their connection by gap junctions, and moreover, the strength of the labeling decrease with distance from the loaded cell, supporting the chain-like connectivity scheme (Haag and Borst, 2005). From two-photon microscopy images as well as from earlier electron micrographs, it became clear that the gap junctions between VS cells resided in the

axons, which lie in close proximity throughout the lobula plate and in the protocerebrum, and not in the dendrites, which are spaced from each other in the lobula plate and do not make direct contacts (Pierantoni, 1976; Haag and Borst, 2004). This was verified using calcium imaging and intracellular current injection – current injected into a VS cell caused depolarization and calcium influx through voltage-gated calcium channels in the entire VS cell, but when the current was injected in a neighboring cell, calcium influx was registered only in the axon. This demonstrated that the VS cells are compartmentalized into an axon-terminal region and a dendritic region (Cuntz et al., 2007).

1.5.2. Functional significance

What is the contribution of input from neighboring VS cells to the receptive fields of a VS cell? To answer this question, receptive fields of VS cells were measured before and after ablation of single neighboring VS cells, filled with carboxyfluorescein, by laser irradiation. As predicted by the chain-like connectivity model, the responsiveness of VS cells to preferred direction motion was reduced on the side of the ablated cell, making their receptive fields narrower, but only on that side (Farrow et al., 2005).

What is the functional significance of the VS cells' broader receptive fields? A modeling study which simulated a biophysically realistic network of VS cells proposed an answer to this question. Cuntz et al. (2007) digitalized images of VS cells from two-photon microscope stacks and built a compartmental model of 10 VS cells, connected in their axons by gap junctions. The model network was fed by an array of Reichardt detectors synapsing on the dendrites of the simulated VS cells as excitatory and inhibitory synapses. When the model was presented with

Introduction

rotating artificial images containing uniform random patterns with high contrast, both the dendritic and the axon-terminal population responses remained relatively stable over time, and it was easy to estimate the axis of rotation of the image from the dendritic population response. The population response measured in the axon terminals was a spatially smoothed version of the dendritic responses, but it was not clear under this stimulation regime what this spatial smoothing achieved. Specifically, the position of the axis of rotation could easily be estimated by looking at the neuron whose response was closest to zero in both the dendritic and the axonal populations.

The contribution of this spatial smoothing was made evident when the network was presented with a naturalistic image in which the distribution of local image characteristics such as contrast and spatial frequency content is highly non-uniform across the different receptive fields of the VS cells. In this case, the dendritic responses were very unstable over time, reflecting the non-uniform naturalistic input and the effect it has on the responses of the Reichardt detectors that synapse on the VS cell dendrites. However, when looking at the spatially smoothed axon-terminal responses, it was immediately clear that in the case of naturalistic images they were much more stable over time than the dendritic responses. Also, it was easier to estimate the axis of rotation by looking at the neuron with the smallest absolute response. This was interpreted as a spatial “interpolation” of the axis of rotation, in the sense that the zero crossing of the population response was more robustly represented in the responses of the axon-terminal population, and not that of the dendritic population.

1.6. Neuronal morphology and intracellular computation

Much of what we know today about the way inputs to a single cell interact is due to the pioneering work by Wilfrid Rall and his students and collaborators from the late 1960s and later (compiled by Segev et al. 1994). Although earlier researchers used elements of linear cable theory to model and understand their results, Rall presented an integrated and comprehensive analytical framework that allowed neurophysiologists to understand how distributed electrical processes that occur in electrotonically remote dendrites affect recordings made predominantly in the soma of neurons (Rall, 1967; Rall et al., 1967). From these theoretical results it became increasingly clear that the relative location of inputs into single cells plays an important role in their interaction, and in the resulting integration at the level of the single neuron.

1.6.1. Segregation and aggregation of inputs

The physical and electrical separation of synaptic, local motion detectors in the dendrites of VS cells from electrical, gap-junction coupling between the axons of neighboring VS cells allows us to ask questions about intracellular computation in this system. Specifically, we can begin to address questions of design in this system – why are certain inputs to a cell spatially and electrotonically aggregated, whereas others are segregated? Using the blowfly lobula plate as a model system, we have a unique opportunity to address these questions in the context of the system's sensory function – the processing of visual motion stimuli related to flow-field estimation.

Introduction

That neighboring excitatory and inhibitory synapses interact divisively, i.e. sublinearly, is an idea that traces back to the discovery of inhibitory synapses by the Eccles group (Brock et al., 1952) and the finding that muscle end-plate potentials in crustaceans are attenuated by inhibitory input without reduction in the baseline potential by Fatt and Katz (1953). Based on Rall's cable theoretical approach to the neuron and his ideas regarding the effect of synaptic location on the somatically-measured EPSP (Rall, 1959; Rall, 1964; Rall et al., 1967), Blomfield suggested that when close together, inhibitory and excitatory synapses will interact divisively,

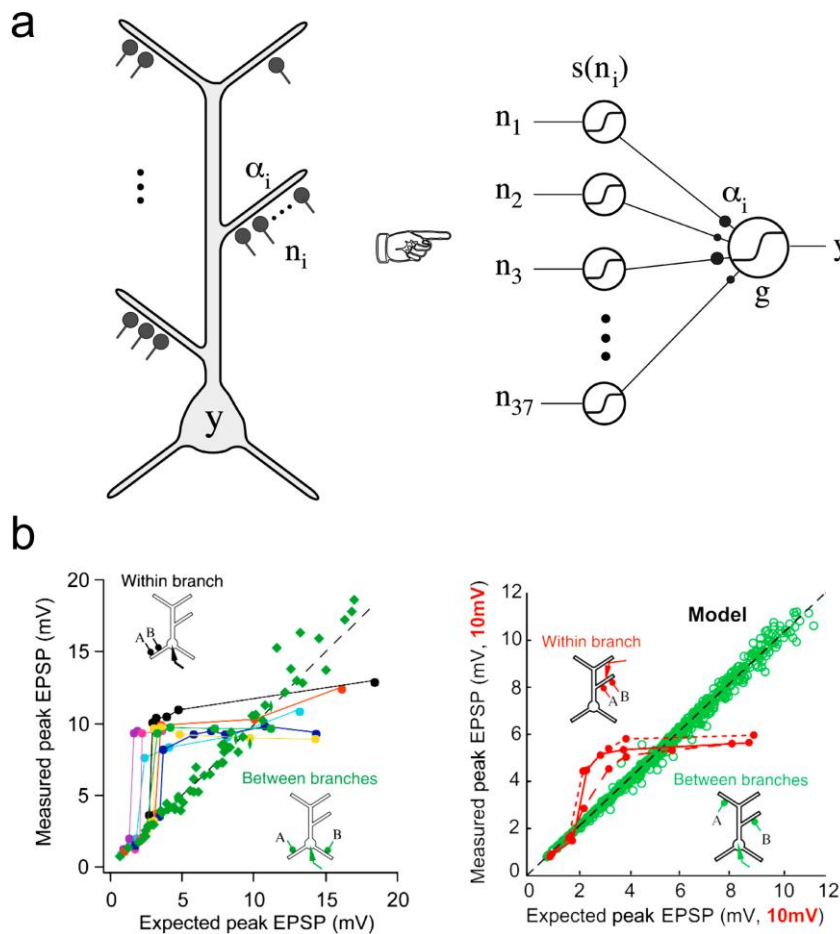


Figure 1-4: Single neurons as dual layer neural networks

(a) Equivalence between an electrically distributed model neuron and a dual layer neural network. The synaptic input to the same dendrite is integrated and passed through a local, dendritic non-linearity before being integrated with inputs from other dendrites at the soma and passed through the spiking non-linearity. Adapted from (Poirazi et al., 2003b). (b) Non-linear and linear integration of synaptic input on the same dendrite and on different dendrites, respectively, demonstrated by local excitation using 2-photon glutamate uncaging (right) and using a compartmental model (left). Adapted from (Polsky et al., 2004)

but when enough electrotonic distance is introduced, the interactions become essentially linear, i.e. subtractive. This idea also was also made explicit in a theoretical proposal for the underlying mechanism of directional selectivity (Torre and Poggio, 1978): “...this type of multiplicative inhibition is critically dependent on the spatial arrangement of the synapses. If the two synapses are not spatially adjacent (their distance being larger than about one-tenth of the membrane length constant), the circuit of figure 2 [i.e. a non-linear, multiplicative interaction] is not a faithful model. In this case the effects of the conductance changes would essentially summate linearly (Rall, 1964; Jack et al., 1975)”.

An important point to be made here is that when one considers spiking responses, shunting inhibition acts linearly even on nearby located excitatory inputs, due to the effect of the shunt on the spike generating mechanism (Holt and Koch, 1997). However, in non-spiking cells such as VS cells where the important interactions are sub-threshold also in the output of the cells, the shunting operation remains divisive.

These ideas, taken together with the various local dendritic non-linearities that were discovered in hippocampal and cortical pyramidal neuron dendrites (Johnston et al., 1996; Magee et al., 1998; Schiller et al., 2000; Häusser et al., 2000; Wei et al., 2001; Reyes, 2001), led to the suggestion that a single neuron could implement a dual-layer artificial neural network. In these networks, each artificial “neuron” sums its inputs linearly and passes the sum through a non-linear output function, and these are implemented in the single-neuron model in the dendrites and in the spiking non-linearity at the axon hillock (Mel et al., 1998; Archie and Mel, 2000; Poirazi et al., 2003a; Poirazi et al., 2003b; Figure 1-8a). The additional computational

mechanism in these models was the local dendritic non-linearity, which in a subthreshold regime allows inputs on the same branch to interact non-linearly while inputs on different branches sum linearly. These model predictions were subsequently tested and verified in hippocampal slices, although the strict one-to-one identification of the thin dendritic branches with the first layer's subunits was dropped in favor of a more continuous compartmentalization in the dendrites (Liu, 2004; Polsky et al., 2004; Figure 1-8b).

1.6.2. Non-linear integration in LPTC dendrites

Are these ideas applicable to the subject of this thesis, the VS cell network? Various non-linear integration mechanisms have been documented in LPTCs, including sub-linear saturation in spatial summation (Hausen, 1982b; Hengstenberg, 1982; Haag et al., 1992; Haag and Borst, 1994; Haag et al., 1999), synaptic gain-control of the saturation level by interactions between inhibitory and excitatory motion-selective inputs (Borst et al., 1995; Single et al., 1997) and supralinear amplification of high-frequency signal components by active properties in the dendrites and axons of HS and VS cells (Haag and Borst, 1996; Haag et al., 1999). There is some evidence for linear summation of inputs arriving at separate dendritic branches of the same VS cell (Haag et al., 1992). However, the existence of gap-junctions between axon terminals of VS cells raises the interesting possibility to view each VS cell as a separate dendrite of a large conglomerate "VS-network" neuron, since connecting two neurons by a gap junction or connecting two neuronal processes with a branching point is biophysically equivalent, assuming the gap junctions are passive.

1.7. Goals and project outline

Considering that the axo-axonal gap-junctions between VS cells are responsible for the broadening of their receptive fields, but that the effects of these interactions can only be seen in the axons, an immediate prediction is that the broader receptive field should be seen only in the axons, and not in the dendrite, which should not be affected by these connections. Thus, it should be possible to measure two distinct receptive fields in a single VS cell: a narrow receptive field in the dendrites, corresponding to the retinotopic feedforward input from local motion detectors, and a broader one in the axon terminals, corresponding to the cell's own dendritic input combined with information from neighboring VS cells (Figure 1-9). I directly tested and visualized this prediction using in-vivo calcium imaging; I showed that in VS cells, the dendritic receptive field is narrower than the axon terminal receptive field, and that this broadening is mediated by the lateral axo-axonal interactions. I also showed that the broader receptive fields are responsible for linearly integrating signals coming from the cells' dendrites and from their neighboring cells, as predicted by previous model studies. I then used a compartmental model to show that spatially separating the gap junction interactions in the axon terminals from the conductive load of the dendritic synapses is essential for this linear integration. Separating axonal interactions from dendritic input sites serves as an explanation for the cells' distinctive T-shaped morphology.

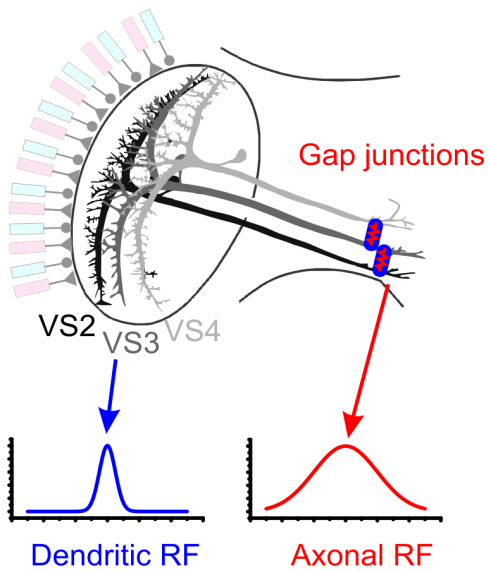


Figure 1-5: Narrow dendritic and broad axonal receptive fields in single VS cells

Top: a schematic depicting 3 example VS cells with their lobula plate input from local motion detectors (left) and the lateral connections between their axon terminals in the protocerebrum. Bottom: the resulting narrow dendritic receptive field, corresponding to input from the local motion detectors, and the broad axon-terminal receptive field, corresponding to the input from the cell's dendrites and from neighboring cells.

Chapter 2. Methods

In this chapter, I present a detailed description of the materials and methods used in gathering and analyzing the data, as well as the modeling techniques used. For a more succinct account of this chapter's contents, the reader is referred to Elyada et al (2009).

2.1. Experiments

2.1.1. Preparation and positioning of the flies

Female blowflies, *Calliphora Vicina*, were prepared as previously described (Haag and Borst, 2004; Farrow et al., 2005; Borst and Haag, 1996; 2-4 day old, laboratory stock). The flies were briefly anesthetized with CO₂, then mounted ventral side up on a piece of glass. The legs were cut off at the base, and the bases of the wings were waxed to prevent them from moving during the recording. The head was then pressed down towards the thorax and waxed, creating an angle of roughly 90° with the rest of the body's axis to allow access to the back of the head. The proboscis was pulled out and cut at the base to separate it from the gut, the antennae were also pulled out and cut and the incisions were closed with wax. An incision was made in the back of the fly's neck, the uppermost muscles removed and the gut was pulled out and waxed to the back of the thorax. The left side of the back of the head capsule was cut out, and air sacs and fat bodies were extracted, exposing the ipsilateral optic neuropils (lamina, medulla, lobula plate) and the dorsal part of the central brain including the bilateral calices, lateral

Methods

deutocerebrum, protocerebral bridge, protocerebrum and suboesophageal ganglion (Figure 2-1).

The piece of glass on which the fly was mounted was used to hold the fly in the recording setup, serving as an insulator to prevent ground loops between the amplifier's ground and that of the headstage. The fly was mounted facing down in front of the screen (see Stimulus presentation), which covered roughly 108° of the ipsilateral visual field from -7° to 101° . An upright epifluorescence microscope (Axioscope, Zeiss, Göttingen) located above the fly's head was used to visualize the brain and the electrodes so as to position the electrodes. A 20x water immersion objective was used in order to minimize optic distortion due to the fly's spontaneous pumping of its haemolymph, and this was also found to be useful in preventing the electrode's capacitance from changing during voltage clamp due to the rising and falling fluid level.

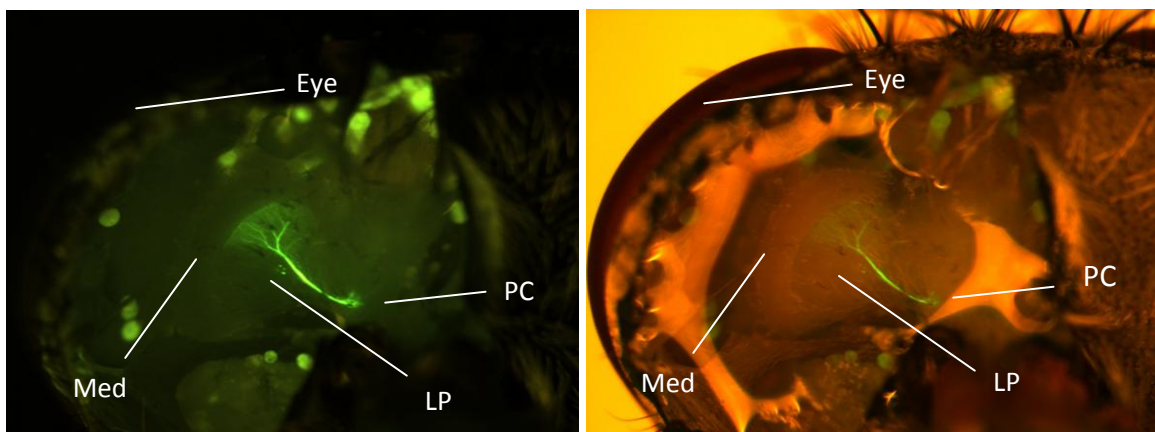


Figure 2-1: Access to the lobula plate and the LPTCs.

Caudal view of the open head capsule showing the brain with a dCH cell filled with fluorescent dye. Left – without external light, right – with external light. Med – medulla, LP – lobula plate, PC – protocerebrum. In the right picture, the lamina between the medulla and the eye is obstructed by a light reflection from the external light source.

2.1.2. Electrophysiology

Micropipettes for intracellular recordings were pulled using a Flaming/Brown puller (P-97, Sutter Instrument Co., Novato, CA), and for switched-mode voltage-clamp recordings coated almost up to the tip with a layer of wax to reduce the pipettes' capacitance. The following combinations of dyes were used in the tip solutions:

- 5mM Oregon Green BAPTA-1 (OGB-1) and 1mM Alexa 594 (A549) for initial access to the cells and receptive field mapping.
- 2mM A594 for electrical access to cells already filled with OGB-1 and A594 in order to voltage clamp them without accidentally introducing calcium dye into other cells.
- Oregon Green BAPTA 6-F (OGB-6F) for imaging of calcium fluctuations while presenting dynamic stimuli.

Dyes were dissolved in 0.5 M Potassium Acetate (all dyes from Molecular Probes, Eugene, Oregon). Electrodes were backfilled with 2M KAc and 500mM KCl. Average electrode resistance was 25M Ω .

VS cells were found by blind search in the lobula plate under visual stimulation and were usually initially impaled in the main dendrite or the axon close to the main dendritic branching point. VS cells were recorded in bridge mode or switched mode at 20-40kHz for voltage clamp (amplifier SEC10-L, NPI Electronic GmbH, Tamm, Germany). The time constant of VS cells (~1.2-1.4ms; Haag and Borst, 2004; Haag, 1994) is one to two orders of magnitude lower than that of

Methods

cells commonly recorded from electrophysiological experiments in other preparations (10ms-100ms), and therefore much closer to the time constants measured from our electrodes ($\sim 100\ \mu\text{s}$). Because of this we found it difficult to reliably balance capacitance in the amplifier by adjusting the voltage responses to square-shaped pulses. We therefore injected a sinusoidal current in the switched mode at 200Hz; since the corner frequency of VS cells is around 80Hz (Borst and Haag, 1996), the cell should not respond significantly to the injected sinusoid, and the only sinusoidal response should be that of the unbalanced electrode. We used this principle to balance the capacitance of the electrode under auditory feedback.

The sinusoidal current was superimposed on a hyperpolarizing DC current which achieved two things: Most importantly, it constrained the capacitance balancing exclusively to negative current injections, mitigating the effects of the non-linear properties of the relatively high-resistance electrode. We experienced a rectification by the electrodes at 0nA, which caused a different voltage drop over the electrode for currents of opposite sign. Since the stimuli we used were excitatory, we expected injection of negative currents while voltage-clamping, and it was therefore important to balance the electrodes using exclusively negative currents. Another thing this achieved was preventing the activation of the cells' active properties which might have distorted their responses to the sinusoidal injection and thus make it difficult to correctly balance the electrode's capacitance. This compensation method was tested with a few test electrodes in the bath and yielded negligible voltage deflections for negative current injections up to -10nA.

The amplifier's output was fed into an analog-to-digital converter board on a PC and sampled at 4kHz using custom software modified from Delphi code (Borland, Austin, TX) written by Juergen Haag. The program also controlled the computer generating the stimuli and triggered the CCD camera. This program was modified to allow automatic repetition of the same experimental protocol.

2.1.3. Visual stimulation

Flies were placed 85mm in front of a CRT monitor with fast, P46 phosphor dots sporting a 300Hz refresh rate (ML15MAX, Image Systems, Plymouth, MN), which resulted in a substantially smaller response of the cells to screen flicker relative to slower, conventional CRT monitors. The screen spanned 108° of the flies' ipsilateral visual field. Stimuli were generated by custom software written in Delphi as a front end for the API of a graphics board (ViSaGe, Cambridge Research Systems, Rochester, UK). The stimuli were presented in pseudo-random order within each repetition of the set of stimuli for a given experiment.

For receptive field mapping, 20° wide square-wave gratings (20° spatial wavelength, 100% contrast, maximal luminance 97.7 cd/m²) measuring 3 wavelengths high were presented at the fly's ipsilateral, medial visual horizon drifting in the preferred direction of the cells at a contrast frequency of 3Hz. The windows were centered at azimuths, from 0° (directly frontal) laterally up to 80°, in 10° steps (overlapping 10° with the two adjacent gratings).

For the calcium influx modeling experiments, whole-field gratings (20° spatial wavelength, 100% contrast, maximal luminance 97.7 cd/m²) were presented to the fly,

Methods

alternating between intervals where the grating drifted at a contrast frequency of 3Hz and intervals where the grating was stationary. This alternation started 1 sec after imaging began, and continued for 3 seconds at switching frequencies of 0.5, 1, 2, 3 and 4 Hz.

In the axon-terminal signal interpolation experiments, receptive fields of the filled cells were first mapped by presenting the same gratings described above for receptive field mapping. The fly was then presented with a pattern comprising sets of horizontal double bars (20° wide, 20° vertical spatial frequency) repeating periodically in the vertical dimension at $100^\circ/\text{cycle}$ and drifting at $50^\circ/\text{sec}$ in the preferred direction of the cell. The bars were positioned in the previously mapped dendritic receptive field or outside of it, laterally shifted by 40° to a position still inside the axon-terminal receptive field and spatially phase-shifted by half a cycle (Figure 3-11a).

2.1.4. Electrical responses

Steady-state membrane-potential responses were calculated from the intracellular recordings by averaging 2 seconds before stimulus onset and 1.5 seconds beginning 0.5 seconds after stimulus onset. The response to each drifting grating was taken as the difference between the two. Receptive fields were normalized to their maximum.

2.2. Data analysis

2.2.1. Cell identification

Identifying VS cells from other tangential cells was done by the directional selectivity of their electrical responses, and later confirmed by visual inspection. To identify each specific VS cell, I used a method developed by Karl Farrow, in which the relative location of the main dendritic branch in the lobula plate is compared to a table (Farrow, 2005). To this end, a fluorescence image of the filled VS cell was taken with a 10x water immersion lens with and without external lighting to illuminate the borders of the lobula plate. The relative location of the VS cell's dendrite was calculated by first marking the medial and lateral borders of the lobula plate in a matlab GUI script, then drawing a line drawn between them and finally marking the crossing point and its projection on that line (Figure 2-2).

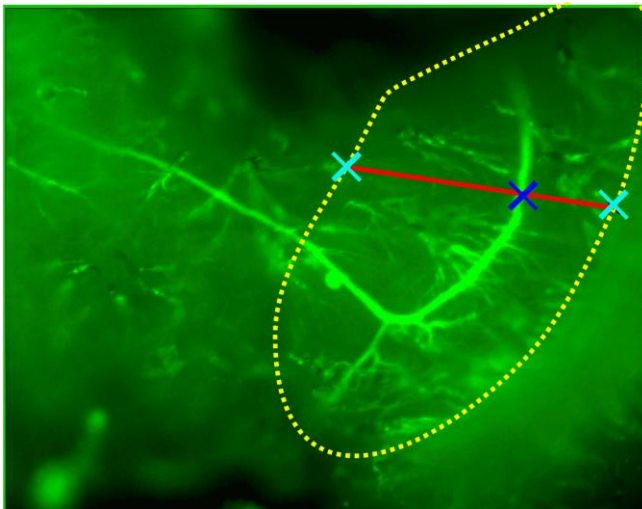


Figure 2-2: Identification of a VS4 cell by the relative position of its main dendrite.

Dotted yellow line illustrate the borders of the lobula plate, cyan X-s are the marked edges of the lobula plate and the blue X is the marked intersection between the connecting line (red) and the VS cell's dendrite.

2.2.2. Calcium imaging

Calcium imaging was performed using an epifluorescence-CCD camera imaging system (CoolSnapHQ, Roper Scientific, Tucson, Arizona) at 2Hz (receptive field mapping and current injection experiments) or 10Hz sampling frequency (image translation experiments). calcium imaging stacks were corrected for motion artifacts (ImageJ, stackreg extension), and $\Delta F/F$ stacks were filtered with a 10x10 pixel median filter and pixel-wise exponentially bleach corrected.

To quantify the steady-state calcium responses for the receptive field mapping experiment, difference images were calculated between the averages of 3 frames during the stimulus and 3 before stimulus onset (“average difference $\Delta F/F$ images”). A region of interest (ROI) was defined by setting a threshold set at 30% of the value of the 95 percentile pixel (see

Figure 2-3), and averaged the difference value over all pixels in the ROI for each of the 9 stimulus conditions. Note that in the dendrite, most of the calcium signal comes from thin dendrites located distally (laterally) from the main dendritic branch. This may reflect the larger

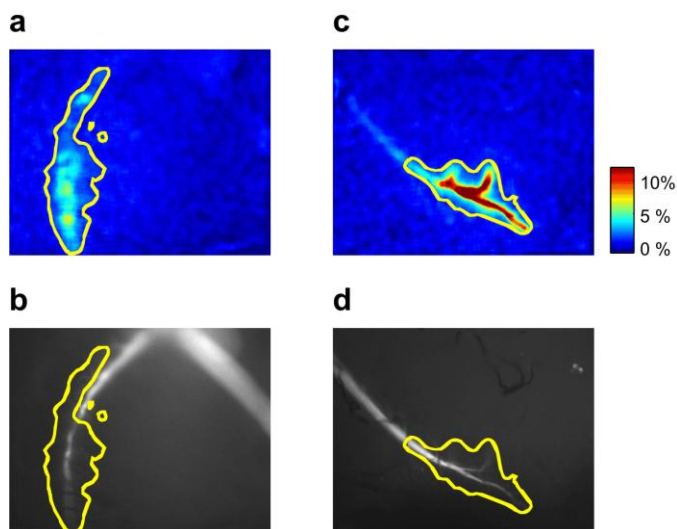


Figure 2-3: Calculating the region of interest (ROI).

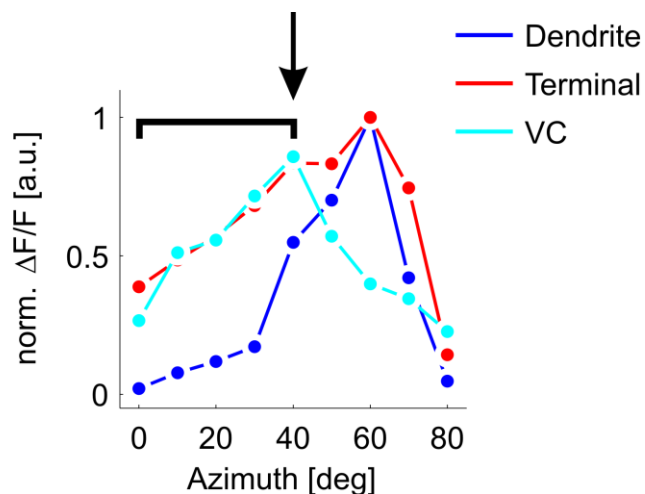
Calculating ROIs for dendrite and axon-terminal. **a.** Average difference $\Delta F/F$ image (see text) for the dendrite of the cell in Fig. 1b,c. ROI boundaries drawn in yellow. **b.** ROI presented on the raw fluorescence image. **c,d.** same as a,b for axon terminal.

increase in $[Ca^{+2}]_i$ caused by the proximity to the direct synaptic channels as well as by the smaller volumes of the respective neuronal processes there.

Calcium-imaging receptive fields measured in the dendrite or in the axon-terminal were normalized to their maximum. This deals with two potential sources of inhomogeneity in the calcium responses across different cells and different cell regions. The first is different cellular and circuit parameters that may result in different membrane potential and calcium responses (Swensen and Bean, 2005; Schulz et al., 2006; Marder and Goaillard, 2006). The second is a shortcoming of wide-field epifluorescence microscopy; because of the inhomogeneous background in an in-vivo preparation, and the optical merging of small branches into the background, it is virtually impossible to carry out a reliable background correction in this preparation (Borst and Egelhaaf, 1992; Haag and Borst, 2000). Background subtraction is an important processing step when trying to relate the $\Delta F/F$ measurements to a physiologically relevant signal such as the intracellular calcium concentration (Grynkiewicz et al., 1985), and I therefore could not obtain good estimations of any such relevant signal. The $\Delta F/F$

Figure 2-4: Normalizing calcium imaging receptive fields.

Maxima of the dendritic and axon-terminal receptive fields normalized to 1. VC: voltage-clamped dendrite, imaging in axon-terminal. Arrow: maximum of the axon-terminal receptive field under dendritic voltage-clamp, bracket: “residual” axon-terminal receptive field which was normalized so as to minimize the sum-of-squares difference from the corresponding points in the unperturbed axon-terminal receptive field.



Methods

measurement variability resulting was thus accounted for by normalization.

To compare axon-terminal receptive field under dendritic voltage clamp (terminal-VC) with the unperturbed axon-terminal responses, we had to take into account that voltage clamping the dendrite might have some effect on the response of the terminal as well, even for responses arriving solely through lateral interactions. We therefore normalized the terminal-VC curves so as to minimize the sum-of-squares difference between the unperturbed terminal receptive field and the axon-terminal receptive field under dendritic voltage-clamp, from the latter's maximum to the edge that is farthest away from the maximum of the dendritic response (see Figure 2-4).

I also modeled the effect that a voltage-clamping electrode has on signals arriving from neighboring cells through the gap junctions. To model this, I used a morphologically realistic compartmental model from Cuntz et al. (2007) kindly supplied by Hermann Cuntz (Figure 2-5a). The model runs in the NEURON environment (Hines and Carnevale, 1997) and incorporates detailed reconstructions of 10 VS cells from 2-photon fluorescence microscopy stacks.

2.3. Modeling

2.3.1. VS cell network model

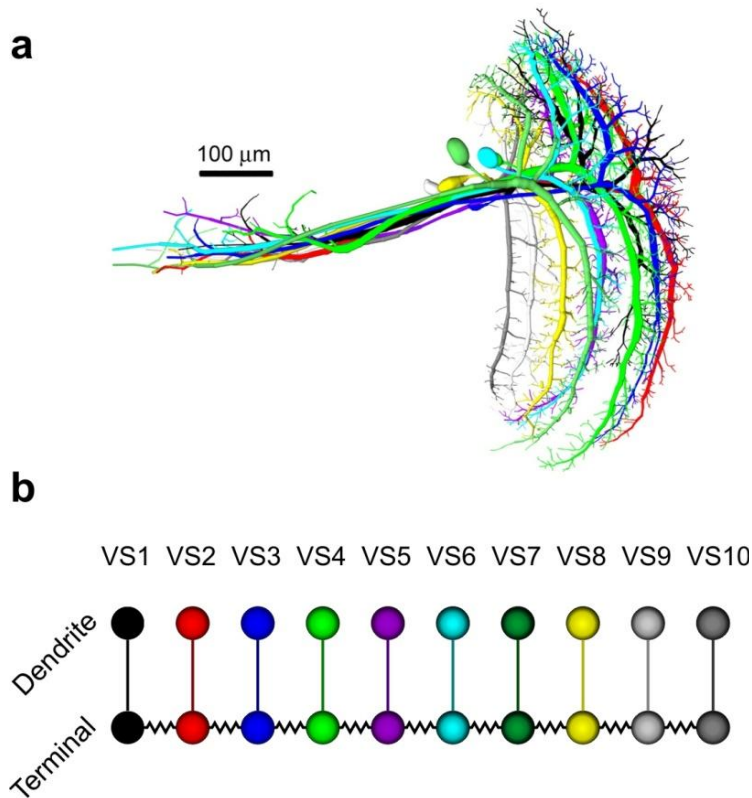


Figure 2-5: VS network models used for simulations.

a. Illustration of the model used for voltage clamp simulations and to extract parameters for the simplified 20-compartment model. Each cell is plotted in a unique color, with full representation of the branching pattern as well as the diameter of each compartment (taken from Cuntz et al., 2007). b. Simplified 20 compartment model extracted from the detailed model.

To simulate the VS cell network, I generated a simplified passive 20-compartment model with each cell being represented by a dendritic and an axon-terminal iso-potential compartment (Figure 2-5b). Each compartment was given a leak current and membrane capacitance, and the two compartments were connected by an axon for each cell, modeled as a simple conductance. Electrical synapses between either the dendrites or the axon-terminals, also modeled as simple conductances, were used to connect the cells in a chain-like fashion (only axon-terminal gap-junctions shown in Figure 2-5b). Synaptic conductances were placed

Methods

exclusively in the dendrites, with batteries of -40mV and +40mV for inhibitory GABA_A synapses and excitatory Acetylcholine synapses, respectively (see below for a description of how the time-dependent synaptic conductances were calculated). VS cells have resting potential of -45mV to -50mV, and in the model this is represented as 0mV. Thus the reversal potentials of Acetylcholine and GABA synapses in the model should be +45 to +50mV and -35 to -30mV, respectively. We used symmetric values as an abstraction step, in order to simplify the analysis of the model. Values of -30mV and +40mV were used by Cuntz et al., (2007), and their results do not differ substantially from ours.

Model simulations were carried out in matlab (MathWorks, Natick, MA) using custom written code adapted from an unpublished manual by Alexander Borst. Essentially, model parameters were incorporated into a conductance matrix M which has the i -th compartment's sum conductances and $\frac{C_m}{\Delta t}$ (taken from the term for capacitive current) on the diagonal M_{ii} , and the conductance between the i -th and j -th compartment in M_{ji} and M_{ij} . Using the vector of membrane potentials at time $t - 1$, $\vec{V}(t - 1)$, the algorithm solves for $\vec{V}(t)$ using the vectors $\vec{I}(t)$ of currents injected into each compartment, $E_{inh} \cdot \vec{g}_{inh}$ and $E_{exc} \cdot \vec{g}_{exc}$ of inhibitory and excitatory synaptic currents to each compartment (the leak potential is taken as zero and does not contribute to this) and $\frac{C_m}{\Delta t} \cdot \vec{V}(t - 1)$ (the other part of the term for capacitive current):

$$\mathbf{M} \cdot \vec{V}(t) = \vec{I}(t) + E_{inh} \cdot \vec{g}_{inh} + E_{exc} \cdot \vec{g}_{exc} + \frac{C_m}{\Delta t} \cdot \vec{V}(t - 1)$$

This is an implementation of the Euler method for solving the underlying differential equations, using a time discretization at $\Delta t = 1\text{msec}$.

A two-dimensional array of vertically oriented local motion detectors of the Reichardt type (Reichardt, 1987) with high-pass filters on the cross arms (Borst et al., 2003; filter time constants: low-pass 35ms; high-pass 75ms) simulated the local motion detection circuitry presynaptic to the lobula plate. Output signals of upward and downward motion detector subunits were thresholded at 0, summed by 10x100 pixel receptive fields, scaled by a gain factor (see model parameters below) and fed into the inhibitory and excitatory synapses, respectively. In models with current-injection synapses, the outputs of the motion detectors were rectified by a square root function immediately before being injected into the dendritic compartments, to account for the synaptic saturation that takes place in conductance based synapses.

2.3.2. Model parameters

For simplicity and abstraction, model parameters were assumed to be identical between all cells except those on the edges (VS1 and VS10, with only one connected electrical synapse). We then used an anatomically realistic model taken from ref. (Cuntz et al., 2007) to calculate responses in the axon-terminal (corresponding to the gap-junction connected compartment in the realistic model) or the dendritic compartment (corresponding to the primary dendritic branching point) to 10nA current injections in either of these compartments, in the injected and in the immediately neighboring cells. To constrain the magnitude of evoked synaptic currents, we also fitted responses in the dendrites and the axon terminal to drifting sinusoid gratings, as well as to a reduction of 25% in input resistance in the dendritic compartment when presenting the same stimulus (Borst et al., 1995).

Methods

We calculated the model's parameters by least sum-of-squares optimization using a score made of the previously described constraints. The resulting model parameters are summarized in Table 2-1.

$g_{\text{Axon}} (\text{VS1, VS10})$	103.5 nS
$g_{\text{Axon}} (\text{VS2-9})$	90.01 nS
$g_{\text{in dendrite}} (\text{VS1, VS10})$	240.8 nS
$g_{\text{in dendrite}} (\text{VS2-9})$	211.4nS
$g_{\text{in axon terminal}} (\text{VS1, VS10})$	6.03 nS
$g_{\text{in axon terminal}} (\text{VS2-9})$	5.29 nS
$g_{\text{gap-junction}}$	473.6 nS
Synaptic scaling coefficient	$10^{-7.4656}$

Table 2-1: Model parameters

2.3.3. Modeling visual input

Six hundred images were taken from an online image database (van Hateren and van der Schaaf A., 1998), rebinned by factor 2 and rescaled by taking the log of the middle 100x100 pixel values minus their mean. This logarithmic transformation mimics the compressive non-linearity of fly photoreceptors that allows them to reliably respond with reasonable signal-to-

noise ratio to light intensities in a very broad range (Juusola et al., 1994) Images were rotated around their centers at 155 deg/sec and 1kHz temporal resolution for 2 seconds. This time sequence was fed into the array of local motion detectors.

2.3.4. Modeling calcium responses

We modeled the Ca^{+2} response to changes in V_m , by measuring the V_m and Ca^{+2} responses to drifting gratings with square-wave velocity profiles repeating in frequencies of 0.5, 1, 2, 3 and 4 Hz. Since the high- K_d dye (OGB-6-F, $K_d \sim 3\mu\text{M}$) operates in the linear domain for cellular concentrations of Ca^{+2} , and assuming a linear dependency of Ca^{+2} influx on V_m fluctuations around the cells' resting potential (Haag and Borst, 2000), we modeled the responses as a second-order time-domain linear filter (Borst and Abarbanel, 2007). Each cell's V_m responses (average responses if V_m recordings were unavailable) were normalized, resampled by a factor of 400 and fitted by the normalized $\Delta F/F$ responses using Steiglitz-McBride iteration (see also Supp. Fig. 3). The modeling resulted in a low-pass filter with cut-off frequency of $\sim 0.4\text{Hz}$. Signal-to-noise ratio was calculated by dividing the Welch power spectral density estimate of the average of all single sweeps (signal) by that of the difference of all single sweeps and the average sweep (noise). For the averaged 5-sweep SNR we divided the noise by $\sqrt{5}$.

Chapter 3. Results

I started my approach to the questions outlined in the introduction by combining full-field epifluorescence calcium imaging and electrical recordings in order to map the receptive fields in different parts of VS cells. I found that dendrites of VS cells have narrow receptive fields, relative to the broader receptive fields in the axon-terminals. Using voltage-clamp blockade of the information flow from the dendrites of single cells, I was able to show that lateral interactions in the axon-terminals, and not in the dendrites, are responsible for this receptive field broadening. Moreover, I was able to demonstrate that the axon-terminal responses are linearly smoothed versions of the dendritic responses, as predicted by previous modeling work (Cuntz et al., 2007; Weber et al., 2008).

The question of why a certain circuit is built one way and not another, however, cannot be answered by experimentation. I therefore turned to compartmental modeling, which allows different configurations and wiring schemes to be tested and compared against each other. For this end I generated a simplified 20-compartment model of the VS cell network. I found that connecting VS cells with gap junctions in their axon-terminals results in significantly more effective interpolative smoothing of the population responses than connecting them in the dendrites, due to the shunting of the gap junction coupling by the dendritic chemical synapses. The need to electrotonically remove the gap junctions from the shunting effect of the synapses serves as a functional explanation for the striking T-shaped morphology of VS cells.

3.1. Two receptive fields in single VS cells

To measure the receptive fields in the two subcellular compartments, I performed simultaneous intracellular recordings and calcium imaging of VS cells using Oregon Green BAPTA 1 (OGB-1) while stimulating the flies with 20° wide gratings drifting in the preferred direction of the cells. The stripes were located at 9 different azimuths along the fly's visual horizon. This allowed me to directly visualize calcium responses in dendrites and terminals by looking at the relative change in fluorescence, $\Delta F/F$.

3.1.1. Linearity and homogeneity of calcium responses

Two important prerequisites for the use of calcium imaging to monitor neuronal activity in subcellular compartments are that the calcium influx is linearly related to the membrane potential deflection, and that this relationship is homogeneous in the various compartments in question. The voltage-gated calcium responses in VS cell dendrites and axon-terminals are linearly related to membrane potential deflections within the activity range of the membrane potentials of these cells (Egelhaaf and Borst, 1995; Haag and Borst, 2000), and the this relationship is homogeneous (Haag and Borst, 2000; Cuntz et al., 2007). I independently corroborated these results in VS cells by injecting current in bridge mode into the main dendritic branching point in 5 VS cells and measuring the calcium responses (Figure 3-1). Positive membrane potential deflections of up to 10mV, within the range of visually induced responses (Haag et al., 1999), can be elicited by injecting currents of 3-3.5nA (Borst and Haag,

Results

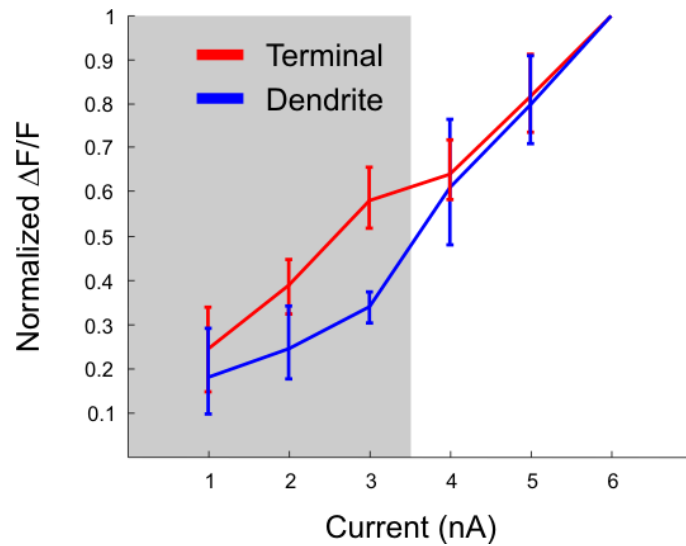


Figure 3-1: Current-calcium influx relationship in VS cell dendrites and axons

Linear relationship between injected current and calcium influx in VS cell dendrites and axon-terminals. Gray shading: functionally relevant range of current injections. See text for details.

1996) . In this range of currents, calcium responses in both dendrites and axon-terminals are linearly related to the injected current, albeit with a different linear slope. VS cells are therefore amenable to calcium imaging of visual-motion induced responses.

3.1.2. Mapping the receptive fields

Taking advantage of these results, I proceeded to map receptive fields in dendrites and axon-terminals of VS cells. I presented the fly with drifting square-wave gratings at various azimuths on the horizon of the fly's eye, and measured the average calcium dye activation over stimulus presentation within defined regions of interest in the dendrites and axon-terminals of the cells. In an example VS3 cell, both axon-terminal and dendrite responded to gratings in lateral azimuths (40°-70°), but only the axon-terminal responded to gratings positioned in frontal azimuths (0°-30°); the dendrite showed no detectable response to these stimuli (Figure 3-2a, example $\Delta F/F$ traces in Figure 3-2b). This confirmed that excitatory input from neighboring VS cells arrives at the axon-terminal and not at the dendrite. I mapped the

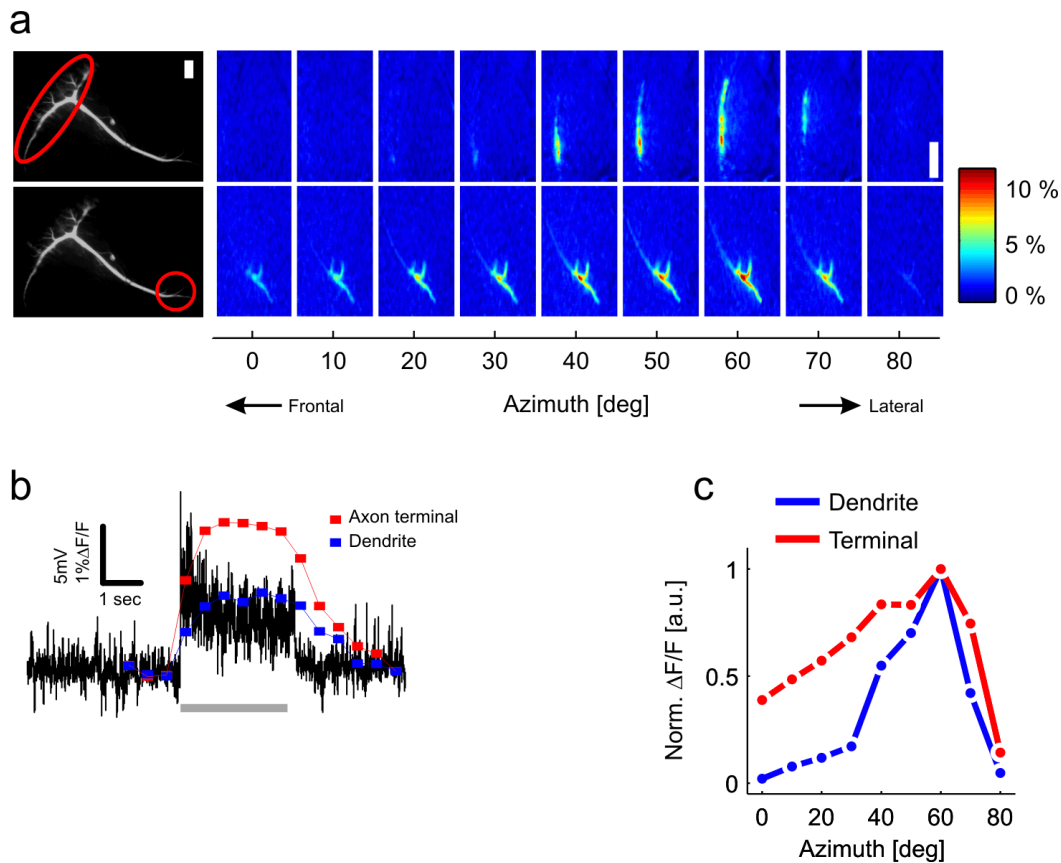


Figure 3-2: Broadening of VS cells' receptive fields within single cells.

(a) Ca^{2+} imaging results for a VS3 cell, top row – dendrite, bottom row – terminal. Each frame is the difference between the averages of 3 $\Delta F/F$ frames before and after stimulus onset. Scale bar – 100 μm , (b) Intracellular recording (black) and $\Delta F/F$ traces (red – axon terminal, blue – dendrite) of the cell's response to a 20° wide grating drifting at 60° azimuth (gray bar). (c) Receptive fields of the cell in b, averaged over the cell's dendrite and terminal.

receptive fields of this cell's dendrite and axon-terminal by averaging the responses over the two defined regions of interest (Figure 3-2c). The terminal receptive field is more than twice as broad as the dendritic one (Gaussian fits: $\sigma \sim 13^\circ$ dendrite, $\sigma \sim 29^\circ$ terminal), and the frontal part of the dendritic responses vanishes, whereas that of the terminal remains above zero.

I measured the receptive fields of 49 VS cells (5 VS1, 14 VS2, 16 VS3 and 14 VS4, Figure 3-3a); data from more medial cells were not acquired because with the stimulus screen it was

Results

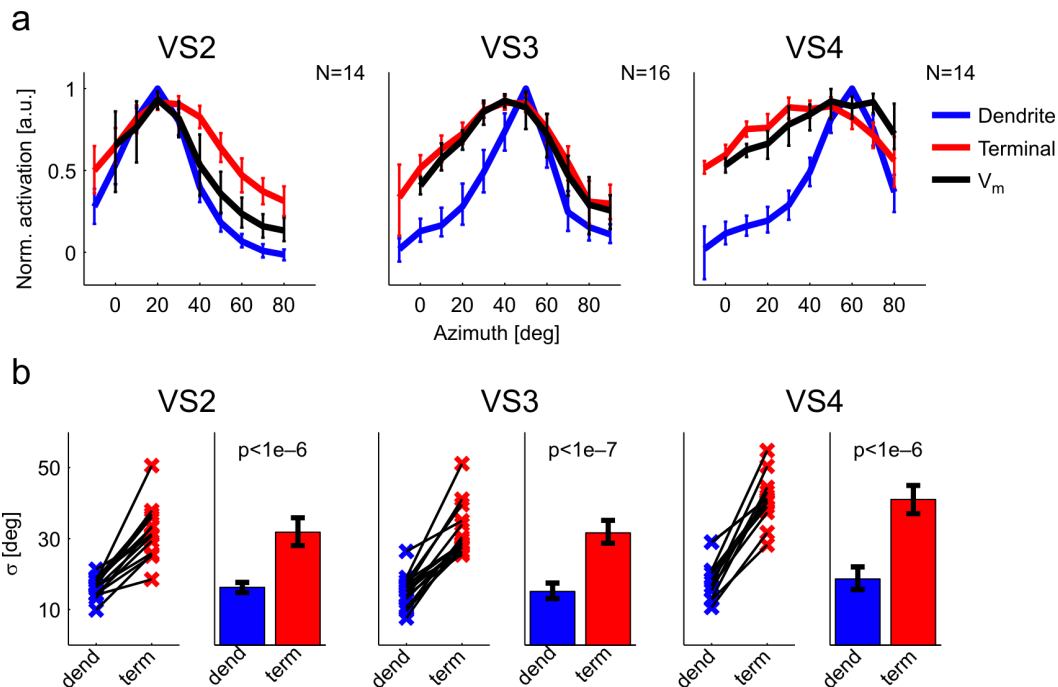


Figure 3-3: Broadening of VS cells' receptive fields – population analysis.

(a) Pooled population responses for dendritic, terminal and V_m receptive fields, means with 95% bootstrap confidence intervals – VS 2 ($n=14$), VS3 ($n=16$) and VS4 ($n=14$) cells. (b) Comparison of σ values from Gaussian fits for dendrite and terminal: left panel – paired responses, right panel – means with 95% bootstrap confidence intervals and t-test p-values.

not possible to measure their receptive fields to their full extent, and in some cases the maximum of their receptive fields fell outside of the stimulation region, which made normalization impossible. Shifts in the receptive fields resulting from variable positioning of the flies in front of the screen were accounted for by aligning all receptive fields according to the maximum of each cell's dendritic receptive field. The dendritic receptive fields of VS2-4 cells vary from frontal to lateral, as expected from their dendritic arborizations in the lobula plate, but their terminal receptive fields are similar, as are their electrical receptive fields (see also (Farrow et al., 2005)). To test for receptive field broadening in the axon-terminal on a population level, I calculated a Gaussian fit for the dendrite and axon-terminal of each of the

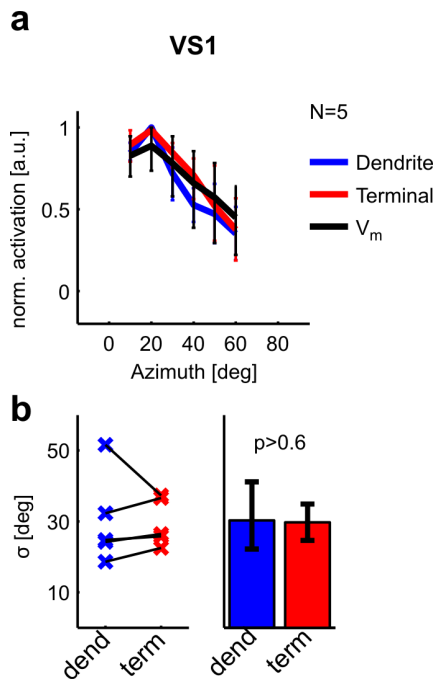


Figure 3-4: No broadening of receptive fields in VS1 cells – population analysis.

Same as Figure 3-3 for VS1 cells (N=5).

cells I measured. Most notably in the present context, I found that the terminal receptive field was substantially broader compared with the dendritic one in all experiments (Figure 3-3b).

3.2. Information flow underlying receptive field broadening

The results of the previous section suggest that in single VS cells, two sources of input dictate the size of receptive fields in dendrites and in axon-terminals. In the dendrites, receptive fields reflect the pooling of retinotopic input from the presynaptic array local motion detectors, and in axons, receptive fields are broadened by axo-axonal gap junctions. However, there is an alternative explanation of these data; it could be the case that due to the lower magnitude of calcium influx into the dendritic compartment, what I demonstrated in Figure 3-2

Results

and Figure 3-3 could be the result of a threshold artifact. In other words, the parts of the axon-terminal receptive field that are not responsive in the dendrite (e.g. azimuths 0° - 30° in Figure 3-2a) are simply below threshold for calcium imaging in the dendrites, but above threshold in the axon-terminal. They are therefore measureable in the axon-terminal but not in the dendrite.

3.2.1. Controlling information flow with voltage clamp

To rule this possibility out, a tool was required that would allow me to control information flow within the cell and therefore to confirm that different sources of information reach different parts of the cell. The tool of choice in this case was single-cell voltage clamping (Finkel and Redman, 1984; see Discussion). I used single-electrode voltage clamp at the site of the main dendritic branching point of VS cells in order to block dendritic inputs from reaching the axon terminal. Although the axon-terminal membrane potential should be partially clamped by the electrode in the dendrite, the electrotonic distance between the two compartments should guarantee substantial residual excitation of the terminal by the neighboring neurons.

To confirm this, I performed current injections and voltage clamp simulations in a biophysically and morphologically realistic compartmental model, kindly supplied by Hermann Cuntz (Cuntz et al., 2007). Voltage responses to current injections of 5 nA into the main dendritic branching point were significantly decayed when they reached the axon-terminal (77.9%, 91.6% and 79% for VS2, VS3 and VS4, respectively, Figure 3-5b,c). The interesting result for the voltage clamp method was that voltage clamping had very little effect on signals coming from neighboring cells at the axon-terminal. Voltage clamp in the dendritic branching point

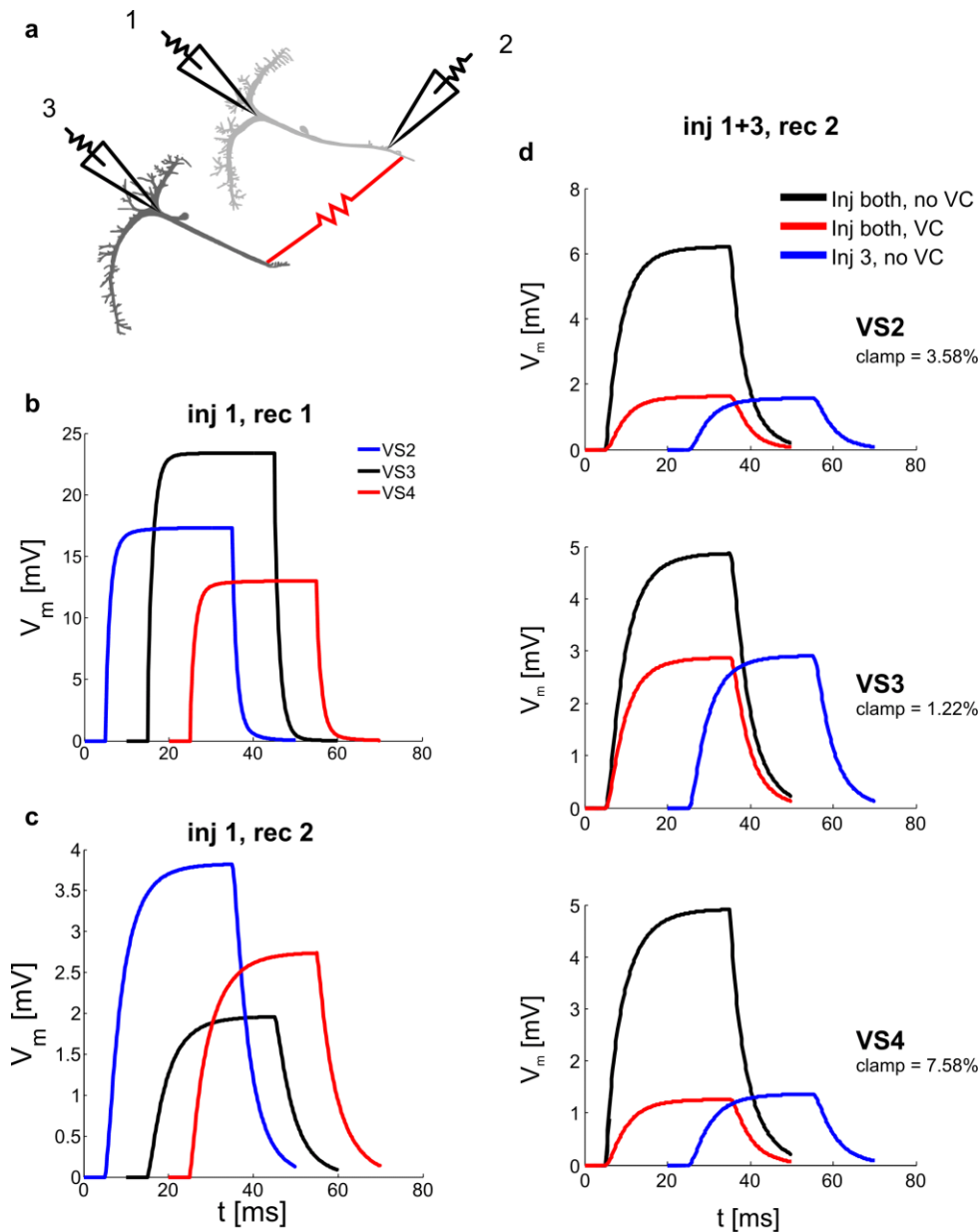


Figure 3-5: Voltage clamp and current injection in a VS cell network model.

(a) Modeling configuration (not all cells shown), access by electrodes in 3 places for each cell – in the main dendritic branching point and in the gap-junction connected compartment of the subject cell (electrodes 1 and 2 respectively, top cell) and in the main dendritic branching point of a neighboring cell (electrode 3, bottom cell). (b) Injection of 5 nA for 30ms into electrode 1, recording in electrode 1. The local effectiveness of current injection is greatest for VS3. (c) Same as b, but recording in electrode 2. Electrotonic decay in VS3 is the strongest relative to VS2 and VS4. (d) Effect of voltage clamp. Currents were injected into both electrode 1 and 3 (black) or only into electrode 3 (blue, shifted in time for clarity), recordings were done in electrode 2. For the red curves, membrane potential was clamped at the location of electrode 1 to the membrane potential by an ideal single-electrode voltage clamp. Clamp percentages show the relative reduction of the signal from the neighboring cell (blue curves) when clamped at the dendrite (red curve).

Results

significantly reduced the axon-terminal responses to simultaneous dendritic current injections in the subject cell and its neighboring cell (Figure 3-5d, compare black and red traces).

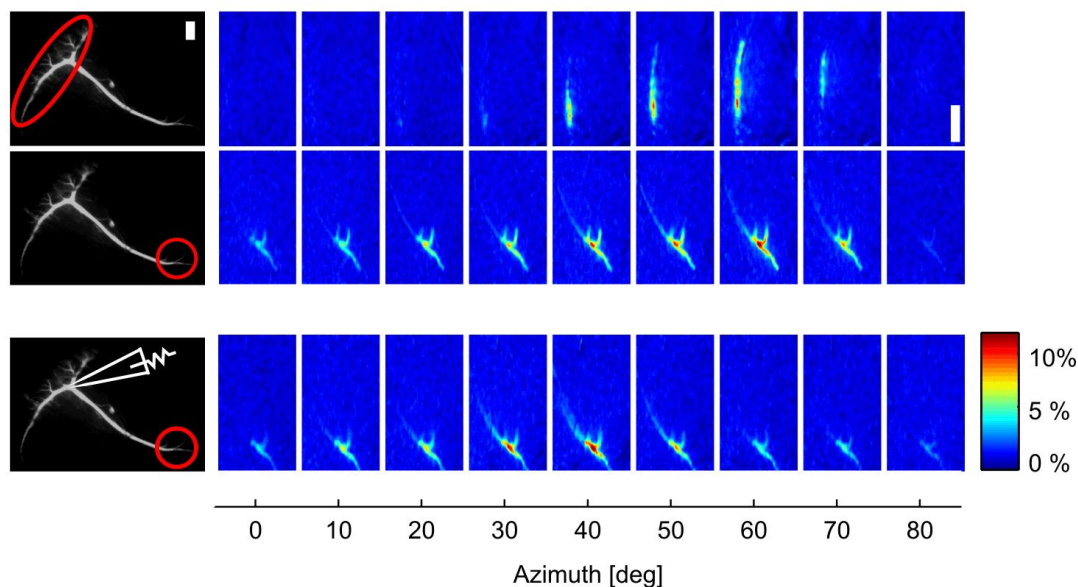
However, this reduction was almost strictly from the voltage response of the subject cell, and not from excitation coming from the neighboring cell through the gap junction connection. These voltage clamped responses were only slightly reduced compared with axon-terminal responses to current injection only in the neighboring cell (3.58%, 1.22% and 7.58% for VS2, VS3 and VS4, respectively, Figure 3-5d, compare red and blue traces), demonstrating that voltage clamping the dendritic branching point had little effect on signals coming from the neighboring cells. This spatial restriction of the voltage clamp perturbation, therefore, makes this method suitable for asking questions about information flow in the VS cell network.

3.2.1. Clamping out dendritic input to the axon terminal

If lateral connectivity takes place in the axon terminals, and synaptic excitation from the dendrite is blocked by voltage clamping in the main dendritic branching point, two predictions can be made: first, responses in the axon terminals should still persist despite blocking dendritic inputs. Second, a “dip” in the terminal receptive field should be observed, corresponding to the location of the peak of the dendritic receptive field, as a result of the cell’s dendritic contribution to the terminal receptive field being suppressed.

The results of a voltage clamp experiment performed in the same VS3 cell as in Figure 3-2a show, as predicted, that the responses in the axon-terminal were not entirely abolished by the dendritic voltage clamp (Figure 3-6a,b). Also, a reduction in the axon-terminal responses

a



b

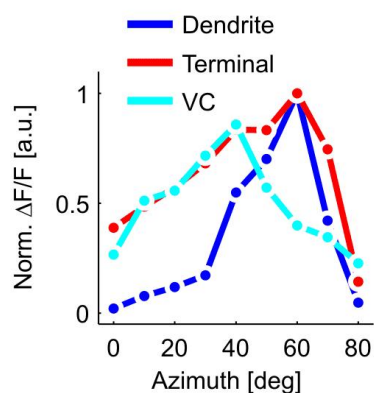


Figure 3-6: Voltage clamping of dendritic input.

(a) Bottom row: calcium imaging results from a voltage-clamp experiment; same cell as in Figure 3-2a, unperturbed dendritic and axon-terminal receptive fields shown for comparison in top rows. (b) Terminal receptive field under dendritic voltage clamp measured from a, compared with the dendritic and terminal receptive fields taken from Figure 3-2a

Results

can be seen only in the lateral parts of the visual field, corresponding to the dendritic receptive field in this particular cell. I measured receptive fields for 20 VS2-4 cells (Figure 3-7a); most importantly, in all 3 cell types it is obvious that terminal responses did not vanish with dendritic voltage clamp. The predicted dip, corresponding to the location of the dendritic RF, was clearest in VS4 cells, less significant but still visible in VS3 cells, and practically non-existent in VS2 cells. We confirmed this notion by plotting the difference curves between the axon-terminal receptive fields and those of the axon-terminals under voltage clamp (Figure 3-7a) as well as by the correlation coefficients between these curves and the dendritic receptive fields

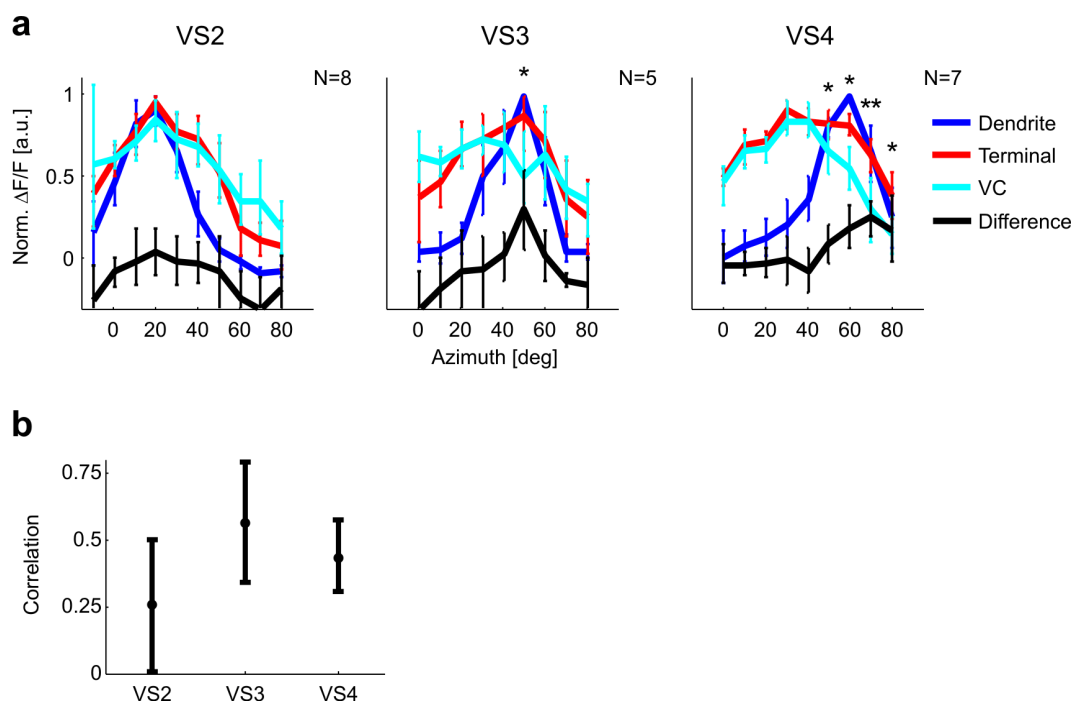


Figure 3-7: Voltage clamping of dendritic input – population analysis.

(a) Population responses as in Figure 3-3 for VS 2 ($n=8$), VS3 ($n=5$) and VS4 ($n=7$). Voltage clamp curves were normalized to minimize the difference between the non-clamped part of the voltage clamp curve and the same positions in the corresponding terminal receptive field (see Methods). Difference trace (black) – difference between the terminal curve (red) and the VC curve (cyan). Means with 95% bootstrap confidence intervals, statistic comparisons are between the terminal curve and the VC curve (* - $p<0.05$, ** - $p<0.005$, one-sided paired t-test). (b) Correlation coefficients between the dendritic receptive fields and the difference traces in (a).

(Figure 3-7b).

3.3. Interpolation of dendritic signals in the terminals

My results from the previous section show for the first time that receptive fields in VS cell dendrites are different from those in axon-terminals. This is a corroboration of a prediction from an experimental and modeling study by (Cuntz et al., 2007 especially Figure 2), and in that sense these results confirm that the lateral interactions between VS cells which are responsible for the broadening of the cells' receptive fields are confined to the axon-terminal.

What is the purpose of broadening the receptive fields of VS cells? In the study by Cuntz et al. (2007), and in a more recent one (Weber et al., 2008), it was suggested that the broader receptive fields of VS cells support a local linear pooling of dendritic responses from neighboring VS cell dendrites. This linear pooling was suggested to result in the spatial smoothing of fluctuations that arise from spatially non-uniform naturalistic input and the effects this non-uniform input has on the responses of the local motion detectors. However, this suggested consequence of the lateral interactions was never tested because of the difficulty of separating the feed-forward synaptic input in the dendrite from the effects of the lateral interactions in the axon-terminals.

3.3.1. Faster reporting of calcium dynamics

I reasoned that since lateral interactions from the terminal do not reach the dendrite, the linear interpolation of the dendritic synaptic signals predicted by those previous modeling studies should be measureable in the axon terminal, but not in the dendrite. In order to

Results

measure faster temporal fluctuations I used a low-affinity dye (Oregon Green BAPTA 6-F, $K_d \sim 3 \mu\text{M}$), allowing for faster resolution of calcium fluctuations (see discussion). Although OGB-1 has become the synthetic calcium indicator of choice in many experimental setups due to its higher affinity and therefore its higher sensitivity to calcium influx, this advantage comes at the price of slower temporal dynamics. Recently, several groups have attempted to overcome this problem by using new-generation low-affinity dyes to image faster calcium dynamics (Bollmann and Sakmann, 2005; Rotschild, G., ISFN 2008). Low-affinity dyes were used before in the lobula plate preparation to demonstrate that the lion's share of calcium buffering in tangential cells results from cell-intrinsic properties, and not from buffering due to the dynamics of the calcium dye (Haag and Borst, 2000). Still, there is a significant difference in the time constant of the calcium influx and efflux between the lower and higher affinity dyes in those measurements (1.69 sec vs. 1.23 sec, or 37% for the decay phase of the calcium response, fits made to graphs extracted from the paper), and I therefore decided to minimize the temporal low-pass filtering introduced by the dye by using a lower affinity dye.

When imaging and comparing temporal fluctuations in the two different compartments, two important issues must be considered. First, the temporal filtering properties of the visually evoked responses by the calcium reporter must be similar, if not identical, in both compartments. If this is not the case, it would present problems in the analysis and comparison of the two signals. Second, when measuring spatial filtering of visual input in a system which is essentially a low-pass filter, it is important to avoid confounding signal smoothing due to temporal low-pass filtering of the calcium imaging system with smoothing due to gap-junction mediated integration.

3.3.2. Frequency response and SNR of the calcium dye

To test the similarity of the filtering properties in dendrites and axon-terminals, I determined the frequency response curves of the calcium dye to the membrane potential responses in the two compartments. I first recorded the electrical responses of the cells together with the calcium responses in their dendrites and axon-terminals, while presenting the fly with full-field gratings alternating between drifting and standing at various frequencies (

Figure 3-8). I then modeled the calcium influx as a function of the membrane potential

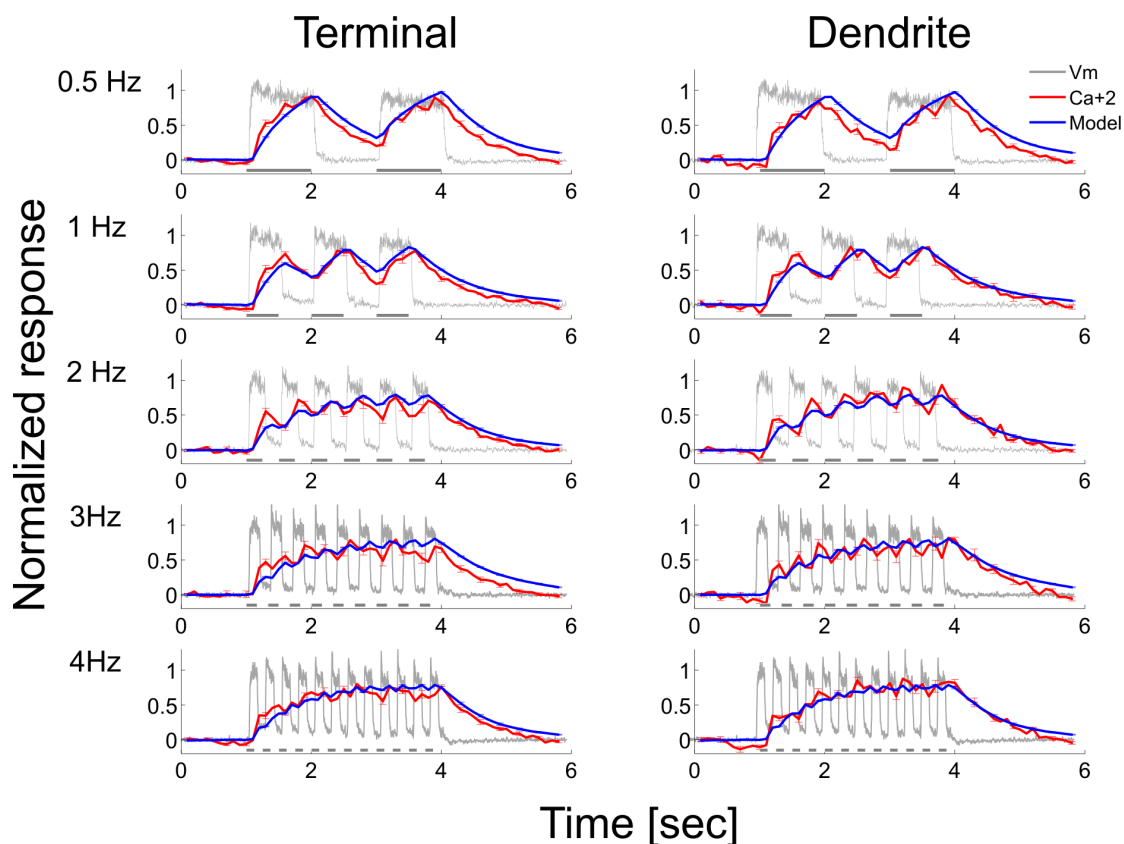


Figure 3-8: Calcium influx modeling results.

Intracellular recordings of responses to full-field gratings drifting at 0.5, 1, 2, 3, and 4 Hz (gray) together with calcium responses (OGB-6-F, red) and calcium response model (blue) in the terminal (left column) and dendrite (right column), means with s.e.m. The same electrical responses were used for terminal and dendrite. Gray bars denote intervals of motion.

Results

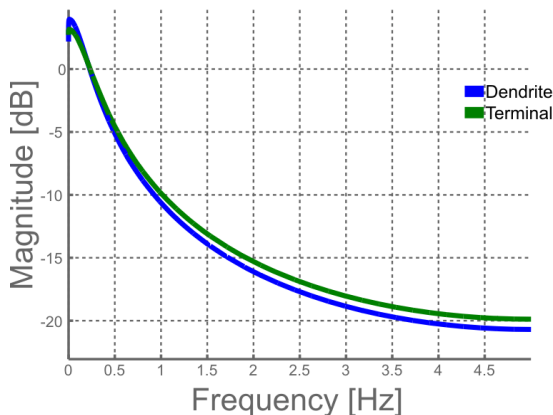


Figure 3-10: Calcium influx model frequency response.

Frequency response of the calcium influx model for dendrites and terminals.

by treating the $\Delta F/F$ responses as a second-order time-domain linear filtered version of the electrical responses (Borst and Abarbanel, 2007; see Discussion). This was done using Steiglitz-McBride iteration, an algorithm that takes an input signal and an output signal, and returns the coefficients of a linear filter of a requested order that will produce a least-squares approximation of the output signal given the input signal (see Methods). The frequency response curves for dendrites and axon-terminals I derived from the linear filter models of the two compartments were similar (Figure 3-9).

In order to be able to distinguish between smoothing due to the calcium reporter's temporal filtering and smoothing due to the lateral interactions, I used visual stimuli whose

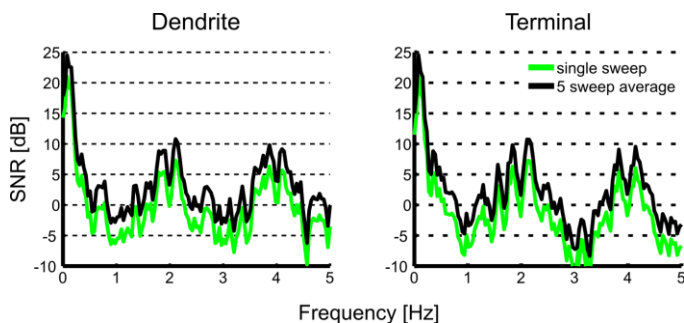


Figure 3-9: Calcium influx signal-to-noise ratio analysis.

Signal-to-noise ratios for dendrite and terminal for single sweeps and the average of 5 sweeps, assuming the noise is Gaussian for each frequency.

main frequency components lie under the low-pass filter cutoff frequency of the dye in these cells. To determine which stimuli fall in this category, I characterized the signal-to-noise ratio (SNR) at different visual stimulation frequencies. To calculate the SNR I took the ratio between the spectra of the signal and of the noise (see Methods). To account for averaging of noise over multiple stimulus presentations, I assumed the noise is Gaussian and divided the noise power spectrum by the square-root of 5, the number of averaged traces. This resulted in a reasonable SNR at signal frequencies of up to 0.5 Hz when averaging 5 trials for each stimulus condition (Figure 3-10).

3.3.3. Smoothing of dendritic fluctuations in the axon terminal

I first measured the dendritic and terminal receptive fields of the cells (Figure 3-11a), and then stimulated the flies with sets of double bars moving inside the dendritic receptive field (“in”-bars) or outside of it but still within the axonal receptive field (“out”-bars), or both sets simultaneously (Figure 3-11b). Each set of bars was repeated at a frequency of 0.5 Hz, and the two sets were out of phase by half a cycle. This stimulus was chosen in order to evoke fluctuations in the dendrites of the target cell, and anti-correlated fluctuations in the dendrites of a neighboring cell, both within the temporal resolution of the calcium dye. The reasoning is that if fluctuations are smoothed out by linear integration in the axon-terminals, the most effective stimulus to demonstrate this is a perfectly anti-correlated pair in which the peaks of the fluctuations caused by one stimulus would cancel out the troughs of the other.

As expected, dendrites responded to the in-bars and fluctuated at their temporal frequency, but did not respond to the out-bars. When both were presented together, the out-

Results

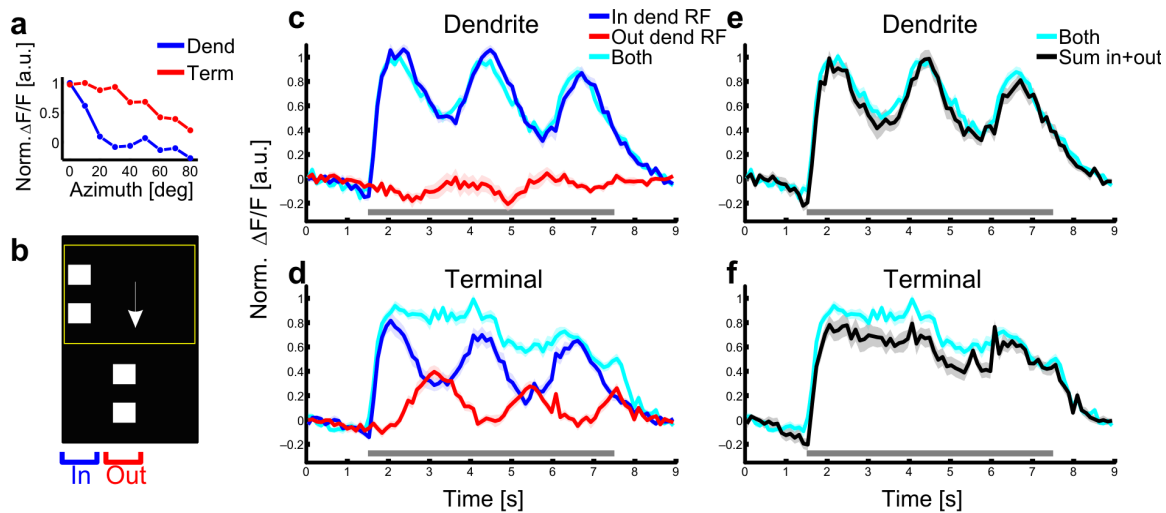


Figure 3-11: Interpolation of dendritic responses in the axon terminal.

a. Dendritic and axon-terminal receptive fields of an example VS2 cell. b. snapshot of the translating image presented to the fly. Yellow rectangle demarcates the screen size, white arrow the direction of image motion. c. Normalized $\Delta F/F$ signals in the dendritic region of interest for double bars drifting inside the dendritic receptive field (red), outside of it (blue) or both (cyan). Means with s.e.m. (shaded). Grey bar marks the interval of stimulus motion. ($n=6$). d. Same as c for the axon-terminals. e.-f. comparison of responses to both sets of bars presented together (cyan) and the algebraic sum of the responses to the single set of bars (black)

bars had no effect on the response and it was the same as that obtained with only the in-bars (Figure 3-11c,e). In contrast, the terminals responded both to the in- and, to a lesser extent, to the out-bars. When presented together, the two responses were smoothly interpolated, as predicted by the models (Figure 3-11d), approximating an algebraic sum of the responses to the two sets of bars (Figure 3-11f).

3.4. Functional consequences

What are the functional consequences of separating the two different input pathways that reach a single neuron? Gap junction connections between neighboring VS cells are thought

to participate in interpolating the responses of the VS cell population, in order to overcome fluctuations in the dendritic responses that arise from the patchy, non-uniform nature of naturalistic visual input. These fluctuations are a result of the dependence of the two dimensional array of local motion detectors on the local structure and contrast of the visual input (Zaagman et al., 1978; Dvorak et al., 1980; Srinivasan and Dvorak, 1980; Eckert, 1980; Egelhaaf et al., 1989b; Egelhaaf et al., 1989b; Single and Borst, 1998; Reisenman et al., 2003; Haag et al., 2004). A previous study showed that the vertically oriented dendrite of each VS cell can smooth out these fluctuations in the vertical dimension (Single and Borst, 1998), but at that time it was not known that VS cells are connected with neighboring VS cells, in the horizontal dimension (Haag and Borst, 2004). After this finding was made, the gap junctions were proposed to deal with such fluctuations in the horizontal dimension, across the receptive fields of different VS cells (Cuntz et al., 2007; Weber et al., 2008). I asked whether the positioning of the gap junction connections bears any significance to this function.

3.4.1. Compartmental model

I generated passive compartmental models of ten VS cells, each consisting of one dendritic and one axon-terminal compartment, connected by a simple conductance to simulate the axon. The cells were connected in a chain-like fashion by gap junctions, also represented by conductances. I compared models with dendritic versus axon-terminal gap junction connections. All model parameters were fitted using a detailed morphological model (Cuntz et al., 2007) and relevant results from electrophysiological measurements (Borst et al., 1995). I calculated the synaptic input to the model using naturalistic images taken from an image

Results

database (van Hateren and van der Schaaf A., 1998); images were rotated around their center and fed into a 2-dimensional array of Reichardt-type local motion detectors (see Methods). I fed the outputs of the preferred- and null-direction motion detectors as conductances to excitatory and inhibitory synapses on the dendrites, respectively. I analyzed the responses of the model to a representative image from the database (Figure 3-12a), shown with the simulated receptive field borders of the modeled VS cells overlaying it.

To visually compare the results of the different models to this example stimulus, I plotted the voltage responses in the axon-terminal compartment over the time period of the simulation (Figure 3-12a-c), as well as the population voltage responses of the ten VS cells at different time points (Figure 3-12d-f). Models connected by gap junctions in their axon terminal clearly implemented better interpolation of the dendritic input signals (Figure 3-12b) than those connected in their dendrites (Figure 3-12c), as was evident from the reduced fluctuations in the voltage responses over time and the smoother population responses of the ten cells at each time point (Figure 3-12e,f). In fact, results of the dendritically connected model differed only slightly (less than 0.1mV) from those of models without gap junctions (results not shown).

3.4.2. Quantifying response smoothness

Finding a suitable quantification for this apparent effect is, however, not a trivial matter. Ideally, given a good understanding of the way the ensemble of post-synaptic neurons use the information they receive from VS cells, I could have directly tested changes in these neurons' functional capabilities as a function of the output of the VS cell network. Unfortunately, despite some promising advances in the last few years (Haag et al., 2007a; Wertz et al., 2008a) we are

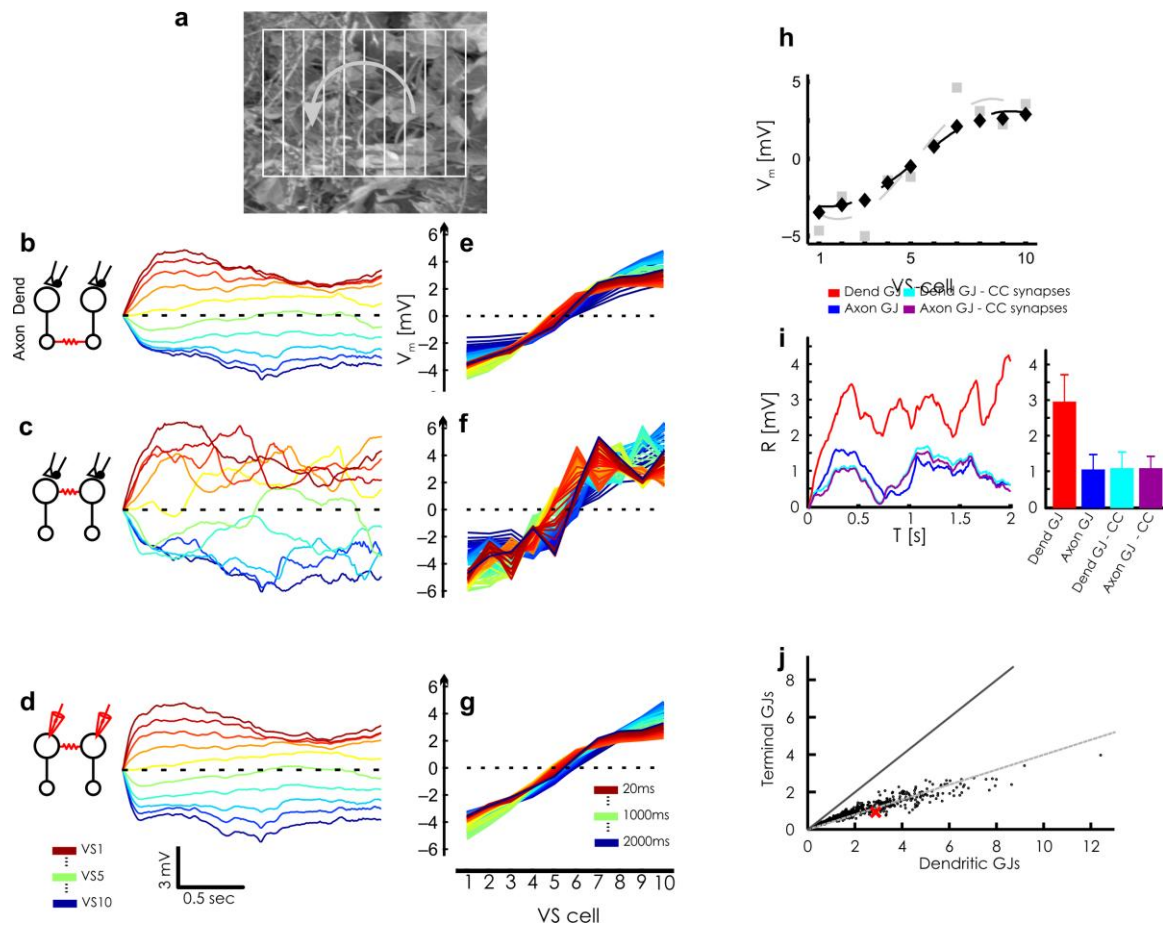


Figure 3-12: Axon terminal coupling results in more robust VS cell population coding

Axon terminal coupling of model VS cells results in more robust population coding than dendritic coupling. (a) Rotated image with modeled VS cell receptive fields, left to right: VS1-10. Arrow shows direction of rotation. (b) Compartmental model with 2 compartments for each of 10 VS cells, electrically coupled in the axon terminal (see text for details): population responses of the axon terminal compartments to the rotating image plotted over time, color coded from red (VS1) through green (VS5) to blue (VS10). Dotted line represents resting potential. (c) Same as b. for the dendritic coupling model. (d) Same as b, dendritic coupling model, conductance-based synapses replaced with current clamp simulation of synaptic input. (e-g) Population responses of axon-terminal compartments from b-d plotted as a connected line for each 20th time point over all VS cells. Time points separated by 20ms, color coded from red (t=20ms) to blue (t=2000ms). (h) RMS error of the population responses for each time point, for models with axonal or dendritic coupling, using conductance based or current-clamp synapses. For each time point, the population response of the 10 VS cells was fitted by a single sinusoid and the RMS of the fit's error calculated. Left panel – population responses and sinusoid fits for t=1848ms from e in blue and f in black. Center panel – RMS error for each time point plotted over time. Right panel – mean and std over the whole simulation period. GJ – gap junction, CC – current-clamp. (i) Comparison of RMS error for all 600 images in the database. Dashed lines: green – linear fit (slope 0.4), red – unity slope. Red x marks the example image in a-g.

still far from having such an understanding. I therefore had to rely on a general measure that would allow for a reasonable space of possible coding schemes in the post-synaptic circuitry; I fit, for each time point, a sinusoid to the population response of the VS cells. The underlying assumption for choosing a sinusoid fit is that given an image with uniform structure (i.e. contrast, spatial frequency, etc.), the vertically oriented Reichardt detectors' output will be roughly proportional to the velocity in the vertical dimension in their receptive fields, up to a certain rotation velocity. When rotating an image around its axis, this velocity depends on the azimuth in a sinusoidal manner (see also Karmeier et al., 2005b). Any deviation from this sinusoidal fit can be therefore attributed to fluctuations arising from the structure of the naturalistic image, and thus I chose the RMS (root mean square) of the fit error as a measure for how good the coding in the VS cell network is (Figure 3-12h). Indeed, model VS cell networks connected in the axon terminals had a smaller RMS error of the sinusoid fit for each time point (Figure 3-12i).

3.4.3. The shunting effect of chemical synapses

At first thought, it is surprising that the position of gap junction coupling should be in any way relevant to the effectiveness of the lateral interactions. To explain this effect, we considered the chemical, conductance-based mechanism of the synapses we used in our model. Strong synaptic conductances, especially inhibitory ones, are known to result in a suppression of neural excitability known as *shunting inhibition* (Fatt and Katz, 1953; Blomfield, 1974; Torre and Poggio, 1978; Alger and Nicoll, 1979; Borg-Graham et al., 1998). Although in

the classical theory of this kind of synaptic interaction (see, e.g., Koch, 1999), the shunting conductance is regarded as a single ionic conductance with a battery close to or equal to the resting potential of the cell, it is easy to show that a combination of two shunting conductances with equal magnitudes and opposing reversal potentials relative to the resting potential is mathematically equivalent.

Adopting the notation of Koch (1999), in a single RC compartment with an excitatory synaptic input and an inhibitory, shunting input we have from his eq. (1.29):

$$C \frac{dV}{dt} = g_e (E_e - V) - g_i V - \frac{V}{R}$$

(3-1)

where C is the capacitance of the compartment, V is the membrane potential with 0mV as the resting potential, g is a constant synaptic conductance with the subscripts e and i denoting excitatory and inhibitory (shunting) synaptic inputs, and R is the compartment's leak resistance. This formulation holds for a single ionic conductance; to generalize it to a scenario with two ionic conductances, we can replace $V = \frac{1}{2}V + \frac{1}{2}E + \frac{1}{2}V - \frac{1}{2}E$ and after rearranging we have:

$$C \frac{dV}{dt} = g_e (E_e - V) + \frac{1}{2} g_i (E - V) + \frac{1}{2} g_i (-E - V) - \frac{V}{R}$$

(3-2)

This results in an equivalent shunt where half of the original conductance is associated with a reversal potential of $+E$ and half with a reversal potential of $-E$, a situation very similar to the dendritic compartment of the simplified VS cell model.

Results

But this analysis is for a single RC compartment; how will a similar shunt affect information arriving from a neighboring compartment via a gap junction? One can replace the excitatory synaptic input in Eq. (3-1) with a gap junction connection g_{GJ} to another compartment which is clamped to a membrane potential V_o :

$$C \frac{dV}{dt} = g_{GJ}(V_o - V) - g_i V - \frac{V}{R}$$

(3-3)

The solution to this differential equation is

$$V(t) = \frac{g_{GJ} V_o}{G_{in}} \left(1 - e^{-t/\tau} \right)$$

3-4

where $G_{in} = g_{GJ} + g_i + \frac{1}{R}$ is the sum of all conductances in the compartment and $\tau = \frac{C}{G_{in}}$ is its time constant. The greater the magnitude of the shunting conductance g_i , the smaller the effect V_o will have on $V(t)$, in other words, the smaller the coupling coefficient between the two compartments induced by the gap junction connection.

I therefore reasoned that the reduction in the effective coupling that occurred in the dendritically connected model should be alleviated by replacing the conductance based excitatory and inhibitory synapses that are responsible for this shunting effect with current-clamp synapses (CC models), i.e. injecting current proportional to the output of the motion detectors without changing the synaptic conductance. When I did this, interpolation in the dendritically connected network was similar to the axon-terminal connected model (Figure

3-12d,g,i). The axon-terminal connected CC model was practically identical to the dendritically-connected CC model (results not shown), suggesting that even though both leak and synaptic conductances contribute to the overall conductivity of the dendritic compartment, the crucial factor behind the interpolation efficacy is the synaptic conductances, due to their larger magnitude. When we compared RMS error values of dendritic versus axon-terminal connected models with chemical synapses, similar results held uniformly over the entire database of natural images we tested (Figure 3-12i).

3.5. Small field selectivity of VS cell dendrites

In the course of our experiments, I encountered a phenomenon that was not reported previously in the VS cell system. Because VS cells are considered to be spatial integrators, it is expected that large-field motion will drive the cells more effectively, resulting in stronger

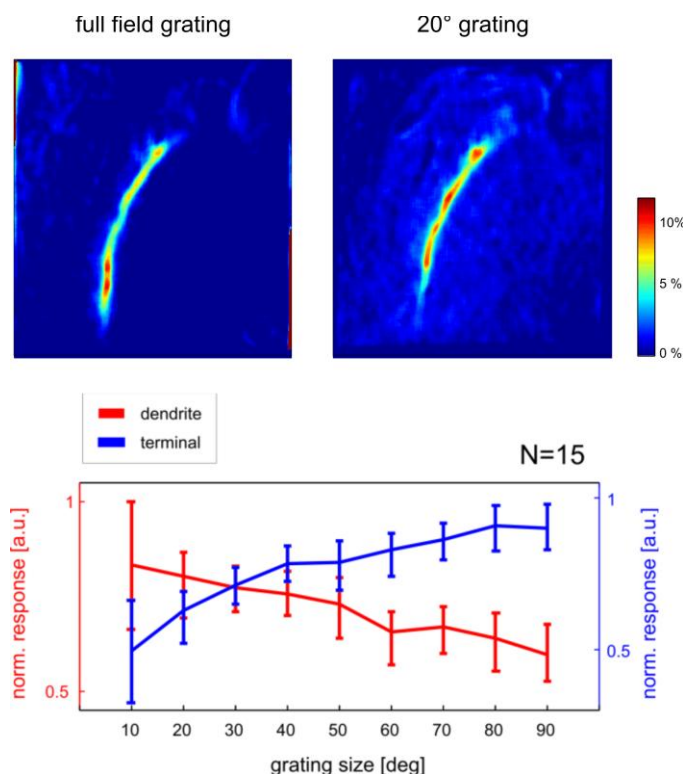


Figure 3-13: Small-field selectivity in VS cell dendrites

(a) Small-field gratings evoke stronger calcium influx in the dendrite of a VS cell than full-field grating. $\Delta F/F$ images averaged over stimulus presentation for a large field (left) and a small-field (right) stimulus. Note that dendritic areas excited by the 20° grating are more strongly excited by it than by the full-field grating. (b) Normalized $\Delta F/F$ responses averaged in dendrites (red) and axon-terminals (blue) of VS cells over stimulus presentation for gratings varying in horizontal width.

Results

responses, than small-field motion. This is indeed the case for electrical responses (Haag et al., 1992; Borst et al., 1995), and when I compared full-field calcium responses to small-field, 20° gratings, this is also what I observed in the axon terminals. But when I measured the dendritic calcium responses, the result was reversed – the small-field gratings elicited larger responses than the full-field gratings (Figure 3-13a). I began an initial quantification of the spatial extent of this small-field selectivity by measuring the responses to gratings varying horizontally in size in 15 VS cells (3 VS2, 6 VS3, 5 VS4, 1 VS5, Figure 3-13b). Here the axon-terminal responses increase by close to 100% on average from the smallest grating to the full-field grating, whereas the dendritic responses unexpectedly dropped approximately 30%.

To check whether this small field selectivity can also be seen in the vertical dimension, I presented gratings that varied in size in the vertical dimension. To keep total luminance constant I presented gratings consisting of an integer number of cycles, from 1 to 4 cycles, at a

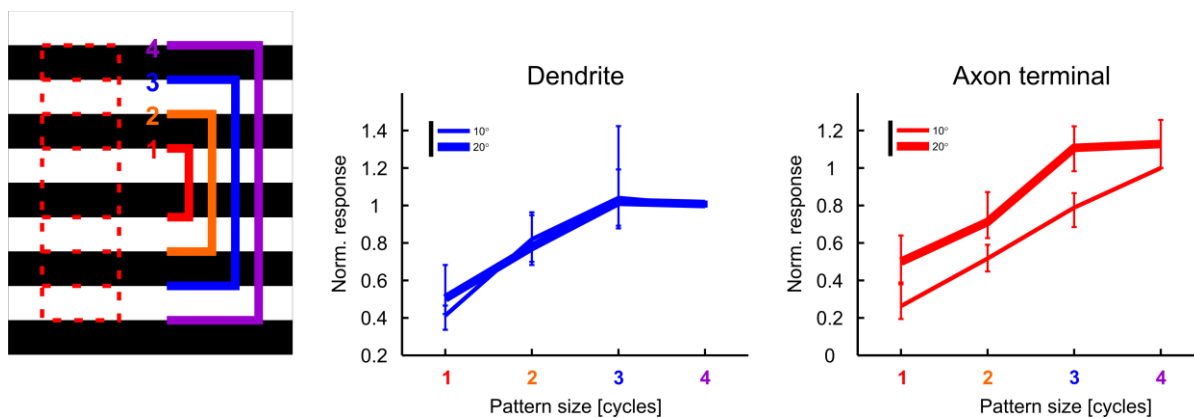


Figure 3-14: Vertical size dependence of dendrites and axons

Left: illustration of stimuli used – gratings presented were 1-4 integer number of cycles long in the vertical dimension and 10° or 20° wide. Right: dependence of dendritic and axon terminal responses on vertical size. Both dendrites and axon terminal responses grow with stimulus size.

width of 10° and 20°. As expected, responses grew with the size of the grating both for the axon terminal and the dendrite, reflecting the integration expected in the vertical dimension of the dendrite (Figure 3-14, same cells as above). This also served as a control for the dendritic calcium imaging, demonstrating that the imaging could register increase in response magnitude as a function of stimulus size.

As putative mechanisms for this small-field dendritic selectivity, I considered either a presynaptic pooling inhibitory mechanism acting isotropically along the horizontal dimension, or a form of presynaptic short-range lateral inhibition. Longer ranges of lateral inhibition, between medial VS cells and the VS1 cell were reported in previous studies (Haag and Borst, 2004; Haag and Borst, 2007), however the shorter range of the effect I describe here, as well as its manifestation in the dendritic compartment of VS2-5 cells, removed from the effect of inhibition coming from VS1 through the axo-axonal gap junctions, suggested that this is a different inhibitory mechanism than any described before.

To differentiate between these two possible mechanisms, I presented a stimulus consisting of the 20° grating that elicited the strongest dendritic response (the “main” grating) and simultaneously another 20° grating horizontally positioned at various distances either lateral or medial to the main grating (the “inhibitory” grating), both drifting in the preferred direction of the cells. If short-range lateral inhibition is the underlying mechanism, the expectation is that further-distanced inhibitory gratings should result in a smaller inhibition. However, if the mechanism is an isotropic pre-synaptic pooling mechanism, we should expect no effect of the position of the inhibitory grating on the inhibition it elicits in the dendrite.

Results

The results of this experiment are presented in Figure 3-15, for the same cells as above. As expected from the linear summation of the responses to the two gratings, the axon terminal responded stronger to both gratings drifting together. In the dendrite, I could not detect a statistically significant effect of the second stripe on the calcium response, neither when I separately analyzed effect of lateral and medial inhibitory gratings (Figure 3-15), nor when I pooled responses to the lateral and medial inhibitory gratings. However, there seems to be a tendency for a stronger effect of medium distances (50°-70°), and this can be seen in a lower mean and lower t-test p-values testing for a difference from responses to the main grating alone (p-values 0.2493, 0.6431, 0.7394, 0.0943, 0.1856, 0.1229 for 20°-70°, respectively). The statistical insignificance of these results may be a result of the small effect for a 40° grating relative to a 20° one (Figure 3-13b), but presenting a larger inhibitory grating and moving it

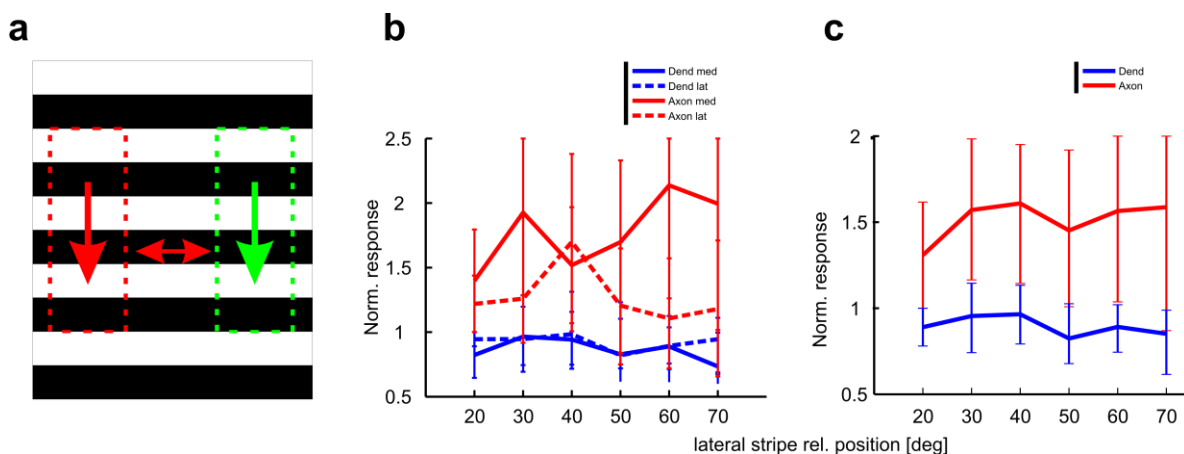


Figure 3-15: Effect of a lateral grating on dendritic and axonal responses

a. Schematic representation of the stimuli used; a main grating (red) is presented together with a horizontally shifted "inhibitory" grating. b. Effect of the inhibitory grating on the axon-terminal and dendritic responses, separated into medially positioned inhibitory gratings and laterally positioned inhibitory gratings. c. Same as b, lateral and medial positioned inhibitory gratings pooled

laterally and medially is not possible using the current stimulus presentation device. Clearly, though, more experimentation is needed in order to obtain a satisfactory description of the underlying mechanism.

Chapter 4. Discussion

In this work I demonstrated that in VS cells, axon terminals have broader receptive fields than dendrites because of the electrotonic separation of feedforward synaptic input from lateral, gap junction interactions. I also showed that this separation ensures effective gap junction connectivity, allowing for the interpolation of dendritic responses and a robust representation of motion information in the axon terminals, the output regions of these cells. The separation between terminal and dendritic receptive fields reveals an important characteristic of sensory neurons: different parts of a cell can have different receptive fields, depending on the proximity of inputs and their intracellular processing. These results also resolve the discrepancy between the dendritic morphology and the shape of the cells' electrical receptive fields (Krapp et al., 1998; Krapp and Hengstenberg, 1996). The dendritic arborization is commensurate with the shape of the dendritic receptive field, whereas the traditionally measured electrical receptive field is more similar to the terminal receptive field.

4.1. Methodology

In this section I will discuss the experimental methodology I used in this work, the potential advantages and disadvantages it incurs and how this might affect the interpretation of the results I obtained.

4.1.1. Calcium imaging

Calcium imaging allows the experimenter, among other things, to independently measure activity in different parts of a single neuron without accessing the different with different electrodes. Calcium imaging uses intracellular fluorescent dyes that change their fluorescence properties in response to changes in calcium concentration. The technique is a popular and well established one; calcium dyes with essentially modern fluorescence and temporal qualities were available from the mid-eighties (Grynkiewicz et al., 1985; Tsien, 1988), and since then have been used in a wide variety of *in-vitro* and *in-vivo* preparations using synthetic as well as genetically encoded dyes (Sobel and Tank, 1994; Miyawaki et al., 1997; Takahashi et al., 1999; Svoboda et al., 1997; Miesenbock, 2004; Mank et al., 2008; Wallace et al., 2008). In the blowfly, this method was first used to demonstrate the retinotopy of the motion detector array that feeds the lobula plate (Borst and Egelhaaf, 1992), and was since used to map input sources (Egelhaaf et al., 1993), lateral connectivity (Haag and Borst, 2002; Cuntz et al., 2007; Haag and Borst, 2007), and input dynamics (Single and Borst, 1998; Haag et al., 2004 reviewed by Kurtz et al., 2008).

Despite being such a ubiquitous and useful technique, one must take a few drawbacks and limitations into account when using calcium imaging as an experimental technique. The main concerns stem from the fact that calcium concentration in a neuronal compartment is only a proxy for the actual electrical activity which is often the desired object of measurement (nevertheless, in many cases calcium concentration itself is the relevant quantity, e.g., Neher and Augustine, 1992; Sobel and Tank, 1994; Helmchen et al., 1996). One of the important pre-requisites is that the cells in question possess low-threshold voltage-gated calcium channels

Discussion

(VGCCs) that are properly activated by the stimulus paradigm used in the study. This is indeed the case for VS cells, and moreover, VGCCs are considered a main source of calcium influx both in the axon-terminal and in the dendrites (Figure 3-1; Haag et al., 1997; Single and Borst, 1998; Haag and Borst, 2000).

Another concern that arises from the use of calcium indicators is the non-linearity of the dependence of calcium indicator fluorescence on the intracellular calcium concentration (Tsien, 1989; Grynkiewicz et al., 1985; Maravall et al., 2000; Borst and Abarbanel, 2007), and of the calcium concentration on membrane potential (Neher and Augustine, 1992; Helmchen et al., 1996; Borst and Abarbanel, 2007). Current injection experiments conducted both by myself (Figure 3-1) and by others in the lab (Haag and Borst, 2000) demonstrated that the dependence of calcium indicator fluorescence on membrane potential in VS cells is reasonably linear within the range of voltage deflections expected from visual stimulation. Although the linear coefficient associated with this dependence is different for axons and dendrites in both datasets, this difference can be accounted for by normalization.

The concentration of calcium in LPTCs was estimated both *in-vivo* (Borst and Egelhaaf, 1992) and in an *in-vitro* preparation (Brotz et al., 1995), in both cases using ratiometric measurement with fura-2 (Oertner et al., 2001; Oertner, 2000). The *in-vivo* measurements resulted in a value of 20-60nM for resting calcium, and 85nM-130nM during preferred direction visual stimulation. The *in-vitro* measurements, on the other hand, resulted in a value of 150nM for the resting state and up to 400nM under carbachol stimulation of the cholinergic receptors. For Oregon Green BAPTA-1 (OGB-1, $K_d = 170\text{nM}$) the *in-vivo* values seem marginally within the

linear regime of the dye where $[Ca^{2+}]_i \ll K_d$, especially if we take into account that the K_d of OGB-1 rises to $\sim 260\text{nM}$ in an *in-vivo* preparation of *Drosophila* larval motoneurons (Hendel et al., 2008). The *in-vitro* values, however, are clearly outside of the linear regime, a result which is at odds both with the above mentioned current injection results and with the *in-vivo* measurements by Borst and Egelhaaf (1992). This discrepancy might be caused by the difference between the two preparations. Specifically, it is well known that severing the descending connectives from the brain to the thoracic ganglion results in loss of visual responses in LPTCs (unpublished), and this “death” of the LPTCs may well be associated with a rise in intracellular calcium. In undocumented observations which I made in the course of this work, cells loaded with calcium dye seemed to undergo an abrupt rise in raw fluorescence, clearly visible in the live feed of the CCD camera, after which the cells ceased to respond electrically or with calcium influx to motion stimulus. This might be another indication that calcium levels in non-responsive, “dead” LPTCs are elevated, although obviously more experimentation is needed to clarify this issue.

To stay on the safe side, in the dynamic motion experiments I changed the calcium indicator to the low-affinity Oregon Green BAPTA 6-F (OGB-6-F, $K_d=3\mu\text{M}$). In the case of this indicator, even the *in-vitro* values cited above are an order of magnitude smaller than the K_d of the dye, well within the linear regime. This allowed me to safely assume linear coding along the framework laid out by Borst and Abarbanel, (2007).

4.1.2. Single electrode voltage clamp

Voltage clamping neurons using two electrodes was invented by Kenneth Cole in the 1940s (e.g., Cole, 1949), and used in the seminal work of Hodgkin and Huxley to characterize the currents involved in action potentials of the squid giant axon (Hodgkin et al., 1952; Hodgkin and Huxley, 1952). The electrical separation of the current injecting electrode and the voltage-measuring electrode in the two-electrode voltage clamp was subsequently replaced by a temporal separation of a current injection interval and a voltage measurement interval within a “switched-mode” cycle of the single-electrode voltage clamp (Brenneck and Lindeman, 1974; Wilson and Monahangoldner, 1975; Finkel and Redman, 1984). However the idea of using a feedback circuit to control the membrane potential of a neuron using current injection remained essentially the same.

Already in the early days of Cole, Hodgkin and Huxley, it was clear that the two electrodes should be inserted parallel and as deep as possible into the axon to avoid electrotonic decay between the measuring and injecting electrodes, and the resulting distortion of the measurement. When taking this intuitive approach into the context of an electrically distributed structure such as an intact neuron, electrotonic decay means that the effect of the voltage clamp on electrotonically removed locations, such as fine dendritic tips or remote axonal projections, should be negligible. This was indeed shown in model simulations (Johnston and Brown, 1983; Spruston et al., 1993; Borg-Graham et al., 1998) and lately measured and quantified in experiments in brain slices (Williams and Mitchell, 2008). These results brought the inevitable conclusion that the single-electrode voltage clamp can only be used to control local membrane potential, and is practically useless in controlling remote structures.

4.1.3. Local voltage clamp as a tool

I propose to turn this argument on its head: If voltage clamp is locally effective but remotely ineffective, the experimenter can use it to block specific sources of input within the cell by placing electrodes in the pathway of these sources and clamping membrane potential to the resting potential. This will block the desired pathway, but will not substantially affect the integration of information sources located further downstream (or upstream, for example in the case of back-propagating action potentials) from the electrode. Naturally, if there is no good spatial and electrotonic separation between different information input sites of the cell, this method will not be useful, and will probably result in significant interference between the desired pathway for blocking and the pathway which is to be left unblocked. However, the model simulations of voltage clamps I carried out, based on a biophysically realistic model of the VS cell network, show that this is not the case in my preparation, at least insofar as the model is a good description thereof.

Another concern with the single-electrode voltage clamp technique is that of over- or undercompensating the capacitance of the electrode. This could cause the micropipette voltage to have insufficient time after the current injection cycle to decay to zero before taking a voltage measurement sample, and the result is referred to as “micropipette clamping” - the micropipette voltage is clamped instead of or in addition to that of the cell. I took two measures to ensure this is not the case with my voltage clamp, namely that of waxing the shaft of the electrode to decrease its capacitance, and thereby its time constant, and the compensation protocol under sinusoidal current injection (see Methods). However, both methods might not

prove sufficient to cover the potential caveat of micropipette clamping. This is of special concern when considering the results of Figure 3-7, where in VS2 and VS3 cells there is very little change in the axon-terminal receptive fields relative to those measured without dendritic voltage clamp, and therefore might be the result of micropipette clamping. However, the fact that under dendritic voltage clamp, VS4 cells show a reduced axon-terminal response to gratings located in the dendritic receptive fields of these cells speak strongly against this interpretation, and in favor of an efficient voltage clamp of the dendritic signal.

4.1.4. The effects of dendritic voltage clamp in VS cells

The masking of the predicted dip in the axon-terminal receptive field in VS2 and its partial masking in VS3 can be explained by the extensive overlap of VS1's dendritic receptive field with those of VS2 and VS3 (Figure 3-4), together with the weaker VS1-VS3 connectivity relative to VS1-VS2 (Haag and Borst, 2004), making the predicted dip in the axon-terminal receptive field of VS2 more effectively masked by connectivity with VS1 than that of VS3. This interpretation also seems plausible considering the small effect of VS3 ablation on the receptive field of VS1, compared to that of ablating VS2 on the receptive field of VS4 (Farrow et al., 2005). The latter result also rules out a similar overlapping effect of VS5 on VS4. Although we could not reliably map VS5's dendritic receptive field, we can dismiss any significant overlap with VS4's dendrite based on morphological evidence (Krapp et al., 1998). VS1's overlapping dendritic receptive field with those of VS2 and VS3 may also explain why the electrically measured receptive fields of VS1-3 overlap extensively at the horizon (Farrow et al., 2005; Krapp et al., 1998).

4.2. Relation to previous results

In this section I will discuss the relevance of the results and the relation they have to previous work in the field. The lobula plate of the fly has been an experimental system for over 40 years, and techniques such as intracellular electrophysiology and *in-vivo* calcium imaging have been available in it for decades. Although in my work I have not introduced new measurement techniques, I will argue that the application of old techniques within the framework of newly available results, the combination of methods, the use of old methods in new approaches, and the methodological control of the stimuli can result in advances of our understanding of this system.

4.2.1. Receptive field broadening in VS cells

The lateral, gap-junction mediated connections between VS cells are thought to underlie the broadening of receptive fields in the VS cell network (Haag and Borst, 2004). This has been demonstrated by others in the lab both experimentally by laser ablation of neighboring cells (Farrow et al., 2005) and in modeling studies by realistically simulating the VS cell network and the inputs to each cell (Cuntz et al., 2007). However, these results have a few drawbacks.

In the ablation experiments by Farrow et al. (2005), despite many of the results being statistically significant, the reduction in the broadening of the receptive fields was in some cases quantitatively not strong enough to fully account for the 3-4 fold broadening of the receptive fields compared to those expected from the width of the dendrite in the lobula plate. This might be ascribed to variable efficiency of the cell ablation technique, but such an explanation seems unlikely as the authors took satisfactory measures to ensure that a cell was

entirely ablated when they carried out the procedure (Farrow et al., 2005; Farrow, 2005). A more likely explanation is overlapping dendritic receptive fields, along the lines of the explanation given above for the masking of the expected “dip” in the axon-terminal receptive field during dendritic voltage clamp. Thus, the contribution of an ablated cell to the receptive field of its neighbor will be compensated by the neighbor’s own, overlapping dendritic receptive field, or by that of the ablated cell’s other neighbor. In this work I have shown strong evidence for the broadening of VS cell receptive fields within single cells (Figures 3-2, 3-3); here one can see two versions of a cell’s receptive field – one with and one without contributions from neighboring cells, allowing me to rule out potential overlaps when considering the latter.

The modeling results by Cuntz et al. (2007) were instrumental in showing that the gap-junction connections could be responsible for the receptive fields broadening, and also suggested a possible explanation why this broadening is advantageous in the context of optic flow coding. However, as modeling results they should be taken as predictions made using the information collected in experiments, to be used in the design of new experiments. I believe this has been done to a large extent in this work.

4.2.2. Information flow in the lobula plate

The unidirectional flow of information in VS cells, from dendrites to axon-terminal but not the other way, could explain some results that seem to be at odds with a lobula plate wiring diagram in which each cell is considered to be a single, equipotential compartment. As described above in the Introduction, injecting positive and negative current into VS1 cells raises and lowers the spiking rate of H1 and H2. However, injecting current into VS2 and VS3 cells

does not have any influence on these cells (Haag and Borst, 2003). This is a surprising result seeing as VS2 and VS3 are both coupled, directly or indirectly, to VS1. This discrepancy can be explained based on the modeling results presented above and on the current injection experiments by Cuntz et al. (2007). VS1 is coupled with H1 and H2 in its dendritic arborization in the lobula plate; current injected directly into VS1 will reach both the dendrite and axon terminal of the cell, invade both H1 and H2, and modify their spiking frequency (Figure 4-1a, blue electrode and arrows). However, current injected into VS2 and VS3 will only reach the axon-terminal of VS1, will not invade the dendrites, and therefore have no influence on H1 and H2's spiking rate (Figure 4-1a, red electrodes and arrows).

In the context of the coupling between VS1 and H1 and H2, one should also note that H1 and H2 receive inhibitory synaptic input on their dendrites from ipsilateral CH cells (Figure 4-1a, dCH only shown). Taken together with the principle of chemical shunting of gap junction connectivity, one should expect that if the CH cells are activated in their dendrites (e.g. by ipsilateral progressive motion or by current injection), the H1 and H2 cells should lose their responsiveness to vertical motion, conveyed to them by the coupling with VS1. However, if CH cells are ablated, the vertical sensitivity should persist even under ipsilateral progressive motion. Thus, vertical input to H1 and H2 may only be relevant to the system when shunting inhibition from CH cells do not veto it under progressive horizontal motion, the null-direction for H1 and H2. This feature might be behaviorally relevant in the context of yaw versus pitch rotational selectivity of these cells. The effect of ipsilateral null direction motion on vertical sensitivity of H1 and H2 is an interesting prediction that can easily be tested experimentally.

An interesting demonstration of the principle of separating gap junctions from synaptic input to ensure effective electric coupling can be found in the coupling of medial VS cell dendrites to the spiking neuron Vi and to dCH (Haag and Borst, 2007). This work showed that the medial-to-lateral direction of the reciprocal inhibitory connection between medial and lateral VS cells is mediated by the spiking neuron Vi, which is coupled dendritically to the

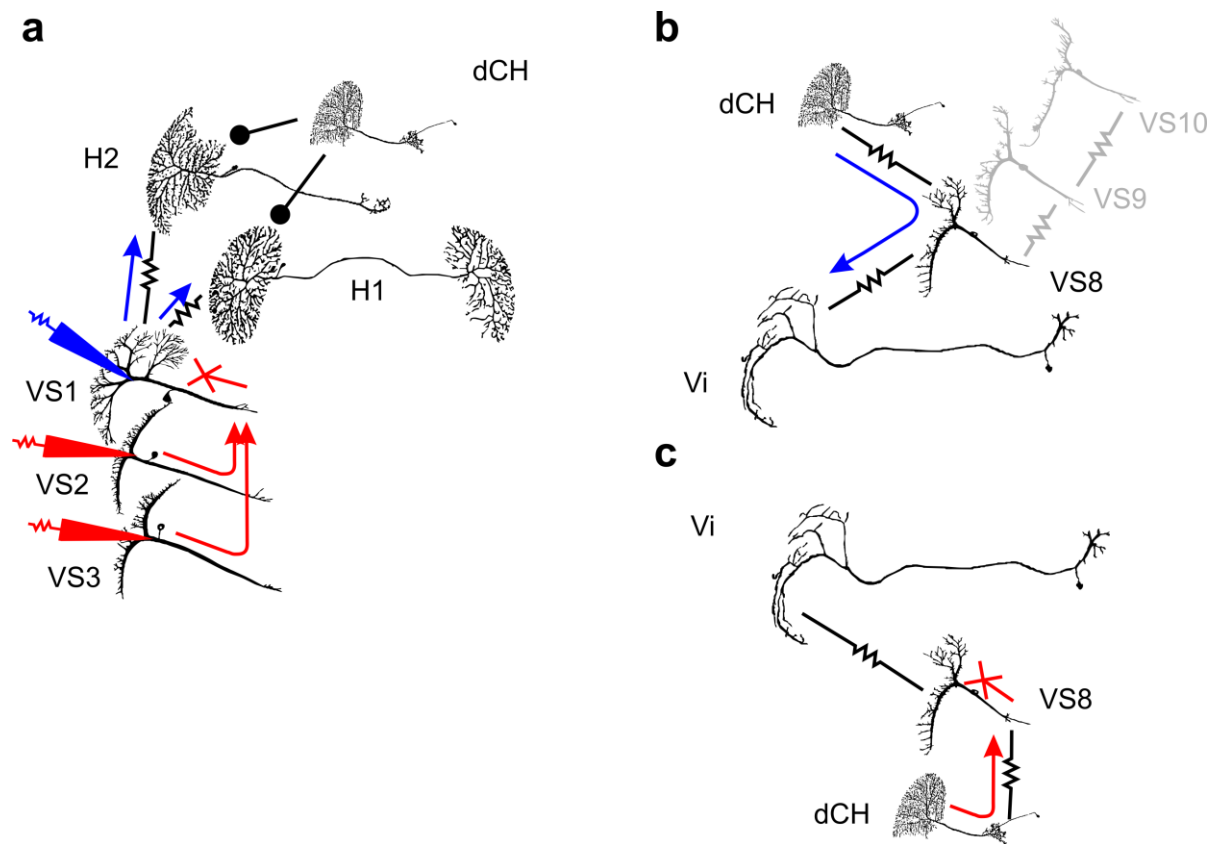


Figure 4-1: Schematic of VS cell connectivity with other LPTCs

a. Dendritic coupling of VS1 with H1 and H2. Current injected in VS1 can pass to H1 and H2 and modulate their spiking frequency (blue arrows), however current injected into VS2 and VS3 is transferred to VS1 in the axon-terminal, cannot invade VS1's dendrite, and cannot pass to H1 and H2 (red arrows). b. Coupling of medial VS cells to Vi and dCH (only connections with VS8 shown for clarity). dCH is coupled to VS8 putatively in the latter's dendrite in the horizontal-selectivity layer of the lobula plate, and so current injected into dCH can pass to the coupled VS8, and on to the dendritically coupled Vi to modify its spiking frequency. c. Implausible connectivity scheme; dCH coupled to VS8 further down the axonal shaft. Current injected into dCH will pass to VS8's axon, will not invade the dendrite and will not pass to Vi.

dendrites of VS7-10 (Figure 4-1b). This fits well with a unidirectional flow of excitation from the VS cells' dendrites to those of Vi, but not vice versa (Vi spikelets recorded in VS9 are attenuated by more than 90%). However, it was also shown that medial VS cells are coupled to dCH cells, a connection responsible for the horizontal motion sensitivity of the medial VS cells in the frontal, dorsal visual field (Figure 4-1b). Considering the results in that paper, and taking into account the anatomy of the Vi cell, which can contact VS cells only in the lobula plate, the dCH-to-medial VS cell coupling can only take place in the lobula plate, and not further down the axonal projections of these two neurons. The reason for this is that the medial VS cells and Vi can be coupled only in the dendrites for anatomical reasons, and that dCH is coupled to Vi indirectly through the medial VS cells, and not directly (Haag and Borst, 2007 diagram in Figure 4-1b, blue arrow). Were the coupling between dCH and the medial VS cells to take place in the axonal projection, current injected into dCH (and also into HSN, transferred to the dCH through their electrical coupling; Haag and Borst, 2004; Haag and Borst, 2007) would not reach the dendrites of the VS cells, invade the Vi cell and change its spiking frequency, contrary to experimental results (Figure 4-1c, red arrow).

This interpretation poses a problem: if dCH input to the medial VS cells arrives at the dendrite through electrical coupling, how is it that the chemical synaptic input to the VS cells does not shunt this input? To understand this, one should consider that the coupling with dCH probably takes place in a separate dendritic branch that ramifies in the frontal, horizontal-selectivity layer of the lobula plate, and not where the synaptic input from vertical-sensitive motion detectors arrives on the other part of the VS cell dendrite (see Figure 1-7a, horizontal layer dendrites marked in gray). On the other hand, it is not known whether vertically sensitive

chemical synapses exist on that dendritic branch (a very unlikely prospect), and so theoretically the dCH-medial VS cell coupling could also be shunted under vertical motion. An alternative explanation for this scenario is that during strong vertical responses, the horizontal input to the medial VS cells is behaviorally irrelevant and will therefore not contribute to the cells' responses. These alternative explanations can once again be tested experimentally.

4.3. Broad receptive fields and population coding

Why are broad receptive fields useful for population coding in the VS cell network? Broad, overlapping tuning curves in a population code might be useful to provide robustness against cell death and to ensure effective excitation of many cells given a certain stimulus (Sanger, 2003). But intuitively, making receptive fields broader should deteriorate the information content of a population, just as reducing the resolution in an image makes the image less sharp and thus contain less information. This intuition has mathematical grounds – generally speaking, narrow receptive fields tend to have steeper slopes, and so discrimination along these slopes is better for a given change in stimulus location. For populations of neurons, this can be quantified using Fisher Information, a measure that is related to the error of parameter estimation through the Cramér-Rao bound and also to Shannon Information, under certain non-restrictive conditions (Blahut, 1987; Brunel and Nadal, 1998; Clarke and Barron, 1990). Indeed, in the case of a population of neurons coding a single variable (not necessarily a spatial one) with independent Gaussian noise, the Fisher information is a sum of the slopes of the tuning curves scaled by the inverse of the noise:

$$I = \sum \frac{f'_i(\theta)^2}{\sigma^2}$$

where f , a function of θ , is the tuning curve and σ is the variance of the Gaussian noise (Seung and Sompolinsky, 1993; Pouget et al., 1999). Interestingly, it was shown that when monkeys are trained for orientation discrimination, cortical cells change their orientation tuning to make the slope of the tuning curve steeper in the tested area in area V1 (Schoups et al., 2001) and V4 (Raiguel et al., 2006).

4.3.1. Noise correlations

However, this simple picture changes dramatically when noise correlations are introduced. Correlative noise between neuronal responses can affect the Fisher Information positively or negatively, depending on many features of the population coding such as the strength and sign of the correlation, the noise model (e.g. additive, multiplicative, Gaussian, Poisson), and the dimension of the coded stimulus (Abbott and Dayan, 1999). An interesting model when considering the VS cell network is that of limited-range correlations, in which the noise correlation between two neurons is a decreasing function of the distance between their tuning curves. Here, the effect of increasing the length and strength of noise correlation on the Fisher Information is non-monotonic, decreasing it when correlations are weak and short, but then gradually turning its sign and increasing it when the correlations are strong and long (Snippe and Koenderink, 1992; Abbott and Dayan, 1999). However, in this case the effect of broadening and overlapping the tuning curves is not explicitly discussed.

4.3.2. Stimulus dimension

Also interesting for the case of VS cells is the effect of the dimensionality of the coded stimulus on the Fisher information content. In a model with multiple, non periodic coding dimensions, radial symmetric tuning curves which are identical in all dimensions, and independent Gaussian noise, broader receptive fields of neurons pays off (in terms of Fisher information) when the encoded variable is of more than two dimensions:

$$J = \eta \sigma^{D-2} K_\phi(F, \tau, D)$$

where J is the Fisher information, η is the number of neurons with tuning curve centers in a given unit of volume, σ is the tuning curve width, D is the dimension of coding space, F is the mean peak firing rate, and τ is the integration window and K_ϕ is an expression that depends on the tuning curves of the neuronal population (Zhang and Sejnowski, 1999). This insight stays essentially the same when noise correlations are added; positive noise correlations will *improve* the Fisher information content, introducing a factor of $\frac{1}{1-q}$ where q is the correlation coefficient.

The intuition to be gained here is that sharpening tuning curves may result in increasing the information carried by *single* neurons; however it also reduces the number of simultaneously active neurons, a factor that is more important in high-dimensional spaces where more information can be extracted from overlaps between different neurons (Zhang and Sejnowski, 1999; Eurich and Wilke, 2000). This can be better seen when the condition of isotropic tuning curves in all dimensions is relaxed. In this case Fisher information in a given dimension i becomes a tradeoff between sharpening the tuning curve in that “informative”

dimension and broadening the tuning curves in the other, “non-informative” dimensions, which essentially ensures that for a given stimulus, enough neurons will be activated:

$$J_i = \eta D K_\phi(F, \tau, D) \frac{\prod_{k=1}^D \sigma_k}{\sigma_i^2}$$

The notation is as before, but here each dimension has its own tuning curve width σ_i , and the information is measured in the dimension i . However, sharpening the tuning curve only works up to a certain point; sufficient overlaps must exist between the tuning curves in the “informative” dimension, otherwise the coding breaks down, leaving patches of uncoded stimuli, and becomes suboptimal. This results in an optimal tuning curve width for any number of stimulus dimensions (Eurich and Wilke, 2000). Broadening of tuning curves in progressive coding stages in the mammalian visual system is a well documented phenomenon; as the complexity of the coded stimulus gets larger, the tuning curves become broader. For example, V1 neurons have narrower tuning curves in macaque than V2 neurons (De Valois et al., 1982; Levitt et al., 1994; Ringach et al., 2002), and V4 neurons (David et al., 2006).

A similar analysis for the coding of periodic stimuli also yields an optimum tuning curve for stimuli with more than two dimensions, the optimum getting broader the more dimensions are added and the larger the period of the stimulus (Montemurro and Panzeri, 2006). This might be of more interest regarding VS cells, in which some coding dimensions such as direction and axis of rotation are periodic. Interestingly, these results fit the broadening of tuning curves found in visual cortex from orientation selective neurons (period of 180°) to directional-selective neurons (period of 360°, see e.g. (Albright, 1984; Kohn and Movshon, 2004)).

4.3.3. Relevance to the VS cell network

It is tempting to speculate that since the stimuli that VS cells encode are high-dimensional (space, direction, contrast, luminosity, speed, contrast frequency and rotational axis), it would make sense to have broader tuning curves, with positive noise correlations, in the non-informative dimensions. However, a comparison between the theoretical results presented above and the actual empirical measurements of VS cells' receptive fields, tuning curves and noise correlations is far from trivial and merits a work of its own. It would also be interesting to see whether the coupling strength between VS cells is optimized to maximize such an informational measure such as Fisher information. The coupling strength of VS cells is essentially a tradeoff between two opposing extremes: at the one end, if the coupling coefficient would be 1, all VS cells would have the exact same output and would not be able to code differences in the rotational axis. On the other hand, if the VS cells would not be coupled at all (coupling coefficient 0), the advantage of local linear integrations would be lost. Somewhere between these two extremities, an optimal solution should be available, given the statistics of the visual input and the utilization of information encoded in the VS cell network by downstream neurons.

It is important to keep in mind, though, that gap junctions between VS cells cannot increase the information content of the entire network, and in that sense do not truly improve the population coding. Rather, this computational intermediate step might benefit downstream neurons by averaging out fluctuations arising from the spatial structure of the visual input. This is especially useful for postsynaptic neurons pooling small subsets of VS cell outputs and

integrating information from other subsystems that might be unaffected by these sources of fluctuations (Haag et al., 2007b; Haag and Borst, 2008; Wertz et al., 2008b).

4.4. Gap junctions

One last point of consideration in the analysis of the results presented above is the question of electrical coupling between VS cells. What are the functional advantages of using gap junctions for receptive field broadening? Connecting neuronal processes with gap junctions or with branching points is biophysically equivalent when the gap-junctions are passive. Thus, it is not inconceivable to have one giant VS cell with ten dendrites and ten different output processes, or, for example, three uncoupled VS cells with three dendrites each, or any other combination along those lines. Likewise it could be possible to account for the broad receptive fields at the level of the VS cell dendrites, simply by integrating broader fields of local motion inputs.

Gap junctions are channel-forming protein structures that connect the plasma membranes of two adjacent cells to allow direct metabolic and electrical communication. Electrically, when connecting two neurons, they function as low-pass filter comparators, transferring current between the cells only when there is a difference in the potentials between both sides (Migliore et al., 2005; Galarreta and Hestrin, 2001; Connors and Long, 2004; Sohl et al., 2005). They do not incur the costs involved in chemical transmission such as maintaining and activating the synaptic mechanism, synthesizing the transmitter and recycling it, and maintaining spatial proximity to the post-synaptic partner. In an electrical synapse, cells need

Discussion

only to invest is synthesizing the innexin proteins and maintaining them. This, in itself, is a good argument against pooling broader, overlapping arrays of local motion detectors on the VS cell dendrite in order to broaden receptive fields – it is simply much more energetically costly. The price for this cost-effectiveness is that electrical synapses cannot be used to amplify transmitted signals, or to invert their signs (e.g. as inhibitory synapses do).

Another alternative circuitry could be achieved by simply replacing the gap junctions with branching points. One argument that could speak against this is that the developmental program of LPTCs might not be able to generate neurons that have multiple main dendrites and multiple output regions. A more interesting prospect is that gap junctions could be used in this system as convenient regulation points both for short-term and long term modifications. Regulation of gap-junction coupling strength by various gap-junction modulators has been described in the vertebrate retina (DeVries and Schwartz, 1989; Hampson et al., 1992; Mills and Massey, 1995), and such regulation is thought to serve as a means of improving the signal-to-noise ratio in darkness by sacrificing spatial acuity both in amacrine cells (Bloomfield et al., 1997; Bloomfield and Volgyi, 2004; Xia and Mills, 2004; Mills et al., 2007). Whether gap junctions between VS cells serve a similar function is an interesting possibility that can be tested experimentally. However, modifications of branch connectivity have been recently demonstrated in hippocampal CA1 pyramidal cells, suggesting that local modifications of membrane permeability and excitability could serve similar functions (Losonczy et al., 2008).

4.5. Separating VS cell input sources

In this work, I showed that in VS cells, separating the lateral, gap junction interactions from chemical synapses serves to separate these interactions from the conductive load generated by the dendritic synapses. This ensures effective gap junction connectivity, allowing for the linear “interpolation” of dendritic responses and a robust representation of motion information in the axon terminals, the output regions of these cells. This provides a functional explanation for the striking T-shaped morphology of the VS cells, and as this separation of input sources is common to many LPTCs, it might serve as a general structural principle in the lobula plate (Pierantoni, 1976; Hausen, 1982a; Eckert and Dvorak, 1983). As mentioned above, in a passive model, connecting two neuronal processes by a branching point or by a gap junction is biophysically equivalent, making the findings presented in this work relevant for understanding the functional structure of neuronal arborizations.

Notably, effects of chemical synapses on electrical synapses have been demonstrated in other systems, such as the dynamic decoupling of mammalian inferior olivary neurons (Llinas et al., 1974; Lang et al., 1996) and of the pharyngeal motor neurons in the mollusk *Navanax* (Spira and Bennett, 1972) by shunting inhibition. In these systems, a complementary principle is implemented: the chemical synapses are located in close proximity to the gap junctions to maximize their shunting effect. In the oculomotor system of teleost fish, the degree of proximity or separation of synaptic inputs from gap junction coupling determines how functionally coupled these inputs are—that is, how synchronous the resulting activation of the coupled cells is (Kriebel et al., 1969; Korn and Bennett, 1975).

4.5.1. Linear and non-linear integration

In addition to enhancing the effectiveness of gap-junction coupling, separating dendrites from the influence of lateral interactions might be useful in isolating local computations that depend on the dendritic membrane potential. For example, the final subtraction step of the Reichardt-type motion detectors, which takes place in the dendrites of lobula plate cells, involves a combination of excitatory and inhibitory inputs that are tuned to opposing motion directions. These inputs exert synaptic driving forces that depend on the postsynaptic potential, and jointly balance this potential at its input-driven value (Borst et al., 1995; Single et al., 1997). Receptive field separation may also allow for nonlinear processing steps, such as amplification of high-frequency components by active properties (Haag and Borst, 1996; Haag et al., 1997), response saturation as a function of stimulus size (Hausen, 1982b; Hengstenberg, 1982; Haag et al., 1992; Haag and Borst, 1994; Haag et al., 1999), and gain control (Borst et al., 1995; Single et al., 1997), to take place before linearly integrating information from neighboring cells.

These speculations are yet to be tested in this system, but modeling (Mel et al., 1998; Archie and Mel, 2000; Poirazi et al., 2003a; Poirazi et al., 2003b) and *in vitro* (Liu, 2004; Polsky et al., 2004) studies of cortical neurons as well as *in vivo* studies of locust visual neurons (Gabbiani et al., 1999; Gabbiani et al., 2002) support the notion that proximal synaptic inputs interact nonlinearly, but inputs coming from separate dendritic branches sum linearly. An interesting question that arises in this context is that of the vertical dendritic structure of the VS cells. One could theoretically conceive of a larger array of VS cells, in which each VS cell pools a small, circular patch of local motion detectors which would then be selectively linearly coupled to form the receptive fields of VS cells in their output regions. Taking that in mind, what is the

functional significance of the non-linear integration of inputs in a vertical stripe, and subsequently a linear integration in the horizontal dimension? A very speculative suggestion could point to the horizon, or a similar horizontal contrast border between dark (trees, foliage, ground) and light (sky, clouds) as a common feature of many naturalistic settings. Thus, the function of the vertical dendrite would be to capture the motion of this landmark in a threshold-like manner, and construct the representation of the axis of rotation in the output regions of the VS cells from the position of this feature.

Another possibility to explain this separation comes from a similar two-tier integration process which has been recently suggested for calculating the likelihood function of a stimulus by a population of sensory neurons (Jazayeri and Movshon, 2006). In this model, each cell in the second layer calculates a weighted sum of the first layer's receptive fields to generate a representation of the likelihood function. An array of dual-compartment cells, such as the one presented above, can achieve this two-step computation faster and energetically more efficiently, without the need for additional synaptic steps.

4.6. Small field selectivity of VS cell dendrites

A surprising result that came from this work was that the dendrites of VS cells are selective for small-field motion, and their responses get attenuated as stimulus size grows in the horizontal, but not the vertical dimension. This serves as a good demonstration for the advantages of being able to separate the feed-forward, motion detector inputs from the lateral,

Discussion

lobula plate interactions in accessing the former in their more “clean” form, without effects being masked by the lateral interactions.

What could be the underlying mechanism for this small-field selectivity? One possibility to consider is presynaptic lateral inhibition between motion detector output channels. Lateral inhibition is a common motif in many sensory systems (Aungst et al., 2003; Balboa and Grzywacz, 2000; Wu et al., 2008), but its function and purpose are still debated (e.g., Series et al., 2004; Oswald et al., 2006). Lateral inhibition was described between laminar columns in the fly (Zettler and Järvilehto, 1972; Laughlin and Hardie, 1978), however, the neurons in these columns are not sensitive to motion, so it is unlikely that this lateral inhibition participates in a such a motion-dependent effect. A more similar, motion-sensitive form of lateral inhibition was found between horizontal motion detectors in the locust visual system (O'Shea and Rowell, 1975), where it is believed to prevent adaptation to wide-field motion in the context of object detection. Thus, the inhibitory effect we observed might be a reflection of phylogenetic similarities in the peripheral visual systems across various insect taxa (Laughlin and Hardie, 1978; Buschbeck and Strausfeld, 1996). However, these two phenomena differ both in magnitude and in direction selectivity, so it is yet unclear whether they both result from the same underlying mechanism. A second possible mechanism could be a large-field cell that inhibits the responses in the dendrites only at larger grating sizes, similar to a mechanism suggested for inhibition of FD-cells by the wide-field CH cells (Warzecha et al., 1993), and also consistent with an alternative model of gain-control by large-field inhibitory cells in the lobula plate (Neri, 2006).

What could be the location of this inhibitory action? The possibility of dendro-dendritic inhibition between VS cell dendrites is easily ruled out since it requires them to have output synapses, as well as physical contacts; both have not been found (Hausen et al., 1980; Haag and Borst, 2004; Raghu et al., 2007). Two remaining possibilities are inhibition by presynaptic elements on the dendrites of the VS cells, and inhibition of the presynaptic elements before they synapse on the VS cell dendrites. A simple experiment can discriminate between these alternatives: if inhibition by larger gratings takes place on the VS cell dendrites, increasing the size of the grating will recruit additional inhibitory synaptic input, reducing the input resistance of the cell. On the other hand, if inhibition affects the presynaptic excitatory inputs to the VS cells, reducing their amplitude before they synapse on the VS cells' dendrites, the input resistance of the cell should grow with the size of the grating.

What could be the functional significance of small-field tuning in the VS cell dendrites? A similar small-field selectivity was found in horizontal selective LPTCs, the so-called figure detection (FD) cells, which are thought to mediate the optomotor orientation of flies towards small-field oscillating gratings (Egelhaaf, 1985a; Gauck and Borst, 1999). The possibility of the existence of a similar, vertically sensitive small-field selective element in the lobula plate has been raised in another study of fly optomotor responses (Hausen and Wehrhahn, 1990) but such a cell in the lobula plate has not yet been described. It remains an intriguing possibility that small-field selectivity in the vertical system is first generated in the dendrites of VS cells or in their immediate presynaptic partners. Still, it seems counter-intuitive that the dendrites should be small-field tuned since the main outputs of VS cells, the axon-terminals, are clearly tuned to large-field stimuli, an important requirement of a system participating in global flow-

Discussion

field processing. Thus, the small-field tuning of the dendrites is lost by the time the signal reaches the cells' post-synaptic partners.

If indeed the underlying mechanism is lateral inhibition, the advantage could indeed be along the lines of the adaptation avoidance effect in the locust (O'Shea and Rowell, 1975). This can be tested by presenting either a small-field or a large-field adaptation stimulus and testing its effect on a subsequently presented small-field stimulus. A large-field stimulus will activate the lateral inhibition and adaptation will be avoided, thus the response to the second stimulus will remain unaffected. On the other hand, a small-field stimulus will not drive lateral inhibition, and the response to the second stimulus will be significantly reduced. Another possible advantage could be seen if the dendrites of VS cells are presynaptic in the lobula plate. Although this was ruled out for chemical synapses based on electron micrographs in *Calliphora* (Hausen et al., 1980) as well as immunohistochemistry in *Drosophila* (Raghu et al., 2007), dendritic gap-junction connectivity between frontally tuned VS cells and H1 and H2 cells (Haag and Borst, 2003) as well as between caudally-tuned VS cells and the spiking neuron Vi (Haag and Borst, 2007) could serve as an output signal for such small-field selective responses.

Finally, are HS-cell dendrites also selective to small-field horizontal motion? The horizontally selective HS-cells are also directly post-synaptic to local motion detectors, and so if a similar presynaptic mechanism for small-field selectivity exists in the horizontal system, it might be found in the dendrites of HS-cells. This is an interesting possibility also considering that lateral inhibition in the locust is between horizontal motion detectors.

References

1. Abbott LF, Dayan P (1999) The effect of correlated variability on the accuracy of a population code. *Neural Comput* 11: 91-101.
2. Adelson EH, Movshon JA (1982) Phenomenal coherence of moving visual patterns. *Nature* 300: 523-525.
3. Albright TD (1984) Direction and orientation selectivity of neurons in visual area MT of the macaque. *J Neurophysiol* 52: 1106-1130.
4. Alger BE, Nicoll RA (1979) GABA-mediated biphasic inhibitory responses in hippocampus. *Nature* 281: 315-317.
5. Archie KA, Mel BW (2000) A model for intradendritic computation of binocular disparity. *Nat Neurosci* 3: 54-63.
6. Aungst JL, Heyward PM, Puche AC, Karnup SV, Hayar A, Szabo G, Shipley MT (2003) Centre-surround inhibition among olfactory bulb glomeruli. *Nature* 426: 623-629.
7. Baarsma EA, Collewij H (1974) Vestibulo-Ocular and Optokinetic Reactions to Rotation and Their Interaction in Rabbit. *Journal of Physiology-London* 238: 603-625.
8. Balboa RM, Grzywacz NM (2000) The role of early retinal lateral inhibition: more than maximizing luminance information. *Vis Neurosci* 17: 77-89.
9. Barlow HB, Levick WR (1965) The mechanism of directionally selective units in rabbit's retina. *J Physiol* 178: 477-504.
10. Barnes GR (1993) Visual-vestibular interaction in the control of head and eye movement: The role of visual feedback and predictive mechanisms. *Prog Neurobiol* 41: 435-472.
11. Bausenwein B, Dittrich APM, Fischbach KF (1992) The optic lobe of *Drosophila melanogaster*. II. Sorting of retinotopic pathways in the medulla. *Cell Tissue Res* 267: 17-28.
12. Bausenwein B, Fischbach K-F (1992) Activity labeling patterns in the medulla of *Drosophila melanogaster* caused by motion stimuli. *Cell Tissue Res* 270: 25-35.
13. Bialek W, Rieke F, de Ruyter van Steveninck R, Warland D (1991) Reading a neural code. *Science* 252: 1854-1857.
14. Bishop CA, Bishop LG (1981) Vertical motion detectors and their synaptic relations in the third optic lobe of the fly. *J Neurobiol* 12: 281-296.
15. Bishop LG, Keehn DG (1966) Two Types of Neurones Sensitive to Motion in Optic Lobe of Fly. *Nature* 212: 1374-&.
16. Blahut RE (1987) Principles and practice of information theory. Reading, MA: Addison-Wesley.
17. Blomfield S (1974) Arithmetical Operations Performed by Nerve-Cells. *Brain Res* 69: 115-124.
18. Blondeau J (1981) Electrically Evoked Course Control in the Fly *Calliphora-Erythrocephala*. *J Exp Biol* 92: 143-153.
19. Blondeau J, Heisenberg M (1982) The three-dimensional optomotor torque system of *Drosophila melanogaster*. *J Comp Physiol* 145: 321-329.
20. Bloomfield SA, Volgyi B (2004) Function and plasticity of homologous coupling between All amacrine cells. *Vision Res* 44: 3297-3306.
21. Bloomfield SA, Xin DY, Osborne T (1997) Light-induced modulation of coupling between All amacrine cells in the rabbit retina. *Vis Neurosci* 14: 565-576.
22. Bollmann JH, Sakmann B (2005) Control of synaptic strength and timing by the release-site Ca^{2+} signal. *Nat Neurosci* 8: 426-434.
23. Borg-Graham LJ, Monier C, Fregnac Y (1998) Visual input evokes transient and strong shunting inhibition in visual cortical neurons. *Nature* 393: 369-377.
24. Borst A, Abarbanel HD (2007) Relating a calcium indicator signal to the unperturbed calcium concentration time-course. *Theor Biol Med Model* 4: 7.

References

25. Borst A, Bahde S (1986) What kind of movement detector is triggering the landing response of the housefly? *Biol Cybern* 55: 59-69.
26. Borst A, Egelhaaf M (1989) Principles of visual motion detection. *Trends Neurosci* 12: 297-306.
27. Borst A, Egelhaaf M (1990) Direction selectivity of fly motion-sensitive neurons is computed in a two-stage process. *Proc Natl Acad Sci USA* 87: 9363-9367.
28. Borst A, Egelhaaf M (1992) In vivo imaging of calcium accumulation in fly interneurons as elicited by visual motion stimulation. *Proc Natl Acad Sci USA* 89: 4139-4143.
29. Borst A, Egelhaaf M (1993) Detecting visual motion: Theory and models. In: *Visual motion and its role in the stabilization of gaze* (Miles FA, Wallman J, eds), pp 3-27. Amsterdam, London, New York, Tokyo: Elsevier.
30. Borst A, Egelhaaf M, Haag J (1995) Mechanisms of dendritic integration underlying gain control in fly motion-sensitive interneurons. *J Computat Neurosci* 2: 5-18.
31. Borst A, Flanagan VL, Sompolinsky H (2005) Adaptation without parameter change: Dynamic gain control in motion detection. *Proceedings of the National Academy of Sciences of the United States of America* 102: 6172-6176.
32. Borst A, Haag J (1996) The intrinsic electrophysiological characteristics of fly lobula plate tangential cells: I. Passive membrane properties. *J Computat Neurosci* 3: 313-336.
33. Borst A, Haag J (2002) Neural networks in the cockpit of the fly. *J Comp Physiol A* 188: 419-437.
34. Borst A, Reisenman C, Haag J (2003) Adaptation of response transients in fly motion vision. II: Model studies. *Vision Res* 43: 1311-1324.
35. Borst A, Single S (2000) Local current spread in electrically compact neurons of the fly. *Neurosci Lett* 285: 123-126.
36. Borst A, Haag J (2007) Optic flow processing in the cockpit of the fly. *Cold Spring Harbor Monograph Series* 49: 101-122.
37. Braitenberg V (1967) Patterns of Projection in Visual System of Fly .I. Retina-Lamina Projections. *Exp Brain Res* 3: 271-&.
38. Braitenberg V (1972) Periodic Structures and Structural Gradients in the Visual Ganglia of the Fly. Wehner, Ruediger (Ed) *Information Processing in the Visual Systems of Arthropods Symposium Zurich, Switzerland, March 6-9, 1972* Xi+334P Illus Springer-Verlag: Berlin, West Germany; New York, N Y , U S A 3-15.
39. Braitenberg V, Debbage P (1974) A regular net of reciprocal synapses in the visual system of the fly, *Musca domestica*. *Journal of Comparative Physiology A: Neuroethology, Sensory, Neural, and Behavioral Physiology* 90: 25-31.
40. Braitenberg V, Taddei-Ferretti C (1966) Landing reaction of *Musca domestica* induced by visual stimuli. *Naturwiss* 53: 155-156.
41. Bremmer F (2005) Navigation in space - the role of the macaque ventral intraparietal area. *Journal of Physiology-London* 566: 29-35.
42. Bremmer F, Duhamel JR, Ben Hamed S, Graf W (2000) Stages of self-motion processing in primate posterior parietal cortex. *Int Rev Neurobiol* 44: 173-198.
43. Brenneck R, Lindeman B (1974) Theory of A Membrane-Voltage Clamp with Discontinuous Feedback Through A Pulsed Current Clamp. *Review of Scientific Instruments* 45: 184-188.
44. Britten KH (2008) Mechanisms of self-motion perception. *Ann Rev Neurosci* 31: 389-410.
45. Brock LG, Coombs JS, Eccles JC (1952) Synaptic Excitation and Inhibition. *Journal of Physiology-London* 117: 8.
46. Brotz TM, Borst A (1996) Cholinergic and GABAergic receptors on fly tangential cells and their role in visual motion detection. *J Neurophysiol* 76: 1786-1799.
47. Brotz TM, Egelhaaf M, Borst A (1995) A preparation of the blowfly (*Calliphora erythrocephala*) brain for in vitro electrophysiological and pharmacological studies. *J Neurosci Meth* 57: 37-46.
48. Brunel N, Nadal JP (1998) Mutual information, Fisher information, and population coding. *Neural Comput* 10: 1731-1757.
49. Buchner E (1976) Elementary movement detectors in an insect visual system. *Biol Cybern* 24: 85-101.
50. Buchner E (1984) Behavioural analysis of spatial vision in insects. In: *Photoreception and vision in invertebrates* (Ali MA, ed), pp 561-621. New York, London: Plenum Press.

51. Buchner E, Buchner S, Bülthoff I (1984) Deoxyglucose mapping of nervous activity induced in *Drosophila* brain by visual movement. *J Comp Physiol A* 155: 471-483.
52. Buchner E, Götz KG, Straub C (1978) Elementary detectors for vertical movement in the visual system of *Drosophila*. *Biol Cybern* 31: 235-242.
53. Buschbeck EK, Strausfeld NJ (1996) Visual motion-detection circuits in flies: small-field retinotopic elements responding to motion are evolutionarily conserved across taxa. *J Neurosci* 16: 4563-4578.
54. Clarke BS, Barron AR (1990) Information-Theoretic Asymptotics of Bayes Methods. *Ieee Transactions on Information Theory* 36: 453-471.
55. Cole KS (1949) Dynamic Electrical Characteristics of the Squid Axon Membrane. *Archives des Sciences Physiologiques* 3: 253-258.
56. Collett TS, Nalbach HO, Wagner H (1993) Visual stabilization in arthropods. In: *Visual Motion and Its Role in the Stabilization of Gaze* (Miles FA, Wallman J, eds), pp 239-263.
57. Connors BW, Long MA (2004) Electrical synapses in the mammalian brain. *Annu Rev Neurosci* 27: 393-418.
58. Coombe PE, Srinivasan MV, Guy RG (1989) Are the large monopolar cells of the insect lamina on the optomotor pathway? *J Comp Physiol A* 166: 23-35.
59. Cuntz H, Haag J, Borst A (2003) Neural image processing by dendritic networks. *Proc Natl Acad Sci U S A* 100: 11082-11085.
60. Cuntz H, Haag J, Forstner F, Segev I, Borst A (2007) Robust coding of flow-field parameters by axo-axonal gap junctions between fly visual interneurons. *Proc Natl Acad Sci U S A* 104: 10229-10233.
61. David SV, Hayden BY, Gallant JL (2006) Spectral receptive field properties explain shape selectivity in area V4. *J Neurophysiol* 96: 3492-3505.
62. De Valois RL, Yund EW, Hepler N (1982) The orientation and direction selectivity of cells in macaque visual cortex. *Vision Res* 22: 531-544.
63. DeVoe RD (1980) Movement sensitivities of cells in the fly's medulla. *J Comp Physiol* 138: 93-119.
64. DeVries SH, Schwartz EA (1989) Modulation of An Electrical Synapse Between Solitary Pairs of Catfish Horizontal Cells by Dopamine and 2Nd Messengers. *Journal of Physiology-London* 414: 351-375.
65. Dickinson MH (1999) Haltere-mediated equilibrium reflexes of the fruit fly, *Drosophila melanogaster*. *Philos Trans R Soc Lond B Biol Sci* 354: 903-916.
66. Douglass JK, Strausfeld NJ (1995) Visual motion detection circuits in flies: peripheral motion computation by identified small-field retinotopic neurons. *J Neurosci* 15: 5596-5611.
67. Douglass JK, Strausfeld NJ (1996) Visual motion - detection circuits in flies : parallel direction -and non-direction-sensitive pathways between the medulla and lobula plate. *J Neurosci* 16: 4551-4562.
68. Douglass JK, Strausfeld NJ (1998) Functionally and anatomically segregated visual pathways in the lobula complex of a calliphorid fly. *J Comp Neurol* 396: 84-104.
69. Douglass JK, Strausfeld NJ (2003) Anatomical organization of retinotopic motion-sensitive pathways in the optic lobes of flies. *Microsc Res Tech* 62: 132-150.
70. Duffy CJ, Wurtz RH (1991) Sensitivity of Mst Neurons to Optic Flow Stimuli .1. A Continuum of Response Selectivity to Large-Field Stimuli. *J Neurophysiol* 65: 1329-1345.
71. Duke-Elder S (1958) *The eye in evolution*. London: Henry Kimpton.
72. Dürre, V. Dendritic Calcium Accumulation in Visual Interneurons of the Blowfly. 1-119. 1998. Doctoral Dissertation, University Bielefeld, Dept. of Neurobiology.
73. Durr V, Egelhaaf M (1999) In vivo calcium accumulation in presynaptic and postsynaptic dendrites of visual interneurons. *J Neurophysiol* 82: 3327-3338.
74. Dvorak D, Srinivasan MV, French AS (1980) The contrast sensitivity of fly movement-detecting neurons. *Vision Res* 20: 397-407.
75. Dvorak DR, Bishop LG, Eckert HE (1975) On the identification of movement detectors in the fly optic lobe. *J Comp Physiol* 100: 5-23.
76. Eckert H (1973) Optomotorische Untersuchungen am visuellen System der Stubenfliege *Musca domestica* L. *Kybernetik* 14: 1-23.
77. Eckert H (1980) Functional properties of the H1-neurone in the third optic ganglion of the blowfly, *Phaenicia*. *J Comp Physiol* 135: 29-39.

References

78. Eckert H (1981) The Horizontal Cells in the Lobula Plate of the Blowfly, *Phaenicia-Sericata*. *J Comp Physiol* 143: 511-526.
79. Eckert H (1982) The vertical-horizontal neurone (VH) in the lobula plate of the blowfly, *Phaenicia*. *J Comp Physiol* 149: 195-205.
80. Eckert H, Bishop LG (1978) Anatomical and Physiological Properties of Vertical Cells in Third Optic Ganglion of *Phaenicia-Sericata* (Diptera, Calliphoridae). *J Comp Physiol* 126: 57-86.
81. Eckert H, Dvorak DR (1983) The centrifugal horizontal cells in the lobula plate of the blowfly *Phaenicia sericata*. *J Insect Physiol* 29: 547-560.
82. Eckert HE (1978) Response Properties of Dipteran Giant Visual Interneurons Involved in Control of Optomotor Behavior. *Nature* 271: 358-360.
83. Eckmeier D, Bischof HJ (2008) The optokinetic response in wild type and white zebra finches. *Journal of Comparative Physiology A-Neuroethology Sensory Neural and Behavioral Physiology* 194: 871-878.
84. Egelhaaf M (1985a) On the neuronal basis of figure-ground discrimination by relative motion in the visual system of the fly. I. Behavioural constraints imposed on the neuronal network and the role of the optomotor system. *Biol Cybern* 52: 123-140.
85. Egelhaaf M (1985b) On the neuronal basis of figure-ground discrimination by relative motion in the visual system of the fly. II. Figure-Detection Cells, a new class of visual interneurons. *Biol Cybern* 52: 195-209.
86. Egelhaaf M (1985c) On the neuronal basis of figure-ground discrimination by relative motion in the visual system of the fly. III. Possible input circuitries and behavioural significance of the FD-Cells. *Biol Cybern* 52: 267-280.
87. Egelhaaf M (1987) Dynamic properties of two control systems underlying visually guided turning in houseflies. *J Comp Physiol A* 161: 777-783.
88. Egelhaaf M, Borst A (1989) Transient and steady-state response properties of movement detectors. *J Opt Soc Am A* 6: 116-127.
89. Egelhaaf M, Borst A (1992) Are there separate ON and OFF channels in fly motion vision? *Vis Neurosci* 8: 151-164.
90. Egelhaaf M, Borst A (1993a) A look into the cockpit of the fly: visual orientation, algorithms and identified neurons. *J Neurosci* 13: 4563-4574.
91. Egelhaaf M, Borst A (1993b) Motion computation and visual orientation in flies. *Comp Biochem Physiol* 104A: 659-673.
92. Egelhaaf M, Borst A (1995) Calcium accumulation in visual interneurons of the fly: stimulus dependence and relationship to membrane potential. *J Neurophysiol* 73: 2540-2552.
93. Egelhaaf M, Borst A, Reichardt W (1989a) Computational structure of a biological motion detection-detection system as revealed by local detector analysis in the fly's nervous system. *J Opt Soc Am A* 6: 1070-1087.
94. Egelhaaf M, Borst A, Reichardt W (1989b) The non-linear mechanism of direction selectivity in the fly motion detection system. *Naturwiss* 76: 32-35.
95. Egelhaaf M, Borst A, Warzecha AK, Flecks S, Wildemann A (1993) Neural circuit tuning fly visual neurons to motion of small objects II. Input organization of inhibitory circuit elements revealed by electrophysiological and optical recording techniques. *J Neurophysiol* 69: 340-351.
96. Egelhaaf M, Hausen K, Reichardt W, Wehrhahn C (1988) Visual course control in flies relies on neuronal computation of object and background motion. *Trends Neurosci* 11: 351-358.
97. Egelhaaf M, Kern R (2002) Vision in flying insects. *Curr Opin Neurobiol* 12: 699-706.
98. Egelhaaf M, Kern R, Krapp HG, Kretzberg J, Kurtz R, Warzecha AK (2002) Neural encoding of behaviourally relevant visual-motion information in the fly. *Trends Neurosci* 25: 96-102.
99. Egelhaaf M, Petrowitz R, Dahmen H, Krapp H (2000) Adaptation of the compound eye geometry to optic flow processing in the blowfly *Calliphora*. *Soc Neurosci Abstr* 26: Abstract-368.
100. Egelhaaf M, Reichardt W (1987) Dynamic response properties of movement detectors: Theoretical analysis and electrophysiological investigation in the visual system of the fly. *Biol Cybern* 56: 69-87.
101. Elyada YM, Haag J, Borst A (2009) Different receptive fields in axons and dendrites underlie robust coding in motion-sensitive neurons. *nature neuroscience* 12: 327-332.
102. Emerson RC, Bergen JR, Adelson EH (1992) Directionally selective complex cells and the computation of motion energy in cat visual cortex. *Vision Res* 32: 203-218.

103. Esch HE, Zhang S, Srinivasan MV, Tautz J (2001) Honeybee dances communicate distances measured by optic flow. *Nature* 411: 581-583.
104. Eurich CW, Wilke SD (2000) Multidimensional encoding strategy of spiking neurons. *Neural Comput* 12: 1519-1529.
105. Exner S (1891) Die Physiologie der Facettirten Augen von Krebsen and Insecten. Eine studie. Die Physiologie der Facettirten Augen von Krebsen and Insecten Eine studie 206.
106. Farrow, K. Lateral Interactions and Receptive Field Structure of Lobula Plate Tangential Cells in the Blowfly. 1-119. 2005. Doctoral Dissertation, Ludwig Maximilians University, Munich.
107. Farrow K, Borst A, Haag J (2005) Sharing receptive fields with your neighbors: tuning the vertical system cells to wide field motion. *J Neurosci* 25: 3985-3993.
108. Farrow K, Haag J, Borst A (2003) Input organization of multifunctional motion-sensitive neurons in the blowfly. *J Neurosci* 23: 9805-9811.
109. Farrow K, Haag J, Borst A (2006) Nonlinear, binocular interactions underlying flow field selectivity of a motion-sensitive neuron. *Nat Neurosci* 9: 1312-1320.
110. Fatt P, Katz B (1953) The effect of inhibitory nerve impulses on a crustacean muscle fibre. *J Physiol* 121: 374-389.
111. Fermi G, Reichardt W (1963) Optomotorische Reaktionen der Fliege *Musca domestica*. Abhängigkeit der Reaktion von der Wellenlänge, der Geschwindigkeit, dem Kontrast und der mittleren Leuchtdichte bewegter periodischer Muster. *Kybernetik* 2: 15-28.
112. Finkel AS, Redman S (1984) Theory and operation of a single microelectrode voltage clamp. *J Neurosci Meth* 11: 101-127.
113. Fischbach KF, Dittrich APM (1989) The optic lobe of *Drosophila melanogaster*. I. A Golgi analysis of wild-type structure. *Cell Tissue Res* 258: 441-475.
114. Fischbach KF, Hiesinger PR (2008) Optic lobe development. *Brain Development in Drosophila Melanogaster* 628: 115-136.
115. Fite KV (1968) Two Types of Optomotor Response in Domestic Pigeon. *Journal of Comparative and Physiological Psychology* 66: 308-&.
116. Fite KV (1985) Pretectal and Accessory-Optic Visual Nuclei of Fish, Amphibia and Reptiles - Theme and Variations. *Brain Behavior and Evolution* 26: 71-90.
117. Fite KV, Reiner A, Hunt SP (1979) Optokinetic Nystagmus and the Accessory Optic-System of Pigeon and Turtle. *Brain Behavior and Evolution* 16: 192-202.
118. Franz MO, Krapp HG (2000) Wide-field, motion-sensitive neurons and matched filters for optic flow fields. *Biol Cybern* 83: 185-197.
119. Frye MA, Tarsitano M, Dickinson MH (2003) Odor localization requires visual feedback during free flight in *Drosophila melanogaster*. *J Exp Biol* 206: 843-855.
120. Fuchs AF, Mustari MJ (1993) The optokinetic response in Primates and its possible neuronal substrate. *Reviews of Oculomotor Research* 5.
121. Gabbiani F, Krapp HG, Hatsopoulos N, Mo CH, Koch C, Laurent G (2004) Multiplication and stimulus invariance in a looming-sensitive neuron. *Journal of Physiology-Paris* 98: 19-34.
122. Gabbiani F, Krapp HG, Koch C, Laurent G (2002) Multiplicative computation in a visual neuron sensitive to looming. *Nature* 420: 320-324.
123. Gabbiani F, Krapp HG, Laurent G (1999) Computation of object approach by a wide-field, motion-sensitive neuron. *J Neurosci* 19: 1122-1141.
124. Galarreta M, Hestrin S (2001) Electrical synapses between GABA-releasing interneurons. *Nat Rev Neurosci* 2: 425-433.
125. Gauck V, Borst A (1999) Spatial response properties of contralateral inhibited lobula plate tangential cells in the fly visual system. *J Comp Neurol* 406: 51-71.
126. Gauck V, Egelhaaf M, Borst A (1997) Synapse distribution on VCH, an inhibitory, motion-sensitive interneuron in the fly visual system. *J Comp Neurol* 381: 489-499.
127. Geiger G, Nässel DR (1981) Visual orientation behaviour of flies after selective laser beam ablation of interneurons. *Nature* 293: 398-399.
128. Gibson JJ (1958) Visually Controlled Locomotion and Visual Orientation in Animals. *British Journal of Psychology* 49: 182-194.

References

129. Gioanni H (1988) Stabilizing Gaze Reflexes in the Pigeon (*Columba-Livia*) .1. Horizontal and Vertical Optokinetic Eye (Okn) and Head (Ocr) Reflexes. *Exp Brain Res* 69: 567-582.
130. Gioanni H, Rey J, Villalobos J, Bouyer JJ, Gioanni Y (1981) Optokinetic Nystagmus in the Pigeon (*Columba-Livia*) .1. Study in Monocular and Binocular Vision. *Exp Brain Res* 44: 362-370.
131. Goodman LJ (1960) The landing response of insects I. The landing response of the fly, *Lucilla seratica*, and other *Calliphoridae*. *J Exp Biol* 37: 854-878.
132. Goodman LJ (1965) Role of Certain Optomotor Reactions in Regulating Stability in Rolling Plane During Flight in Desert Locust *Schistocerca Gregaria*. *J Exp Biol* 42: 385-&.
133. Götz KG (1964) Optomotorische Untersuchungen des visuellen Systems einiger Augenmutanten der Fruchtfliege *Drosophila*. *Kybernetik* 2: 77-92.
134. Götz KG (1968) Flight control in *Drosophila* by visual perception of motion. *Kybernetik* 4: 199-208.
135. Götz KG, Wenking H (1973) Visual control of locomotion in the walking fruitfly *Drosophila*. *J Comp Physiol* 85: 235-266.
136. Grynkiewicz G, Poenie M, Tsien RY (1985) A new generation of Ca indicators with greatly improved fluorescence properties. *J Biol Chem* 260: 3440-3450.
137. Gu Y, Watkins PV, Angelaki DE, DeAngelis GC (2006) Visual and nonvisual contributions to three-dimensional heading selectivity in the medial superior temporal area. *J Neurosci* 26: 73-85.
138. Haag J. Aktive Und Passive Membraneigenschaften Bewegungsempfindlicher Interneurone Der Schmeissfliege. 11-3-1994. Doctoral Dissertation, Eberhard-Karls-Universität Tübingen.
139. Haag J, Borst A (1994) Membrane parameters and potential spread in fly lobula-plate neurons. In: Göttingen Neurobiology Report 1994 (Elsner N, Breer H, eds), pp 447. Stuttgart, New York: Georg Thieme.
140. Haag J, Borst A (1996) Amplification of high-frequency synaptic inputs by active dendritic membrane processes. *Nature* 379: 639-641.
141. Haag J, Borst A (2000) Spatial distribution and characteristics of voltage-gated calcium signals within visual interneurons. *J Neurophysiol* 83: 1039-1051.
142. Haag J, Borst A (2001) Recurrent network interactions underlying flow-field selectivity of visual interneurons. *J Neurosci* 21: 5685-5692.
143. Haag J, Borst A (2002) Dendro-dendritic interactions between motion-sensitive large-field neurons in the fly. *J Neurosci* 22: 3227-3233.
144. Haag J, Borst A (2003) Orientation tuning of motion-sensitive neurons shaped by vertical-horizontal network interactions. *J Comp Physiol A Neuroethol Sens Neural Behav Physiol* 189: 363-370.
145. Haag J, Borst A (2004) Neural mechanism underlying complex receptive field properties of motion-sensitive interneurons. *Nat Neurosci* 7: 628-634.
146. Haag J, Borst A (2005) Dye-coupling visualizes networks of large-field motion-sensitive neurons in the fly. *J Comp Physiol A Neuroethol Sens Neural Behav Physiol* 191: 445-454.
147. Haag J, Borst A (2007) Reciprocal inhibitory connections within a neural network for rotational optic-flow processing. *Front Neurosci* 1: 111-121.
148. Haag J, Borst A (2008) Electrical coupling of lobula plate tangential cells to a heterolateral motion-sensitive neuron in the fly. *J Neurosci* 28: 14435-14442.
149. Haag J, Denk W, Borst A (2004) Fly motion vision is based on Reichardt detectors regardless of the signal-to-noise ratio. *Proc Natl Acad Sci U S A* 101: 16333-16338.
150. Haag J, Egelhaaf M, Borst A (1992) Dendritic integration of motion information in visual interneurons of the blowfly. *Neurosci Lett* 140: 173-176.
151. Haag J, Theunissen F, Borst A (1997) The intrinsic electrophysiological characteristics of fly lobula plate tangential cells: II. active membrane properties. *J Computat Neurosci* 4: 349-369.
152. Haag J, Vermeulen A, Borst A (1999) The Intrinsic Electrophysiological Characteristics of Fly Lobula Plate Tangential Cells: III. Visual Response Properties. *J Computat Neurosci* 7: 213-234.
153. Haag J, Wertz A, Borst A (2007a) Integration of lobula plate output signals by DNOVS1, an identified premotor descending neuron. *J Neurosci* 27: 1992-2000.
154. Haag J, Wertz A, Borst A (2007b) Integration of lobula plate output signals by DNOVS1, an identified premotor descending neuron. *J Neurosci* 27: 1992-2000.
155. Hampson ECGM, Vaney DI, Weiler R (1992) Dopaminergic Modulation of Gap Junction Permeability Between Amacrine Cells in Mammalian Retina. *J Neurosci* 12: 4911-4922.

156. Hardie RC (1984) Functional organization of the fly retina. In: Progress in Sensory Physiology 5 (Autrum H, Ottoson D, Perl ER, Schmidt RF, Shimazu H, Willis WD, eds), pp 1-79. Berlin, Heidelberg, New York, Tokyo: Springer-Verlag.
157. Hassenstein B, Reichardt W (1956) Systemtheoretische Analyse der Zeit-, Reihenfolgen- und Vorzeichenauswertung bei der Bewegungsperzeption des Rüsselkäfers *Chlorophanus*. Z Naturforsch 11b: 513-524.
158. Hausen, K. The Neural Architecture of the Lobula Plate of the Blowfly, *Calliphora Erythrocephala*. unpublished work.
159. Hausen K (1976) Functional characterization and anatomical identification of motion sensitive neurons in the lobula plate of the blowfly *Calliphora erythrocephala*. Z Naturforsch 31c: 629-633.
160. Hausen K (1977) Struktur, Funktion und Konnektivität bewegungsempfindlicher Interneurone im dritten optischen Neuropil der Schmeißfliege *Calliphora erythrocephala*. dtb.
161. Hausen K (1981) Monocular and binocular computation of motion in the lobula plate of the fly. Verh Dtsch Zool Ges 74: 49-70.
162. Hausen K (1982a) Motion sensitive interneurons in the optomotor system of the fly. I. The Horizontal Cells: Structure and signals. Biol Cybern 45: 143-156.
163. Hausen K (1982b) Motion sensitive interneurons in the optomotor system of the fly. II. The Horizontal Cells: Receptive field organization and response characteristics. Biol Cybern 46: 67-79.
164. Hausen K (1984) The lobula-complex of the fly: Structure, function and significance in visual behaviour. In: Photoreception and vision in invertebrates (Ali MA, ed), pp 523-559. New York, London: Plenum Press.
165. Hausen K, Egelhaaf M (1989) Neural mechanisms of visual course control in insects. In: Facets of vision (Stavenga DG, Hardie RC, eds), pp 391-424. Berlin, Heidelberg, New York, London, Paris, Tokyo: Springer.
166. Hausen K, Wehrhahn C (1983) Microsurgical lesion of horizontal cells changes optomotor yaw response in the blowfly *Calliphora erythrocephala*. Proc R Soc Lond B 219: 211-216.
167. Hausen K, Wehrhahn C (1989) Neural circuits mediating visual flight control in flies. I. Quantitative comparison of neural and behavioral response characteristics. J Neurosci 9: 3828-3836.
168. Hausen K, Wehrhahn C (1990) Neural circuits mediating visual flight control in flies. II. Separation of two control systems by microsurgical brain lesions. J Neurosci 10: 351-360.
169. Hausen K, Wolburg-Buchholz W, Ribi WA (1980) The synaptic organization of visual interneurons in the lobula complex of flies. A light and electron microscopical study using silver-intensified cobalt-impregnations. Cell Tissue Res 208: 371-387.
170. Häusser M, Spruston N, Stuart GJ (2000) Diversity and dynamics of dendritic signaling. Science 290: 739-744.
171. Hecht S, Wald G (1934) THE VISUAL ACUITY AND INTENSITY DISCRIMINATION OF DROSOPHILA. The Journal of General Physiology 17: 517-547.
172. Heisenberg M, Buchner E (1977) The role of retinula cell types in visual behavior of *Drosophila melanogaster*. J Comp Physiol 117: 127-162.
173. Heisenberg M, Wolf R, Brembs B (2001) Flexibility in a single behavioral variable of *Drosophila*. Learning & Memory 8: 1-10.
174. Heisenberg M, Wonneberger R, Wolf R (1978) Optomotor-blind (H31) -a *Drosophila* mutant of the lobula plate giant neurons. J Comp Physiol 124: 287-296.
175. Helmchen F, Imoto K, Sakmann B (1996) Ca^{2+} buffering and action potential - evoked Ca^{2+} signaling in dendrites of pyramidal neurons. Biophys J 70: 1069-1081.
176. Hendel T, Mank M, Schnell B, Griesbeck O, Borst A, Reiff DF (2008) Fluorescence changes of genetic calcium indicators and OGB-1 correlated with neural activity and calcium in vivo and in vitro. J Neurosci 28: 7399-7411.
177. Hengstenberg R (1981) Visuelle Drehreaktionen von Vertikalzellen in der Lobula Platte von *Calliphora*. Verhandlungen der Deutschen Zoologischen Gesellschaft 74: 180.
178. Hengstenberg R (1982) Common visual response properties of giant vertical cells in the lobula plate of the blowfly *Calliphora*. J Comp Physiol A 149: 179-193.
179. Hengstenberg R, Hausen K, Hengstenberg B (1982) The number and structure of giant vertical cells (VS) in the lobula plate of the blowfly *Calliphora erythrocephala*. J Comp Physiol A 149: 163-177.

References

180. Hengstenberg R, Hengstenberg B (1980) Intracellular staining of insect neurons with procion yellow. In: Neuroanatomical techniques (Strausfeld NJ, Miller TA, eds), pp 308-323. New York, Heidelberg, Berlin: Springer Verlag.
181. Hennig P, Müller R, Egelhaaf M (2008) Distributed Dendritic Processing Facilitates Object Detection: A Computational Analysis on the Visual System of the Fly. PLoS ONE 3: e3092.
182. Higgins, C. M., Douglass, J. K., and Strausfeld, N. J. (2004) The Computational Basis of an Identified Neuronal Circuit for Elementary Motion Detection in Dipterous Insects. Vis Neurosci 21, 567-568.
183. Hildreth EC, Koch C (1987) The Analysis of Visual Motion: From Computational Theory to Neuronal Mechanisms. Ann Rev Neurosci 10: 477.
184. Hines ML, Carnevale NT (1997) The NEURON simulation environment. Neural Comput 9: 1179-1209.
185. Hodgkin AL, Huxley AF (1952) A Quantitative Description of Membrane Current and Its Application to Conduction and Excitation in Nerve. Journal of Physiology-London 117: 500-544.
186. Hodgkin AL, Huxley AF, Katz B (1952) Measurement of Current-Voltage Relations in the Membrane of the Giant Axon of Loligo. Journal of Physiology-London 116: 424-448.
187. Holt GR, Koch C (1997) Shunting inhibition does not have a divisive effect on firing rates. Neural Comput 9: 1001-1013.
188. Holub RA, Morton-Gibson M (1981) Response of Visual Cortical-Neurons of the Cat to Moving Sinusoidal Gratings - Response-Contrast Functions and Spatiotemporal Interactions. J Neurophysiol 46: 1244-1259.
189. Horridge GA (1986) A Theory of Insect Vision - Velocity Parallax. Proceedings of the Royal Society of London Series B-Biological Sciences 229: 13-27.
190. Horstmann W, Egelhaaf M, Warzecha AK (2000) Synaptic interaction increase optic flow specificity. Eur J Neurosci 12: 2157-2165.
191. Huang YY, Neuhauss SCF (2008) The optokinetic response in zebrafish and its applications. Frontiers in Bioscience 13: 1899-1916.
192. Hyzer WG (1962) Flight Behavior of A Fly Alighting on A Ceiling. Science 137: 609-&.
193. Ibbotson MR, Mark RF, Maddess TL (1994) Spatiotemporal response properties of direction-selective neurons in the nucleus of the optic tract and dorsal terminal nucleus of the wallaby, *Macropus eugenii*. J Neurophysiol 72: 2927-2943.
194. Jack JJB, Noble D, Tsien RW (1975) Electric current flow in excitable cells. Oxford: Clarendon Press.
195. Jarvilehto M, Zettler F (1973) Electrophysiological-histological studies on some functional properties of visual cells and second order neurons of an insect retina. Z Zellforsch Mikrosk Anat 136: 291-306.
196. Jarvilehto M, Zettler F (1971) Localized intracellular potentials from pre- and postsynaptic components in the external plexiform layer of an insect retina. Journal of Comparative Physiology A: Neuroethology, Sensory, Neural, and Behavioral Physiology 75: 422-440.
197. Jazayeri M, Movshon JA (2006) Optimal representation of sensory information by neural populations. Nat Neurosci 9: 690-696.
198. Joesch M, Plett J, Borst A, Reiff DF (2008) Response properties of motion-sensitive visual interneurons in the lobula plate of Drosophila melanogaster. Current Biology 18: 368-374.
199. Johnston D, Brown TH (1983) Interpretation of voltage-clamp measurements in hippocampal neurons. J Neurophysiol 50: 464-486.
200. Johnston D, Magee JC, Colbert CM, Cristie BR (1996) Active properties of neuronal dendrites. Annu Rev Neurosci 19: 165-186.
201. Juusola M, Kouvalainen E, Jarvilehto M, Weckstrom M (1994) Contrast gain, signal-to-noise ratio, and linearity in light-adapted blowfly photoreceptors. J Gen Physiol 104: 593-621.
202. Kalb J, Egelhaaf M, Kurtz R (2006) Robust Integration of Motion Information in the Fly Visual System Revealed by Single Cell Photoablation. The Journal of Neuroscience 26: 7898-7906.
203. Kalmus HH (1949) Optomotor responses in Drosophila and Musca. Physiol Comp Ocol Int J Comp Physiol Ecol 1: 127-147.
204. Karmeier K, Krapp HG, Egelhaaf M (2005a) Population coding of self-motion: Applying Bayesian analysis to a population of visual Interneurons in the fly. J Neurophysiol 94: 2182-2194.
205. Karmeier K, Krapp HG, Egelhaaf M (2005b) Population coding of self-motion: applying bayesian analysis to a population of visual interneurons in the fly. J Neurophysiol 94: 2182-2194.

206. Katsov AY, Clandinin TR (2008) Motion Processing Streams in *Drosophila* Are Behaviorally Specialized. *Neuron* 59: 322-335.
207. Keng MJ, Anastasio TJ (1997) The Horizontal Optokinetic Response of the Goldfish. *Brain, Behavior and Evolution* 49: 214-229.
208. Kirschfeld K (1967) Die Projektion der optischen Umwelt auf das Raster der Rhabdomere im Komplexauge von MUSCA. *Exp Brain Res* 3: 248-270.
209. Koch C (1999) The membrane equation. In: *Biophysics of Computation* pp 5-24. New York, NY: Oxford University Press.
210. Koenderink JJ (1986) Optic Flow. *Vision Res* 26: 161-179.
211. Koenderink JJ, Vandoorn AJ (1975) Invariant Properties of Motion Parallax Field Due to Movement of Rigid Bodies Relative to An Observer. *Optica Acta* 22: 773-791.
212. Kohn A, Movshon JA (2004) Adaptation changes the direction tuning of macaque MT neurons. *nature neuroscience* 7: 764-772.
213. Korn H, Bennett MV (1975) Vestibular nystagmus and teleost oculomotor neurons: functions of electrotonic coupling and dendritic impulse initiation. *J Neurophysiol* 38: 430-451.
214. Kral K (1998) Side-to-side head movements to obtain motion depth cues: A short review of research on the praying mantis. *Behavioural Processes* 43: 71-77.
215. Kral K (2003) Behavioural-analytical studies of the role of head movements in depth perception in insects, birds and mammals. *Behavioural Processes* 64: 1-12.
216. Krapp HG (2000) Neuronal matched filters for optic flow processing in flying insects. *Int Rev Neurobiol* 44: 93-120.
217. Krapp HG, Hengstenberg B, Hengstenberg R (1998) Dendritic structure and receptive-field organization of optic flow processing interneurons in the fly. *J Neurophysiol* 79: 1902-1917.
218. Krapp HG, Hengstenberg R (1996) Estimation of self-motion by optic flow processing in single visual interneurons. *Nature* 384: 463-466.
219. Krapp HG, Hengstenberg R, Egelhaaf M (2001) Binocular Contributions to Optic Flow Processing in the Fly Visual System. *J Neurophysiol* 85: 724-734.
220. Kriebel ME, Bennett MV, Waxman SG, Pappas GD (1969) Oculomotor neurons in fish: electrotonic coupling and multiple sites of impulse initiation. *Science* 166: 520-524.
221. Kunze P (1961) Untersuchung des Bewegungsehens fixiert fliegender Bienen. *Z vergl Physiol* 44: 656-684.
222. Kurtz R (2004) Ca²⁺ clearance in visual motion-sensitive neurons of the fly studied in vivo by sensory stimulation and UV photolysis of caged Ca²⁺. *J Neurophysiol* 92: 458-467.
223. Kurtz R (2007) Direction-selective adaptation in fly visual motion-sensitive neurons is generated by an intrinsic conductance-based mechanism. *Neurosci* 146: 573-583.
224. Kurtz R, Kalb J, Spalthoff C (2008) Examination of fly motion vision by functional fluorescence techniques. *Frontiers in Bioscience* 13: 3009-3021.
225. Kurtz R, Warzecha AK, Egelhaaf M (2001) Transfer of visual motion information via graded synapses operates linearly in the natural activity range. *J Neurosci* 21: 6957-6966.
226. Land M, Stavenga D, Hardie R (1989) Variations in the structure and design of compound eyes. *Facets of vision* 90-111.
227. Land MF (1997) Visual acuity in insects. *Annu Rev Entomol* 42: 147-177.
228. Land MF, Eckert H (1985) Maps of the acute zones of fly eyes. *J Comp Physiol A* 156: 525-538.
229. Land MF, Nilsson D-E (2002a) Apposition compound eyes. In: *Animal Eyes* pp 125-155. New-York: Oxford University Press.
230. Land MF, Nilsson D-E (2002b) What makes a good eye? In: *Animal Eyes* pp 33-55. New-York: Oxford University Press.
231. Lang EJ, Sugihara I, Llinas R (1996) GABAergic modulation of complex spike activity by the cerebellar nucleoolivary pathway in rat. *J Neurophysiol* 76: 255-275.
232. Lappe M, Bremmer F, Pökel M, Thiele A, Hoffmann KP (1996) Optic flow processing in monkey STS: A theoretical and experimental approach. *J Neurosci* 16: 6265-6285.
233. Lappe M, Hoffmann KP (1999) Optic flow and eye movements. In: *Neuronal Processing of Optic Flow* (Lappe M, ed), pp 29-48.

References

234. Laughlin SB, Hardie RC (1978) Common strategies for light adaptation in the peripheral visual systems of fly and dragonfly. *J Comp Physiol* 128: 319-340.
235. Lee DN (1980) The optic flow field: the foundation of vision. *Philos Trans R Soc Lond B Biol Sci* 290: 169-179.
236. Levitt JB, Kiper DC, Movshon JA (1994) Receptive fields and functional architecture of macaque V2. *J Neurophysiol* 71: 2517-2542.
237. Liu G (2004) Local structural balance and functional interaction of excitatory and inhibitory synapses in hippocampal dendrites. *Nat Neurosci* 7: 373-379.
238. Llinas R, Baker R, Sotelo C (1974) Electrotonic coupling between neurons in cat inferior olive. *J Neurophysiol* 37: 560-571.
239. Losonczy A, Makara JK, Magee JC (2008) Compartmentalized dendritic plasticity and input feature storage in neurons. *Nature* 452: 436-4U3.
240. Magee J, Hoffman D, Colbert C, Johnston D (1998) Electrical and calcium signaling in dendrites of hippocampal pyramidal neurons. *Annu Rev Physiol* 60: 327-346.
241. Mank M, Santos AF, Drenth S, Mrcic-Flogel TD, Hofer SB, Stein V, Hendel T, Reiff DF, Levelt C, Borst A, Bonhoeffer T, Hubener M, Griesbeck O (2008) A genetically encoded calcium indicator for chronic in vivo two-photon imaging. *Nat Methods* 5: 805-811.
242. Maravall M, Mainen ZF, Sabatini BL, Svoboda K (2000) Estimating intracellular calcium concentrations and buffering without wavelength ratioing. *Biophys J* 78: 2655-2667.
243. Marder E, Goaillard JM (2006) Variability, compensation and homeostasis in neuron and network function. *Nat Rev Neurosci* 7: 563-574.
244. Marr D, Ullman S (1981) Direction selectivity and its use in early visual processing. *Proc R Soc Lond B* 211: 151-180.
245. Matic T, Laughlin SB (1981) Changes in the intensity-response function of an insect's photoreceptors due to light adaptation. *Journal of Comparative Physiology A: Neuroethology, Sensory, Neural, and Behavioral Physiology* 145: 169-177.
246. McCann GD, Arnett DW (1972) Spectral and Polarization Sensitivity of Dipteran Visual System. *J Gen Physiol* 59: 534-&.
247. McCann GD, Foster SF (1971) Binocular interactions of motion detection fibers in the optic lobes of flies. *Kybernetik* 8: 193-203.
248. McCann GD, MacGinitie GF (1965) Optomotor response studies of insect vision. *Proc R Soc Lond B* 163: 369-401.
249. Meinertzhagen IA, Hanson TE (1993) The development of the optic lobe. In: *The development of Drosophila melanogaster* (Bate M, Martinez-Arias A, eds), pp 1363-1491. Cold Spring Harbor Laboratory Press.
250. Meinertzhagen IA, Oneil SD (1991) Synaptic Organization of Columnar Elements in the Lamina of the Wild-Type in *Drosophila-Melanogaster*. *J Comp Neurol* 305: 232-263.
251. Meinertzhagen IA, Sorra KE (2001) Synaptic organization in the fly's optic lamina: few cells, many synapses and divergent microcircuits. *Prog Brain Res* 131: 53-69.
252. Mel BW, Ruderman DL, Archie KA (1998) Translation-invariant orientation tuning in visual "complex" cells could derive from intradendritic computations. *J Neurosci* 18: 4325-4334.
253. Meyer EP, Matute C, Streit P, Nüssel DR (1986) Insect optic lobe neurons identifiable with monoclonal antibodies to GABA. *Histochemistry and Cell Biology* 84: 207-216.
254. Miesenbock G (2004) Genetic methods for illuminating the function of neural circuits. *Curr Opin Neurobiol* 14: 395-402.
255. Migliore M, Hines ML, Shepherd GM (2005) The role of distal dendritic gap junctions in synchronization of mitral cell axonal output. *J Comput Neurosci* 18: 151-161.
256. Mills SL, Massey SC (1995) Differential Properties of 2 Gap Junctional Pathways Made by Aii Amacrine Cells. *Nature* 377: 734-737.
257. Mills SL, Xia XB, Hoshi H, Firth SI, Rice ME, Frishman LJ, Marshak DW (2007) Dopaminergic modulation of tracer coupling in a ganglion-amacrine cell network. *Vis Neurosci* 24: 593-608.
258. Miyawaki A, Llopis J, Heim R, McCaffery JM, Adams JA, Ikura M, Tsien RY (1997) Fluorescent indicators for Ca^{2+} based on green fluorescent proteins and calmodulin. *Nature* 388: 882-887.

259. Montemurro MA, Panzeri S (2006) Optimal tuning widths in population coding of periodic variables. *Neural Comput* 18: 1555-1576.
260. Movshon JA, Thompson ID, Tolhurst DJ (1978) Receptive field organization of complex cells in the cat's striate cortex. *J Physiol* 283: 79-99.
261. Nakayama K (1985) Biological image motion processing: a review. *Vision Res* 25: 625-660.
262. Nakayama K, Loomis JM (1974) Optical Velocity Patterns, Velocity-Sensitive Neurons, and Space Perception - Hypothesis. p 3: 63-80.
263. Nalbach G (1993) The Halteres of the Blowfly *Calliphora* .1. Kinematics and Dynamics. *Journal of Comparative Physiology A-Sensory Neural and Behavioral Physiology* 173: 293-300.
264. Nalbach G, Hengstenberg R (1994) The Halteres of the Blowfly *Calliphora* .2. 3-Dimensional Organization of Compensatory Reactions to Real and Simulated Rotations. *Journal of Comparative Physiology A-Sensory Neural and Behavioral Physiology* 175: 695-708.
265. Neher E, Augustine GJ (1992) Calcium Gradients and Buffers in Bovine Chromaffin Cells. *Journal of Physiology-London* 450: 273-301.
266. Neri P (2006) Spatial integration of optic flow signals in fly motion-sensitive neurons. *J Neurophysiol* 95: 1608-1619.
267. O'Shea M, Rowell CH (1975) Protection from habituation by lateral inhibition. *Nature* 254: 53-55.
268. Oertner, T. G. Mechanismen Dendritischer Kalzimdynamik: Eine in-Vitro-Studie an Insektenneuronen. 1-95. 2000. Doctoral Dissertation, Max-Planck Institute of Cybernetics.
269. Oertner TG, Brotz TM, Borst A (2001) Mechanisms of dendritic calcium signaling in fly neurons. *J Neurophysiol* 85: 439-447.
270. Oswald AM, Schiff ML, Reyes AD (2006) Synaptic mechanisms underlying auditory processing. *Curr Opin Neurobiol* 16: 371-376.
271. Pailhous J, Ferrandez AM, Fluckiger M, Baumberger B (1990) Unintentional Modulations of Human Gait by Optical-Flow. *Behavioural Brain Research* 38: 275-281.
272. Patla AE (1997) Understanding the roles of vision in the control of human locomotion. *Gait & Posture* 5: 54-69.
273. Petrowitz R, Dahmen H, Egelhaaf M, Krapp HG (2000) Arrangement of optical axes and spatial resolution in the compound eye of the female blowfly *Calliphora*. *J Comp Physiol* 168: 737-746.
274. Pflugfelder GO, Heisenberg M (1995) *Optomotor-blind* of *Drosophila melanogaster*: a neurogenetic approach to optic lobe development and optomotor behaviour. *Comp Biochem Physiol* 110: 185-202.
275. Pierantoni R (1976) A look into the cock-pit of the fly. *Cell Tissue Res* 171: 101-122.
276. Poggio T, Reichardt W (1973) Considerations on models of movement detection. *Kybernetik* 13: 223-227.
277. Poggio T, Reichardt W (1976) Visual control of orientation behaviour in the fly II. Towards the underlying neural interactions. *Quart Rev Biophys* 9: 377-438.
278. Poirazi P, Brannon T, Mel BW (2003a) Arithmetic of subthreshold synaptic summation in a model CA1 pyramidal cell. *Neuron* 37: 977-987.
279. Poirazi P, Brannon T, Mel BW (2003b) Pyramidal neuron as two-layer neural network. *Neuron* 37: 989-999.
280. Polsky A, Mel BW, Schiller J (2004) Computational subunits in thin dendrites of pyramidal cells. *Nat Neurosci* 7: 621-627.
281. Pouget A, Deneve S, Ducom JC, Latham PE (1999) Narrow versus wide tuning curves: What's best for a population code? *Neural Comput* 11: 85-90.
282. Prazdny K (1980) Egomotion and relative depth map from optical flow. *Biol Cybern* 36: 87-102.
283. Pringle JWS (1948) The Gyroscopic Mechanism of the Halteres of Diptera. *Philosophical Transactions of the Royal Society of London Series B, Biological Sciences* 233: 347-384.
284. Raghu SV, Joesch M, Borst A, Reiff DF (2007) Synaptic organization of lobula plate tangential cells in *Drosophila*: gamma-aminobutyric acid receptors and chemical release sites. *J Comp Neurol* 502: 598-610.
285. Raghu SV, Joesch M, Sigrist SJ, Borst A, Reiff DF (2009) Synaptic Organization of Lobula Plate Tangential Cells in *Drosophila*: D7 Cholinergic Receptors. *J Neurogenet* 23: 200-209.
286. Raiguel S, Vogels R, Mysore SG, Orban GA (2006) Learning to see the difference specifically alters the most informative V4 neurons. *J Neurosci* 26: 6589-6602.
287. Rall W (1959) Branching dendritic trees and motoneuron membrane resistivity. *Exp Neurol* 1: 491-527.

References

288. Rall W (1964) Theoretical significance of dendritic trees for neuronal input-output relations. In: *Neural theory and modeling* (Reiss RF, ed), Stanford University Press.
289. Rall W (1967) Distinguishing theoretical synaptic potentials computed for different soma-dendritic distributions of synaptic input. *J Neurophysiol* 30: 1138-1168.
290. Rall W, Burke RE, Smith TG, Nelson PG, Frank K (1967) Dendritic location of synapses and possible mechanisms for the monosynaptic EPSP in motoneurons. *J Neurophysiol* 30: 1169-1193.
291. Reichardt W (1961) Autocorrelation, a principle for the evaluation of sensory information by the central nervous system. In: *Sensory Communication* (Rosenblith WA, ed), pp 303-317. New York, London: The M.I.T. Press and John Wiley & Sons.
292. Reichardt W (1969) Movement perception in insects. In: *Processing of Optical Data by Organisms and by Machines* (Reichardt W, ed), pp 465-493. New York: Academic.
293. Reichardt W (1987) Evaluation of optical motion information by movement detectors. *J Comp Physiol A* 161: 533-547.
294. Reichardt W, Egelhaaf M (1988) Properties of individual movement detectors as derived from behavioural experiments on the visual system of the fly. *Biol Cybern* 58: 287-294.
295. Reichardt W, Guo A (1986) Elementary pattern discrimination (Behavioral experiments with the fly *Musca domestica*). *Biol Cybern* 53: 285-306.
296. Reichardt W, Poggio T (1976) Visual control of orientation behaviour in the fly I. A quantitative analysis. *Quart Rev Biophys* 9: 311-375.
297. Reichardt W, Poggio T (1979) Figure-ground discrimination by relative movement in the visual system of the fly. Part I: Experimental results. *Biol Cybern* 35: 81-100.
298. Reichardt W, Poggio T, Hausen K (1983) Figure-Ground discrimination by relative movement in the visual system of the fly. Part II: Towards the neural circuitry. *Biol Cybern* 46: 1-30.
299. Reichardt W, Varjú D (1959) Übertragungseigenschaften im Auswertesystem für das Bewegungssehen. *Z Naturforsch* 14b: 674-689.
300. Reichardt WE, Poggio T (1981) Visual control of flight in flies. In: *Theoretical approaches in neurobiology*. (Reichardt WE, Poggio T, eds), pp 135-150. Cambridge, Mass. and London: The MIT Press.
301. Reichert H, Rowell CHF, Griss C (1985) Course correction circuitry translates feature detection into behavioural action in locusts. *Nature* 315: 142-144.
302. Reisenman C, Haag J, Borst A (2003) Adaptation of response transients in fly motion vision. I: Experiments. *Vision Res* 43: 1293-1309.
303. Reyes A (2001) Influence of dendritic conductances on the input-output properties of neurons. *Annu Rev Neurosci* 24: 653-675.
304. Ribi WA (1978) Gap junctions coupling photoreceptor axons in the first optic ganglion of the fly. *Cell and Tissue Research* 195: 299-308.
305. Ringach DL, Shapley RM, Hawken MJ (2002) Orientation selectivity in macaque V1: diversity and laminar dependence. *J Neurosci* 22: 5639-5651.
306. Rister J, Pauls D, Schnell B, Ting CY, Lee CH, Sinakevitch I, Morante J, Strausfeld NJ, Ito K, Heisenberg M (2007) Dissection of the peripheral motion channel in the visual system of *Drosophila melanogaster*. *Neuron* 56: 155-170.
307. Robert D, Rowell CHF (1992) Locust flight steering. *Journal of Comparative Physiology A: Neuroethology, Sensory, Neural, and Behavioral Physiology* 171: 41-51.
308. Safran MN, Flanagan VL, Borst A, Sompolsky H (2007) Adaptation and information transmission in fly motion detection. *J Neurophysiol* 98: 3309-3320.
309. Sanger TD (2003) Neural population codes. *Curr Opin Neurobiol* 13: 238-249.
310. Schiller J, Major G, Koester HJ, Schiller Y (2000) NMDA spikes in basal dendrites of cortical pyramidal neurons. *Nature* 404: 285-289.
311. Schmitz D, Schuchmann S, Fisahn A, Draguhn A, Buhl EH, Petrasch-Parwez E, Dermietzel R, Heinemann U, Traub RD (2001) Axo-axonal coupling: A novel mechanism for ultrafast neuronal communication. *Neuron* 31: 831-840.
312. Schoups A, Vogels R, Qian N, Orban G (2001) Practising orientation identification improves orientation coding in V1 neurons. *Nature* 412: 549-553.

313. Schulz DJ, Goaillard J-M, Marder E (2006) Variable channel expression in identified single and electrically coupled neurons in different animals. *Nature Neuroscience* 9: 356-362.
314. Segev I, Rinzel J, Shepherd GM (1994) *The theoretical foundation of dendritic function*. Cambridge, MA: The MIT Press.
315. Series P, Latham PE, Pouget A (2004) Tuning curve sharpening for orientation selectivity: coding efficiency and the impact of correlations. *Nat Neurosci* 7: 1129-1135.
316. Seung HS, Sompolinsky H (1993) Simple-Models for Reading Neuronal Population Codes. *Proceedings of the National Academy of Sciences of the United States of America* 90: 10749-10753.
317. Shaw SR (1975) Retinal Resistance Barriers and Electrical Lateral Inhibition. *Nature* 255: 480-483.
318. Shaw SR (1989) The retina-lamina pathway in insects, particularly diptera, viewed from an evolutionary perspective. In: *Facets of Vision* (Stavenga DG, Hardie RC, eds), pp 185-212. Berlin, Heidelberg: Springer.
319. Simmons P (1980) A Locust Wind and Ocellar Brain Neuron. *J Exp Biol* 85: 281-294.
320. Simpson JI (1984) The Accessory Optic System. *Ann Rev Neurosci* 7: 13.
321. Simpson JI, Leonard CS, Soodak RE (1988) The accessory optic system of rabbit. II. Spatial organization of direction selectivity. *J Neurophysiol* 60: 2055-2072.
322. Single S, Borst A (1998) Dendritic integration and its role in computing image velocity. *Science* 281: 1848-1850.
323. Single S, Haag J, Borst A (1997) Dendritic computation of direction selectivity and gain control in visual interneurons. *J Neurosci* 17: 6023-6030.
324. Smakman JGJ, Hateren JH, Stavenga DG (1984) Angular sensitivity of blowfly photoreceptors: intracellular measurements and wave-optical predictions. *Journal of Comparative Physiology A: Neuroethology, Sensory, Neural, and Behavioral Physiology* 155: 239-247.
325. Snippe HP, Koenderink JJ (1992) Discrimination Thresholds for Channel-Coded Systems. *Biol Cybern* 66: 543-551.
326. Sobel EC (1990) The locust's use of motion parallax to measure distance. *J Comp Physiol A* 167: 579-588.
327. Sobel EC, Tank DW (1994) In vivo Ca^{2+} dynamics in a cricket auditory neuron: an example of chemical computation. *Science* 263: 823-826.
328. Sohl G, Maxeiner S, Willecke K (2005) Expression and functions of neuronal gap junctions. *Nature Reviews Neuroscience* 6: 191-200.
329. Soohoo SL, Bishop LG (1980) Intensity and motion responses of giant vertical neurons of the fly eye. *J Neurobiol* 11: 159-177.
330. Spira ME, Bennett MV (1972) Synaptic control of electrotonic coupling between neurons. *Brain Res* 37: 294-300.
331. Spruston N, Jaffe DB, Williams SH, Johnston D (1993) Voltage- and space-clamp errors associated with the measurement of electrotonically remote synaptic events. *J Neurophysiol* 70: 781-802.
332. Srinivasan M, Zhang S, Lehrer M, Collett T (1996) Honeybee navigation en route to the goal: visual flight control and odometry. *J Exp Biol* 199: 237-244.
333. Srinivasan MV (1977) A visually-evoked roll response in the housefly. *J Comp Physiol* 119: 1-14.
334. Srinivasan MV, Dvorak DR (1980) Spatial processing of visual information in the movement-detecting pathway of the fly. *J Comp Physiol* 140: 1-23.
335. Srinivasan MV, Poteser M, Kral K (1999) Motion detection in insect orientation and navigation. *Vision Res* 39: 2749-2766.
336. Srinivasan MV, Zhang SW (2004) Visual motor computations in insects. *Ann Rev Neurosci* 27: 679-696.
337. Srinivasan MV, Zhang S, Altwein M, Tautz J (2000) Honeybee Navigation: Nature and Calibration of the "Odometer". *Science* 287: 851-853.
338. Steveninck RRV, Lewen GD, Strong SP, Koberle R, Bialek W (1997) Reproducibility and variability in neural spike trains. *Science* 275: 1805-1808.
339. Strausfeld NJ (1970) Golgi Studies on Insects .2. Optic Lobes of Diptera. *Philosophical Transactions of the Royal Society of London Series B-Biological Sciences* 258: 135-&.
340. Strausfeld NJ (1976) *Atlas of an insect brain*. Berlin: Springer Verlag.
341. Strausfeld NJ (1984) Functional neuroanatomy of the blowfly's visual system. In: *Photoreception and vision in invertebrates* (Ali MA, ed), pp 483-522. Plenum Publishing Corporation.

References

342. Strausfeld NJ, Campos-Ortega JA (1973) The L4 monopolar neurone: a substrate for lateral interaction in the visual system of the fly *Musca domestica* (L). *Brain Res* 59: 97-117.
343. Strausfeld NJ, Lee JK (1991) Neuronal basis for parallel visual processing in the fly. *Vis Neurosci* 7: 13-33.
344. Svoboda K, Denk W, Kleinfeld D, Tank DW (1997) In vivo dendritic calcium dynamics in neocortical pyramidal neurons. *Nature* 385: 161-165.
345. Swensen AM, Bean BP (2005) Robustness of burst firing in dissociated purkinje neurons with acute or long-term reductions in sodium conductance. *J Neurosci* 25: 3509-3520.
346. Taddei-Ferretti C, Perez de Talens AF (1973) Landing reaction of *Musca domestica*, III: Dependence on the luminous characteristics of the stimulus. *Z Naturforsch* 28c: 568-578.
347. Takahashi A, Camacho P, Lechleiter JD, Herman B (1999) Measurement of intracellular calcium. *Physiol Rev* 79: 1089-1125.
348. Tanaka K, Saito HA (1989) Analysis of Motion of the Visual-Field by Direction, Expansion Contraction, and Rotation Cells Clustered in the Dorsal Part of the Medial Superior Temporal Area of the Macaque Monkey. *J Neurophysiol* 62: 626-641.
349. Thorson J (1966) Small-signal analysis of a visual reflex in the locust. I. Input parameters. *Kybernetik* 3: 41-53.
350. Torre V, Poggio T (1978) Synaptic Mechanism Possibly Underlying Directional Selectivity to Motion. *Proceedings of the Royal Society of London Series B-Biological Sciences* 202: 409-416.
351. Trujillo O, Melamed J (1966) Compound Eye of Dipterans - Anatomical Basis for Integration - An Electron Microscope Study. *Journal of Ultrastructure Research* 16: 395-&.
352. Tsien RY (1988) Fluorescent measurement and photochemical manipulation of cytosolic free calcium. *Trends Neurosci* 11: 419-424.
353. Tsien RY (1989) Fluorescent probes of cell signaling. *Annu Rev Neurosci* 12: 227-253.
354. Ullman S (1983) The measurement of visual motion. *Trends Neurosci* 6: 177-179.
355. van den Berg AV, van de Grind WA (1989) Reaction times to motion onset and motion detection thresholds reflect the properties of bilocal motion detectors. *Vision Res* 29: 1261-1266.
356. van Doorn AJ, Koenderink JJ (1982a) Spatial properties of the visual detectability of moving spatial white noise. *Brain Res* 45: 189-195.
357. van Doorn AJ, Koenderink JJ (1982b) Temporal properties of the visual detectability of moving spatial white noise. *Brain Res* 45: 179-188.
358. van Hateren JH, van der Schaaf A. (1998) Independent component filters of natural images compared with simple cells in primary visual cortex. *Proc Biol Sci* 265: 359-366.
359. van Santen JPH, Sperling G (1984) Temporal covariance model of human motion perception. *J Opt Soc Am A* 1: 451-473.
360. Virsik R, Reichardt W (1974) Tracking of Moving Objects by Fly *Musca-Domestica*. *Naturwiss* 61: 132-133.
361. Virsik RP, Reichardt W (1976) Detection and Tracking of Moving-Objects by Fly *Musca-Domestica*. *Biol Cybern* 23: 83-98.
362. Wagner H (1982) Flow-field variables trigger landing in flies. *Nature* 297: 147-148.
363. Wallace DJ, zum Alten Borgloh SM, Astori S, Yang Y, Bausen M, Kugler S, Palmer AE, Tsien RY, Sprengel R, Kerr JND, Denk W, Hasan MT (2008) Single-spike detection in vitro and in vivo with a genetic Ca²⁺ sensor. *Nat Meth* 5: 797-804.
364. Wallace GK (1959) Visual Scanning in the Desert Locust *Schistocerca-Gregaria* Forskal. *J Exp Biol* 36: 512-525.
365. Wang YC, Frost BJ (1992) Time to Collision Is Signaled by Neurons in the Nucleus Rotundus of Pigeons. *Nature* 356: 236-238.
366. Warren WH, Hannon DJ (1988) Direction of self-motion is perceived from optical flow. *Nature* 336: 162-163.
367. Warzecha AK, Borst A, Egelhaaf M (1992) Photo-ablation of single neurons in the fly visual system reveals neural circuit for the detection of small moving objects. *Neurosci Lett* 141: 119-122.
368. Warzecha AK, Egelhaaf M, Borst A (1993) Neural circuit tuning fly visual interneurons to motion of small objects. I. Dissection of the circuit by pharmacological and photoinactivation techniques. *J Neurophysiol* 69: 329-339.

369. Weber F, Eichner H, Cuntz H, Borst A (2008) Eigenanalysis of a neural network for optic flow processing. *New Journal of Physics* 10: 015013.
370. Wehner R (1981) Spatial vision in arthropods. In: *Handbook of Sensory Physiology* (Autrum H, ed), pp 287-616. Berlin: Springer-Verlag.
371. Wehrhahn C, Hausen K (1980) How is tracking and fixation accomplished in the nervous system of the fly? A behavioural analysis based on short time stimulation. *Biol Cybern* 38: 179-186.
372. Wei DS, Mei YA, Bagal A, Kao JP, Thompson SM, Tang CM (2001) Compartmentalized and binary behavior of terminal dendrites in hippocampal pyramidal neurons. *Science* 293: 2272-2275.
373. Wertz A, Borst A, Haag J (2008a) Nonlinear integration of binocular optic flow by DNOVS2, a descending neuron of the fly. *J Neurosci* 28: 3131-3140.
374. Wertz A, Borst A, Haag J (2008b) Nonlinear integration of binocular optic flow by DNOVS2, a descending neuron of the fly. *J Neurosci* 28: 3131-3140.
375. Williams SR, Mitchell SJ (2008) Direct measurement of somatic voltage clamp errors in central neurons. *Nat Neurosci* 11: 790-798.
376. Wilson HR (1985) A model for direction selectivity in threshold motion perception. *Biol Cybern* 51: 213-222.
377. Wilson WA, Monahangoldner M (1975) Voltage Clamping with A Single Microelectrode. *J Neurobiol* 6: 411-422.
378. Wolf-Oberhollenzer F, Kirschfeld K (1994) Motion sensitivity in the nucleus of the basal optic root of the pigeon. *J Neurophysiol* 71: 1559-1573.
379. Wu CF, Pak WL (1978) Light-induced voltage noise in the photoreceptor of *Drosophila melanogaster*. *The Journal of General Physiology* 71: 249-268.
380. Wu GK, Arbuckle R, Liu BH, Tao HW, Zhang LI (2008) Lateral sharpening of cortical frequency tuning by approximately balanced inhibition. *Neuron* 58: 132-143.
381. Wylie DRW, Frost BJ (1999) Responses of neurons in the nucleus of the basal optic root to translational and rotational flowfields. *J Neurophysiol* 81: 267-276.
382. Xia XB, Mills SL (2004) Gap junctional regulatory mechanisms in the AII amacrine cell of the rabbit retina. *Vis Neurosci* 21: 791-805.
383. Yarnaguchi S, Wolf R, Desplan C, Heisenberg M (2008) Motion vision is independent of color in *Drosophila*. *Proceedings of the National Academy of Sciences of the United States of America* 105: 4910-4915.
384. Zaagman WH, Mastebroek HAK, Buyse T, Kuiper JW (1977) Receptive field characteristics of a directionally selective movement detector in the visual system of the blowfly. *J Comp Physiol* 116: 39-50.
385. Zaagman WH, Mastebroek HAK, Kuiper JW (1978) On the correlation model: performance of a movement detecting neural element in the fly visual system. *Biol Cybern* 31: 163-168.
386. Zbikowski R (2005) Fly like a Fly. *IEEE Spectrum* 42: 46-51.
387. Zettler F, Järvilehto M (1972) Lateral Inhibition in An Insect Eye. *Zeitschrift fur Vergleichende Physiologie* 76: 233-&.
388. Zhang K, Sejnowski TJ (1999) Neuronal tuning: To sharpen or broaden? *Neural Comput* 11: 75-84.

Acknowledgements

First and foremost, I would like to thank my supervisor and Doktorvater, Axel Borst, for the opportunity to carry out this work in his lab, and for turning me into a neuroscientist, for the constant encouragement, patience and advice, even when results were few and far-between, and for his support in changing to the project whose results are presented in this thesis. I would also like to thank him for helping me in planning the next steps in my scientific career. Thanks to Jürgen Haag, my direct boss and the most talented and knowledgeable electrophysiologist I have ever known. Thank you for teaching me to be an electrophysiologist, a calcium imager and a lobula plate scientist, for countless suggestions, criticisms, methodological and systemic insights and for always having the time and patience to answer my many questions.

Thanks also to Mark Hübener who was on my thesis committee, especially for his suggestions on planning the small-field selectivity experiments. Thanks also to Yong Choe, who was a constant source of knowledge about anything related to neuroscience, and whose discussions helped me a lot along the way. Thanks to Deusdedit Spavieri for help with programming and for many discussions about the more mathematical and informational sides of neuroscience, and to Karl Farrow for helping me with the preparation and electrophysiology. To Renate Gleich who kept the flies happy and helped me find everything I needed, to the MPI mechanics and electrical workshops for building fantastic contraptions that do all you need and more. To the rest of the Borst group, Adrian, Hubert, Franz, Friedrich, Max, Bettina, Johannes, Väinö, Nicola, Benji and Sham for their support, help and many nice discussions in our fly meetings. To the Bonhoeffer group for help with calcium dyes, and to the Stein Group for help with channel blockers.

Curriculum Vitae

Yishai Michael Elyada, b. Feb 24, 1976, Jerusalem, Israel

Education

2004-2009 MPI of Neurobiology, Martinsried, Germany

Ph.D. student, Department of Systems and Computational Neurobiology. Supervisor: Prof. Alexander Borst. Subject: Intracellular processing of motion information in a network of blowfly visual interneurons.

Ph.D. students' representative of the institute for 2007

1999-2004 University of Tel-Aviv, Israel

Adi Lautman Interdisciplinary Program for Outstanding Students.

The Adi Lautman Interdisciplinary Program for Outstanding Students is a 4-year full scholarship program for direct M.A. studies with an interdisciplinary orientation. Freshman or sophomore students are admitted, and are exempt from completing their B.A. requirements. After 2 years of extra-facultatory studies within the program, students join one of the departments in a faculty of their choice as M.A. students, still as part of the program.

M.A. summa cum laude in the department of Computer Science, Faculty of Exact Sciences. Supervisors: Prof. David Horn (Physics) and Prof. Eytan Ruppin (Computer Science). Dissertation: Can Dynamic Neural Filters Create Pseudo-Random Sequences?

1998-1999 University of Tel-Aviv, Israel

Research-Oriented Honors Program, Faculty of Life Sciences, Tel-Aviv University.

Honors, Awards and Scholarships

1998-1999 Partial scholarship for the Research-Oriented Honors Program, Faculty of Life Sciences

1999 Dean's Prize, Faculty of Life Sciences

1999-2003 4-years full scholarship, The Adi Lautmann Interdisciplinary Program for Outstanding Students, Tel-Aviv University

2005-2007 The Minerva Foundation Scholarship (Max-Planck Society)

Courses

2006 In-vivo intracellular electrophysiology course, the Otto Loewi Minerva center, Eilat, Israel. In this course students learned and successfully implemented intracellular patch-clamp recordings of cortical and cerebellar neurons in anesthetized rats.

Publications

Elyada, Y. M., Haag, J. and Borst, A. Different receptive fields in axons and dendrites underlie robust coding in motion-sensitive neurons. *Nature Neuroscience* **12**, 327-332 (2009)

Elyada, Y. M. and Horn, D. Can Dynamic Neural Filters Produce Pseudo-Random Sequences? Lecture Notes in Computer Science – Proceedings of ICANN 2005, Vol. 3696 211-216 (2005)

Employment

2003-2004 Researcher and algorithm developer, Peldec Decision Systems, Tel-Aviv. Development of an event-based neural network system for bankruptcy prediction in commercial companies.

2002-2003 Teaching assistant, The Department of Computer Science, IDC College, Herzliya. Calculus for computer science students in Hebrew and in English as part of the international program for computer science.

2000-2003 Course instructor, The Department of Mathematics, The Open University. Introduction to mathematics, Linear algebra for mathematics and computer science students.

1998-2000 Mathematics and Logics teacher in a private university-preparatory institute, "Lachmann", textbook editor.

Language Skills

Fluent in Hebrew and English, conversational level German, rudimentary Spanish

Personal interests

Nature photography

Sports: member of the Munich Irish Rovers Football Club since 2005